Design and Development of a Roll-to-Roll Machine for Continuous High-Speed Microcontact Printing

by

Adam Stagnaro

M.Eng Manufacturing, MIT 2008

Submitted to the Department of Mechanical Engineering
in partial fulfillment of the requirements for the degree of

Masters of Engineering

at the

MASSACHUSETTS INSTITUTE OF TECHNOLOGY

August 2008

Author .. ..

Department of Mechanical Engineering
19 August 2008

Certified by ....

David E. Hardt
Professor of Mechanical Engineering
Thesis Supervisor

Accepted by ....

Lallit Anand
Chairman, Departmental Committee on Graduate Studies
Department of Mechanical Engineering

Design and Development of a Roll-to-Roll Machine for Continuous High-Speed Microcontact Printing

by

Adam Stagnaro

Submitted to the Department of Mechanical Engineering on 19 August, 2008,
in partial fulfillment of the requirements for the
Degree of Masters of Engineering in Manufacturing
Advisor: Dr. David E. Hardt

Abstract

Microcontact printing (μCP) is an emerging technique for patterning micro-scale features for electronics, optics, surface modifications, and a variety of other applications. Its many advantages over traditional techniques like photolithography include lower cost, ability to pattern on non-planar surfaces, and compatibility with a variety of materials. Low production rates are one of the major limitations, as the process remains primarily a lab-scale technique at this point. Commercialization of the process depends on the development of innovative ways of applying the techniques to fast and flexible process paradigms. This thesis proposes the use of roll-to-roll techniques to increase the throughput, flexibility, and printable area for μCP, while maintaining high quality outputs. A three-part literature review is presented comprising microcontact printing, traditional printing techniques, and roll-to-roll web handling best practices. The development of a printing machine and continuous etching machine used to explore the application of μCP in a high-speed roll-to-roll paradigm is then detailed. Finally, the results of the experimentation carried out are documented including effects on quality and limitations for high throughputs. It is concluded that roll-to-roll microcontact printing can produce high quality results over large areas at rates up to 400 feet per minute and possibly beyond.

Acknowledgements

First, thanks to my wonderful teammates: Kanika Khanna and Shawn Shen. Their hard work and bright ideas helped carry this project. Each of us brought something unique and interesting to the table, and our minds and ideas melded and mixed into a fantastic team.

Many thanks also to my advisor Dr. David Hardt for his guidance, insight, and open-door. The meetings in his office always seemed to bring up new ideas and questions that steered our project along a successful path.

Thank you to everyone at NanoTerra for being friendly, professional, and ever so helpful to three manufacturing engineers thrown into a chemistry laboratory.

A million thanks to Karan Chauhan. He and NanoTerra put an incredible amount of trust in us, and that is truly what made this a worthwhile experience, both for us and, hopefully, for NanoTerra. Karan took a great deal of time out of his day to teach us the fundamentals of soft lithography, throw around ideas, discuss potential problems, offer advice, show us how to present to scientists and managers (at the same time), how to apply useful statistical and engineering tools, steer us towards the right questions and goals, show us interesting new developments, and more. Whether at NanoTerra, in the top floor at 100 Memorial Dr, or the Muddy, he was always available and open.

Last, and definitely not least, thanks to my family for their patience and continuing support of everything and anything I pursue.

Table of Contents

List of Figures

List of Tables

Chapter 1

Introduction

1.1 Motivation

Currently, nanostructures are commonly fabricated using techniques such as photolithography, electron-beam writing and X-ray lithography. Although they are proven technologies that provide high-quality outputs, there are inherent problems. These techniques are generally expensive, slow, and the production of large patterns is difficult. Another technology is required that can enable economical manufacturing of nanostructures at high production rates and good quality.

Microcontact printing (μCP) is a promising technology in which a patterned elastomeric stamp is used to transfer patterns of self-assembled monolayers (SAMs) onto a substrate by conformal contact. It has been demonstrated with a resolution of 30nm and a minimum feature size of 40nm with millisecond deposition times. Currently, the art remains primarily a research topic, but by adapting the technology to new processes it is a feasible large scale manufacturing method.

Roll-to-roll printing techniques such as gravure and flexography have been successfully used to print components such as antennas in RFID tags and other flexible electronics. They achieve good results at low costs and high throughput, but the technique

is limited to feature sizes of about 15μm. This has led to the novel idea that traditional printing processes can be applied to the fabrication of nano-scale components for mass manufacturing by applying the techniques and tools to microcontact printing (illustrated in Figure 1-1). In doing so, much higher rates can be achieved and more sophisticated structures patterned. The result must be reliable, its output accurate and repeatable, and its throughput comparable to traditional printing methods.

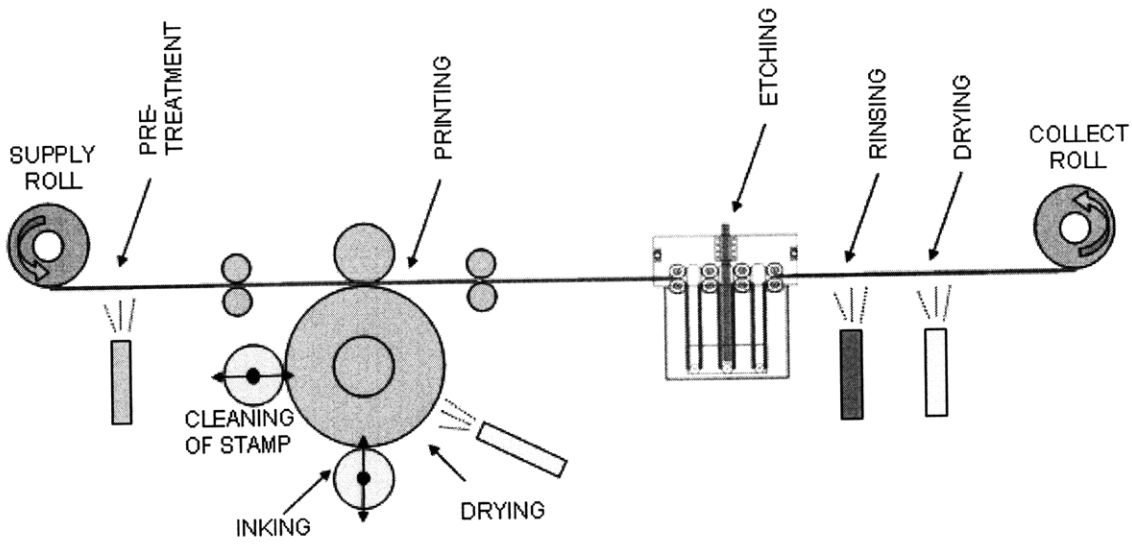

Figure 1-1: A schematic approach to the motivation behind this research; taking a primarily lab-scale technique and applying it to the roll-to-roll paradigm to make it suitable for high-production manufacturing.

This thesis will discuss our research into the melding of μCP with traditional printing techniques to produce nano-structures at higher rates than current methods. Included is a synopsis of the literature regarding soft lithography and traditional printing techniques, a description of the devices we developed to test the method, analysis of the input factors and effects on quality of the finished product, lessons learned throughout the project, and opportunities for future work.

Research was funded by and in cooperation with NanoTerra LLC, a Cambridge, Massachusetts company that specializes in soft lithography. Their resources and wealth of knowledge in the science of nano-manufacturing has been invaluable and has contributed greatly to our work.

1.2 Objectives

The primary objective of this project was to expand on knowledge relating to the continuous processing of flexible substrates using μCP printing. Specifically, this encompassed three key objectives:

1. Develop a set of modular tools to enable continuous μCP to pattern flexible gold-on-plastic substrates
2. Demonstrate high quality output over large areas at fast processing times
3. Develop a quantitative knowledge base around process input-output causality

Key areas to be addressed by experimentation were the maximization of throughput and optimization of print quality (global distortions, dimensional variation, and yield). Originally, a target of 100 feet per minute for throughput was set, however much higher rates were achieved.

1.3 Summary of Findings

This paper presents the following results and insights into roll-to-roll μCP

- Printing pressure and speed have little effect on dimensional variation, spatial distortions, and yield. Dimensional variation is small (COV~.5%) and randomly distributed.
- 100% pattern transfer is relatively easy to achieve using roll-to-roll techniques.
- It is possible to print a robust etch-resisting SAM at very high speeds (400 ft/min, unit area contact time ~ 5ms).
- At very high speeds (400ft/min), some systematic air trapping occurs.
- PDMS is a *very* durable stamp material that can last for many prints in the roll-to-roll format (we estimate that the printing cylinder made ~20,000 revolutions during testing).

1.4 Approach

A number of designs were discussed in the infancy of this project; some that were very similar to traditional printing methods and others that were quite different. The roll-to-roll paradigm was the obvious choice as it is a proven robust method used by many industries for the fast processing of flexible materials. Also, it is perceived by many in the field of soft lithography to be a key industrial implementation paradigm for the technique. The perceived challenges to accommodate the unique characteristics associated with microcontact printing included the following:

- Large area stamp fabrication
- Stamp mounting on a cylindrical surface
- Method of applying and measuring printing pressure (impression)
- Inking method
- Control of substrate tension
- Automated material handling

In addition to the printing machine, several additional tools were developed. This included a new stamp fabrication method for large area stamps and an etching machine prototype to experiment with continuous etching of the printed substrate.

1.5 Scope

The scope of our project is limited to printing octadecanethiols on gold substrates using microcontact printing in a roll-to-roll paradigm. Developing a useful tool, optimizing the quality of the print, and maximizing rate are the key outputs that we wished to explore.

Byproducts of this project include improvements in large area stamp manufacturing and demonstration of continuous etching.

Although the machine is primarily intended for microcontact printing, modularity was a key design goal, and with the proper modifications it could be used in the future for

micromolding, polymeric ink printing, and a host of other processes at NanoTerra's discretion.

1.6 Task Division

The project was initially divided into three main activities: mechanical design/execution, electrical & programming design/execution, and experimental design/execution. Each group member took the lead on one activity and delegated responsibility for anything that needed to be done in that area. I was primarily responsible for mechanical design of the printing and etching machine, Shawn Shen was responsible for electrical design and programming, and Kanika Khanna was in charge of experimental design. All group members participated in machine assembly, running experiments, and the myriad of other activities that accompanied the project.

Chapter 2

Soft Lithography and μCP

This section first discusses the general field of soft lithography. Next, the key elements and inputs to microcontact printing are presented. As it is the focus of this project, this chapter emphasizes μCP, rather than other techniques that fall under the umbrella of soft lithography.

2.1 Soft Lithography

Soft lithography is a collection of technologies that enable the formation of structures for nanofabrication separate from the photolithographic paradigm. These techniques are a relatively low-cost and effective method for creating features as small as 10 nanometers based on the concept of self assembly and replica molding of molecular layers. Applications include microelectronics, polarizers, filters, wire grids, surface acoustic wave devices, surface modifications, aesthetic features for consumer products, and an expanding array of other products.

Projection photolithography tends to be the de-facto technology for producing patterned microstructures down to 250 nm. However, there is an apparent barrier for features smaller than 100nm due to optical limitations. Other problems include the in-

ability to pattern non-planar surfaces, lack of control of surface chemistry, patterns only in two dimensions, and material limitations (can only work on photoresists). The state-of-the-art also includes emerging technologies such as UV lithography, soft X-ray lithography, electron beam writing, focused-ion-beam writing, and proximal-probe lithography. These methods are well suited for the production of extremely small feature sizes (several nanometers); however cost has limited their feasibility for wide-scale production.

Soft lithography has many advantages over the photolithography methods in a number of applications. It can create patterns down to ~10nm on a wide range of materials (Au, Ag, Cu, polymer beads, organic and inorganic salts to name a few), on non-planar and planar surfaces, and can create 2D and 3D structures. The technology is also low in capital cost and relatively easy to learn and apply [1].

2.1.1 The Soft Lithography Taxonomy

Soft Lithography encompasses five core techniques. These include: Microcontact Printing, Near Field Optical Lithography, Replica Molding, Micromolding in Capillaries, Microtransfer Molding, and Solvent Assisted Microcontact Molding. In common to all of these are the three following attributes (also refer to Figure 2-1):

1. A master pattern with desired topography (typically silicone or glass)
2. Fabrication of a molded stamp from the master by the application of a functional organic material (typically Polydymethylsiloxane, PDMS)
3. Generating a replica of the original pattern in a functional material [1]

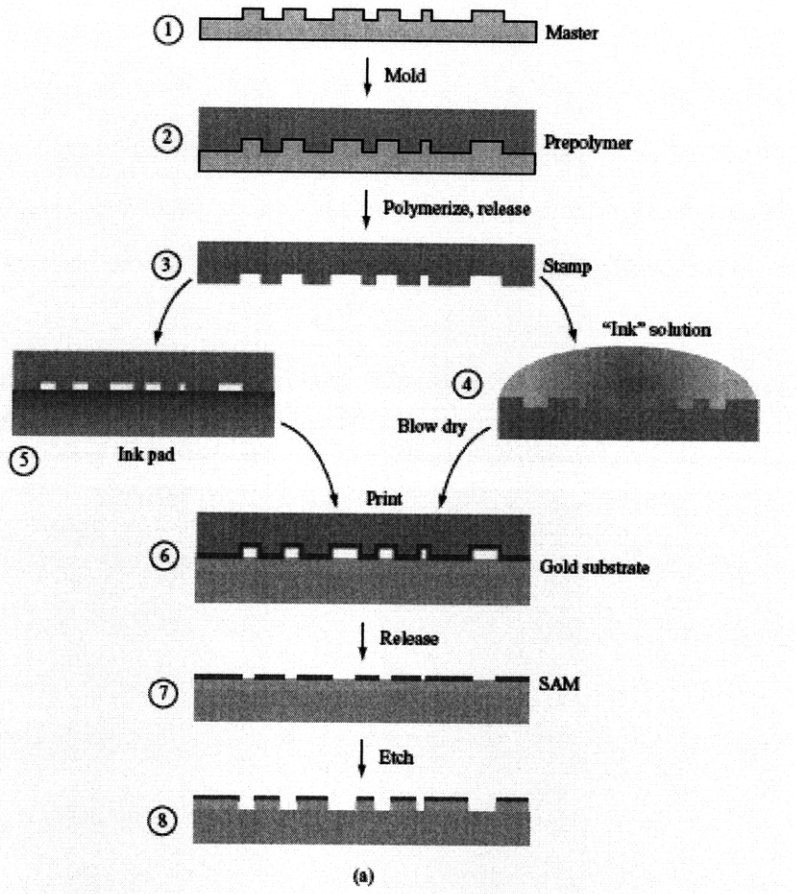

Figure 2-1: Overview of soft lithographic technique (μCP, in this example) [2]

Because the whole of soft lithography is out of the scope of this paper, and our project is focused on only one of these techniques (μCP), further explanation of other techniques will be omitted. There is a plethora of literature that can be referred to if the reader so desires. A detailed overview of microcontact printing is presented in the following section.

2.2 Microcontact Printing

In μCP, a relief pattern on the surface of a Polydimethylsiloxane (PDMS) stamp is used to transfer *self-assembled* monolayers to a substrate by conformal contact. Self-assembly is the key differentiator from other printing methods.

This section describes the key characteristics of μCP technology, the parameters that affect the output, and the various considerations and limitations for manufacturing feasibility.

2.2.2 Process

μCP differs from other printing methods primarily in its use of self-assembly (especially the use of Self-Assembled Monolayers) to form patterns. An elastomeric stamp with a relief pattern is inked with a molecular ink and brought into contact with a substrate with a small force, forming a monolayer which can be used as a resist layer for etching or other processes. Because the stamp is flexible, the process is insensitive to surfaces that are not completely flat or smooth [2].

Self assembly is the spontaneous aggregation and subsequent organization of molecules or meso-scale objects into a stable, well-defined structure via noncovalent interactions (Figure 2-2). They tend to form spontaneously and reject defects because the assembled structures are close to or at their thermodynamic equilibrium. The subunit properties determine the final structure by coming to their equilibrium at the lowest energy form. Self Assembled Monolayers (SAM's) are prepared by immersing a substrate in a solution containing a ligand ($Y(CH_2)_nX$); the thickness of the monolayer can be changed by the number (n) of methylene groups in the alkyl chain. Depositing SAM's on gold and silver tends to be the easiest compared to other materials, however it is possible on a number of other metals. SAM's work well in microcontact printing because they are easy to prepare, have good stability in ambient laboratory conditions, and exhibit very few defects in the final structures [1].

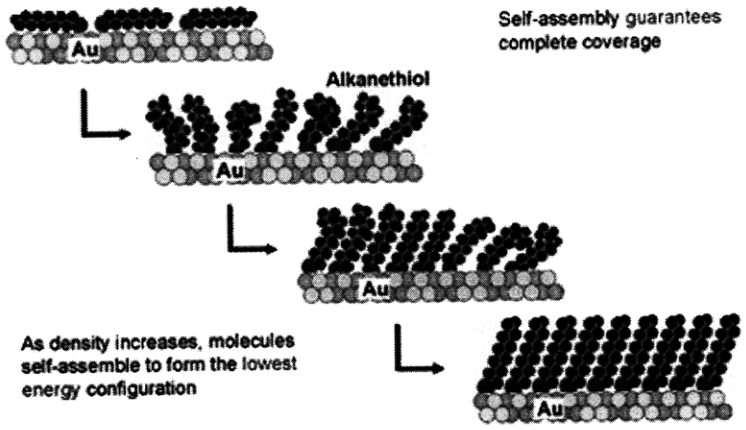

Figure 2-2: A schematic of the self-assembly process [14]

2.2.3 Printing Parameters of Interest

The μCP process can be broken down into two steps: inking and printing. There are several key factors that influence these steps. Those that were of interest to this project were selected, namely conformal contact, stamp elasticity, contact time, printing pressure, ink type and concentration, and inking method. Other factors, such as temperature, humidity, propagation method, and several others were left out for the sake of brevity.

2.2.3.1 Conformal contact

Printing is generally divided into two logical steps: defining an accurate pattern and bringing it close enough to the substrate to transfer the pattern. The second step in this process requires the adaptation of the printing plate to execute the transfer. Conformal contact in μCP is the mediator for the intimate contact between ink on the elastomeric stamp and the substrate. Although it is strongly related to the elasticity of the stamp, soft backings and other techniques are often used to accomplish the conformity of the stamp to the substrate. Its definition is twofold: it is 1) the macroscopic adaptation to the overall shape of the substrate, and 2) the microscopic adaptation of a soft polymer layer to a rough surface [2]. Figure 2-3 depicts these two functions of conformal contact. Stamp elasticity is one of the key enablers of conformal contact and is explained in the following paragraph.

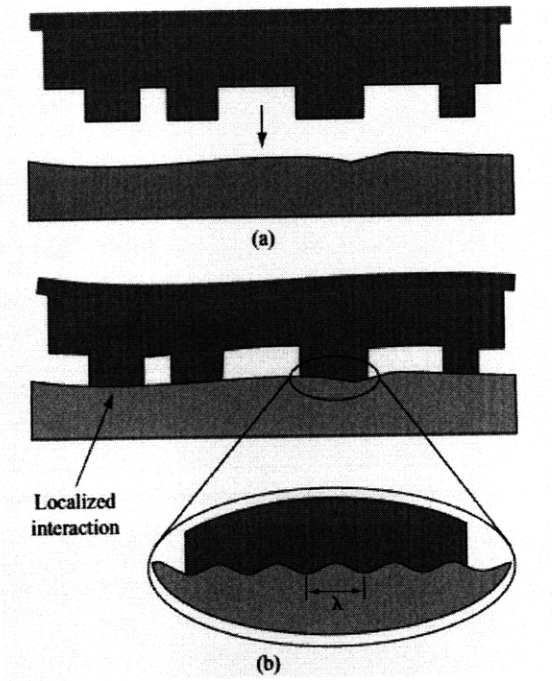

Figure 2-3: Macroscopic and microscopic adaptation to the substrate [2].

2.2.3.2 Stamp elasticity

Young's Modulus for the stamp in μCP is one of the key determinants of conformal contact. It also has a large effect on dimensions of small features; harder stamps are required for smaller feature sizes. It is primarily determined by the mixing ratio of the prepolymer and curing agent, as well as the curing time and temperature during preparation.

Three characteristics of the elasticity are required for good patterning: 1) A low and defined modulus, as well as high toughness, is required to avoid local overload and defects from brittle failure; 2) a rubber-elastic behavior allow recovery from significant strain; and 3) a low work of adhesion to ease separation of the stamp from the substrate at low force [2].

2.2.3.3 Contact Time

Thickness of the SAM layer is largely determined by the contact time of the stamp and substrate. Effects on print width and yield are also influenced by the printing

time (Figure 2-4), both being negatively correlated. Contact times of 1ms have been shown to be feasible [8], but times in the tens of millisecond range are more common. Vapor transport tends to cause undesired results in the pattern for contact times greater than 30 seconds.

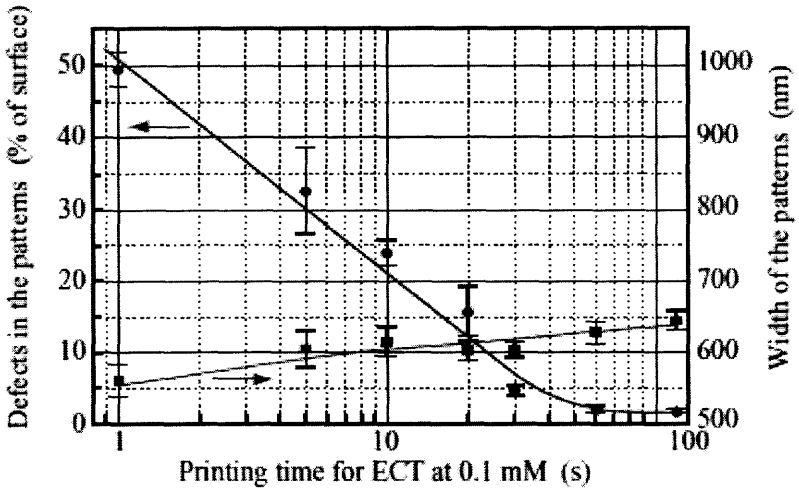

Figure 2-4: effect of contact time on width and yield [2].

An interesting point is that it is not the diffusion of the ink that sets a minimum limit to the formation of a sturdy SAM, but it is the establishment of a conformal contact that limits it (Figure 2-5). Hence in a continuous printing paradigm, where conformal contact is continuously taking place; it is possible to print even faster [8].

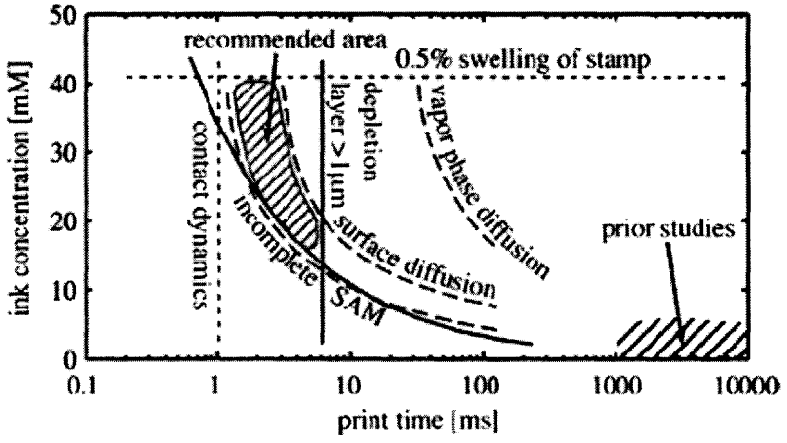

Figure 2-5: Process window for high speed µCP from recent literature [8]

2.2.3.4 Print pressure

Some amount of pressure is required to initiate and establish conformal contact between the stamp and substrate. However, higher pressures may cause the roof of the stamp to collapse and come in contact with the substrate, printing in areas which are undesirable. The pressure is concentrated locally based on the inverse of the fill factor (percentage of area of printed pattern). Figure 2-6 shows the pressures required to initiate collapse as a function of the fill factor. It shows that the pressure for onset of collapse is dependant on the fill factor of the stamp and increases with it. Further for the same fill factor, stamps which have posts of larger diameter tend to collapse at lower pressures.

The aspect ratio of the features also has an effect on the stamp's stability. Features with low aspect ratios of less than 0.2 may sag while features with high aspect ratios, greater than 2, show a tendency to bunch or sag [18].

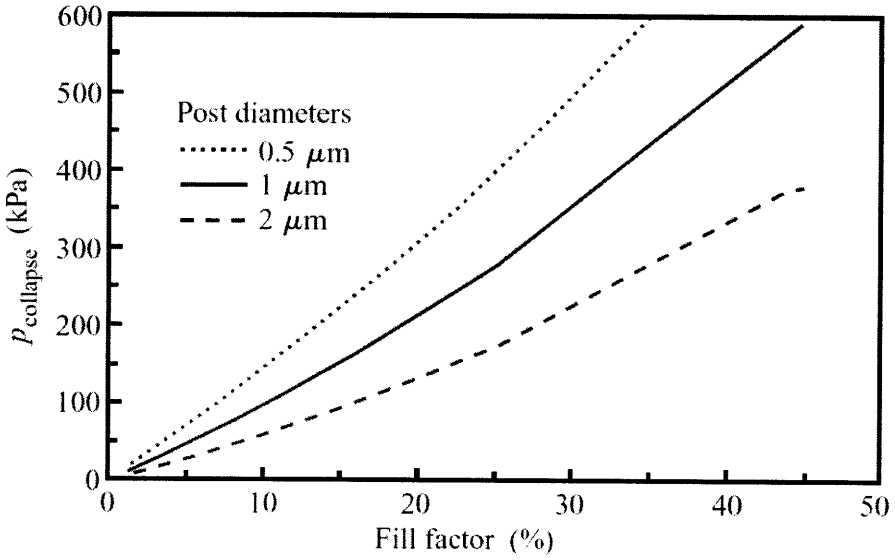

Figure 2-6: Pressure required for onset of collapse as a function of the fill factor [19]

2.2.3.5 Ink Type and Concentration

Use of alkanethiols with increasing molecular weights, decreases the surface and vapor phase transport during printing and consequently results in more precise di-

mensions. However, extremely long thiols have limited solubility and tend to crystallize on the surface of the stamp [2]. Figure 2-7 shows that the print made with higher molecular weight inks have better contrast.

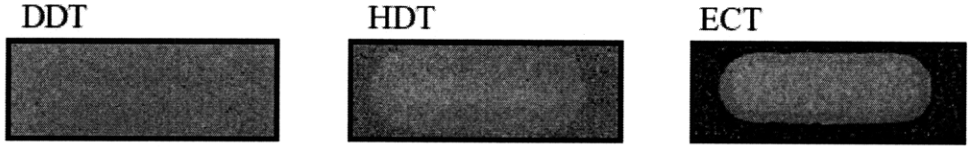

Figure 2-7: Inks of different molecular weights result in better contrast [2]

The concentration of ink has an effect similar to the duration of print. Extremely high concentrations of the ink lead to larger dimensions due to diffusion of the ink molecules. However, as can be seen in Figure 2-8, the SAM is not sturdy enough with low concentrations and there are a large number of defects. Another noteworthy fact is that the stamp swells at high ink concentrations leading to poor quality.

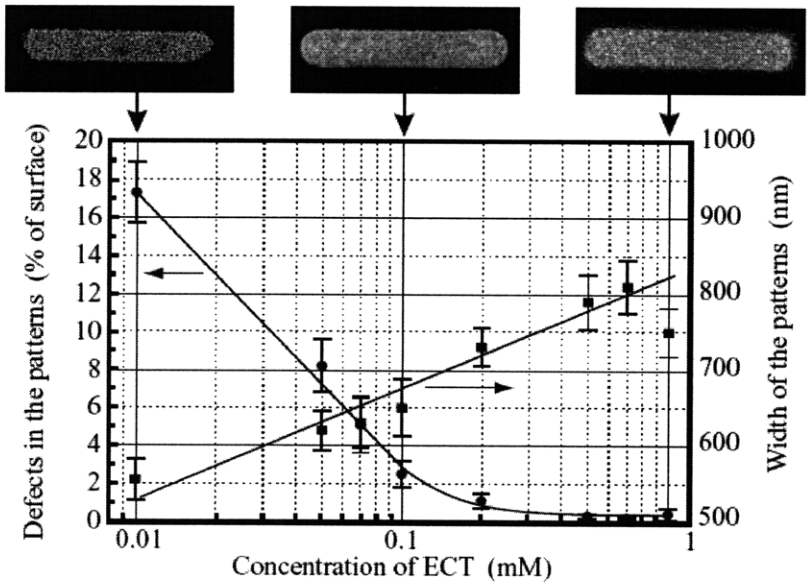

Figure 2-8: Contrast Optimization as a function of Ink Concentration [2]

2.2.3.6 Inking method

Three primary methods for inking stamps are commonly used, as well as a host of variants. Immersive inking, or direct inking, is accomplished by dipping all or part the stamp in a tray of ink. Variants include spray inking or vapor phase inking. Res-

ervoir inking (also known as pen-inking), is done by placing the ink on the un-patterned side of the stamp and allowing it to absorb and travel through the stamp. This method too impregnates the complete surface with ink molecules. However, in contrast to wet type inking, it is possible to maintain the concentration of ink in the stamp over time and subsequent prints. Contact inking is similar to a stamp pad used for traditional patterning; a piece of PDMS is immersed in ink until fully absorbed. The pad is then used to transfer thiols to the stamp. The advantage of this technique is that during printing, there will be no diffusion from the side walls of features because the ink is present only where it is required. Secondly, the stamp will swell by a smaller percentage as well [2].

A higher per area amount of ink is available for smaller features with lower fill factors, as can be seen in Figure 2-9. This results in a non uniform distribution of ink at the stamp-substrate interface. This situation of pattern-dependant ink delivery is worsened when the stamp is re-used without inking for several consecutive prints, as is the case in continuous printing. Standardized printing conditions can be ensured by continuous re-inking and/or having long waiting times to establish equilibrium. However, high speed printing has the advantage that the depletion layer is limited to only the features [8].

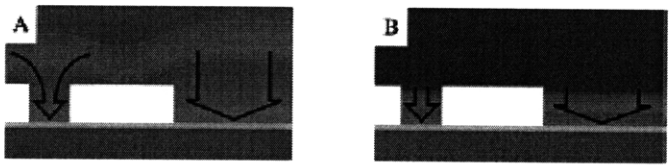

Figure 2-9: Depletion layer in stamps after printing A) at low speeds and B) at high speeds [8]

Chapter 3

Traditional Printing Techniques

This chapter details the techniques and tools used in traditional printing techniques, namely Gravure and Flexography. A comparison of these techniques and μCP is then presented.

3.1 Traditional Methods: Gravure and Flexography

Gravure and flexography are two of the most common methods of large-scale printing used today. They are very similar in method, but differ mainly in the type of stamp, applications, setup costs, and quality.

Flexography is commonly used to print corrugated containers, folding cartons, sacks, plastic bags, milk and beverage cartons, disposable cups and containers, labels, adhesive tapes, envelopes, newspapers, and various applications in electronics. The process uses a stamp with raised surfaces to print on the substrate. [17]

Gravure is typically used on packaging, labels, electronics (RFID tags, sensors, etc.), and magazines. This is the preferred method for printing on flat materials. The stamp used in gravure is a negative of the print pattern and consists of many tiny cells. Gra-

vure is typically more repeatable than flexography and more suited for long production runs due to higher setup costs. [5]

Both can be divided into three sub-processes: prepress, press, and postpress.

3.1.4 Prepress, Flexography

The prepress step involves the manufacture of the relief stamp (Figure 3-1). Typical materials for flexography include rubber and photopolymers. Stamps can be made via laser etching and photolithography. Minimum feature size is on the order of 50-75 μm with registration repeatability of around 200 μm or better. Costs vary considerably depending on size, complexity of the pattern, and process used. Typically costs are approximately $100-150 for a 16"x18" plate of average complexity plus other costs such as backing materials, mounting materials, and labor for installation of the stamp onto the machine. [17]

Figure 3-1: A close-up of a relief stamp used in flexographic printing [17]

Typical waste outputs in flexography during plate manufacture include: Film, paper, developer, fixer, cleaning solutions, scrap plates and materials, plate-processing solvent, and water. [4]

3.1.5 Prepress, Gravure

Stamps for gravure are typically made of copper. The features are comprised of a series of cells made by laser drilling (Figure 3-2). Minimum feature size is 75 μm with registration repeatability of 20 μm or better. Because the cell depth can be controlled, gravure printing has the added benefit of being able to print variable film thickness. For gravure, costs scale with size, rather than complexity, as the features are comprised of cells. Costs for a stamp are higher than flexo, typically costing around several thousand dollars per plate, making this process more suitable for long runs, where the stamp costs can be amortized across the entire run. [5]

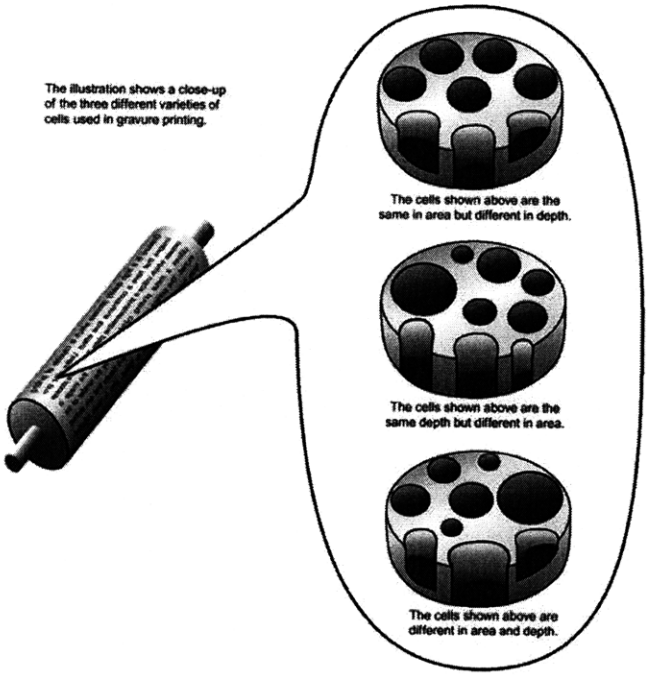

Figure 3-2: A blown-up view of the cells in a gravure printing cylinder [5]

Waste outputs during gravure plate manufacturing include: Waste from laser etching, cleaning solvents, and water.

3.1.6 Press

This step involves the actual printing of the substrate. Costs are typically driven by large capital costs for equipment, variable costs for materials (ink and printing material), and labor costs for setup and operation. Machine prices vary considerably de-

pending on speed, size capability, color capability, and used vs. new. Larger, full-featured machines (5' and up width, 6-color, fast) typically are $1 million and up. Smaller machines with limited features and speeds typically cost around $100,000.

Gravure can typically produce better quality than flexography; both having a minimum feature size of approximately 50 μm, however gravure has better registration accuracy and is the preferred method for high quality printing applications such as magazines. It is well suited for printing high quality metallic and fluorescent inks. Gravure is also used for microelectronics; 50 μm conductors of Ag, Au, and Pt are common. It also excels in printing lightweight films at high speeds with tight registration control [5]. Roof collapse can occur in flexography due to feature geometry [17]. In gravure printing however, roof collapse is not an issue because the stamp consists of cells in a metallic plate. Printing plates and inks are the greatest factors in achieving high quality prints.

Both Gravure and flexo allow for a variety of materials, from plastic films to laminates, however each excels at certain materials. Depending on the machine, widths from very narrow up to 10' are possible. Color also depends on machine configuration. Some machines also have the flexibility to be retrofitted with additional printing processes or post-processes such as drying, cutting, creasing, etc.

The printing station on a typical machine is comprised of a plate cylinder, anilox metering cylinder (flexo only), and ink pan; illustrated in Figure 3-3. Gravure uses a third roller called a fountain roller or a "doctor blade" (for improving ink distribution).

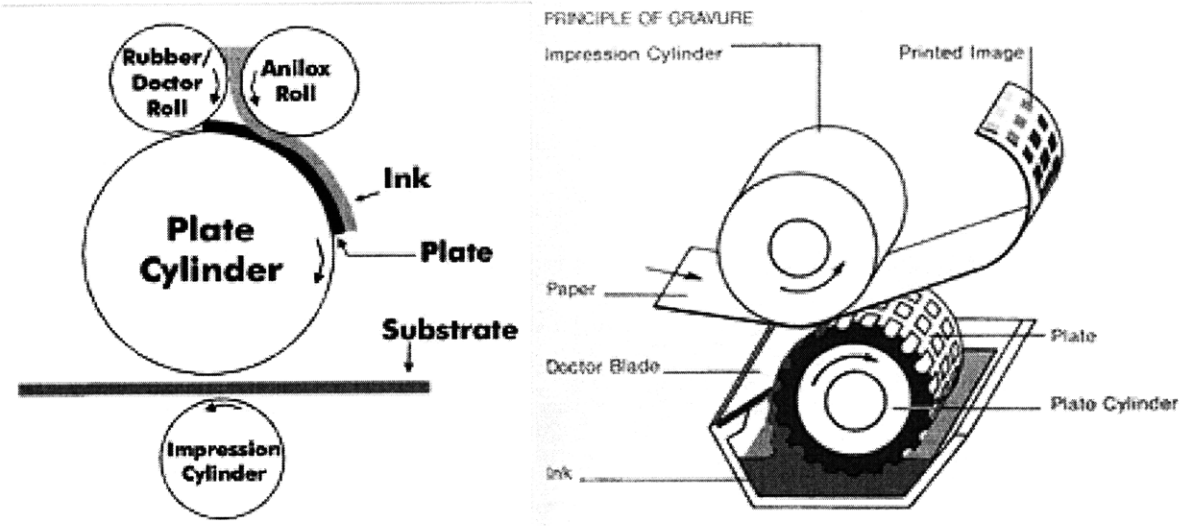

Figure 3-3: Roller setup for flexography (left) [17] and gravure (right) [5]

Speeds vary considerably. Lower end machines advertise rates of 150-300 feet per minute (FPM), while 1000-2000 FPM or more is common on higher end machines. There are a variety of different configurations; following is an explanation of the most common:

- Stack
    - Vertical stacks with separate printing stations
    - Easy to interface other equipment like cutters, creasers, etc.
    - Poor registration
- Central impression cylinder (CIC)
    - Single central impression cylinder surrounded color printing stations
    - Precise registration, good color impressions
- In-line
    - Similar to stacked printing press, but horizontal
    - Same problems and advantages as stack machine
- Newspaper unit
    - Multiple printing stations arranged back to back to allow printing both sides at once in one pass

- Dedicated 4-, 5-, or 6-color commercial flexo press
    - Typically uses two 4-color units back to back
    - Infrared driers
    - Compact, high speed, wide web printing possible

Waste outputs during printing are similar for both gravure and flexo and include: Ink, wasted paper, old/outdated plates, solvents, and water [4].

3.2 A Comparison with Microcontact Printing

3.2.7 Prepress, μCP

Masters costs about $100 when prepared in the lab including the silicon. However, one master can be used to produce many stamps, and each stamp can be used about 100 times. PDMS used to prepare the stamp is also inexpensive (~$75/kg.). High quality HDT (>99% purity) costs $200/g but the technical grade HDT costs only $10/g. Microcontact printing is still in its experimental lab stage, however, if utilized in large volume for mass-production these prices have nowhere to go but down.

3.2.8 Press

A variety of methods have been developed for the press operation in microcontact printing. Machine costs vary greatly as the technology is in its infancy and most machines are one-off laboratory devices.

Quality is a major issue that is being evaluated and optimized by many companies and universities. Minimum feature sizes achievable have been found to be about 5 μm. While the densities of defects in patterns of inks of alkanethiols formed by μCP have been evaluated, the errors in registration of patterns produced by μCP have not been determined. There are three primary sources of inaccuracies in μCP: i) in positioning the elastomeric element relative to the substrate, ii) intrinsic distortions of the element

introduced during its fabrication, and iii) distortions caused by elastic deformation of the element when it is brought into contact with the substrate [2].

It has been demonstrated that when thin 0.1 mm elastomeric elements are cast against a rigid backplane and the lithography is controlled with translation stages, absolute distortions are 500 nm over square areas 1 cm2. When the lithography is performed by hand, relative distortions of pairs of patterns can be as small as 500 nm over 0.25 cm2 if stiff, thick stamps are used. The distortions in both of these cases are comparable to the limit of sensitivity of the measurements. [7]

At present, μCP is limited to thiols on metals such as Ag, Au and Cu. However, developments are being made in printing of alkylsiloxanes on silicon dioxide and glass, as well as copper and polypyrole on fluoropolymers. Other inks and substrates are also being developed.

The feasibility of continuous Micro-contact printing has already been demonstrated by a group at MIT. They demonstrated acceptable results up to 100 FPM [16]. Once developed this technology may be able to give good quality prints at much higher speeds.

Waste outputs in μCP include: chemicals used in photolithography for master manufacture, PDMS waste, thiol inks, etchants, water, etc.

Table 3-1 offers a side-by-side comparison of the three processes discussed in this chapter.

Table 3-1: A side-by-side comparison of the three printing techniques detailed in this chapter.

	Gravure	Flexography	Micro-contact Printing
Cost			
Setup-costs	High	Lower than gravure	Existing Flexography machines can be modified. Still in experimental stages
Stamp Costs	Scales linearly with sizes	Increases with complexity and size	If applied to mass production, the cost of the master can be amortized over many stamps making them cost effective.
Production			
Production Rate	Typically ~500 m/min	Similar to gravure	Rates of 30.5 m/min have been demonstrated. However, it is possible to achieve higher rates.
Runs	Preferred for long runs	Used mainly for medium to long runs.	Continuous micro-contact printing is being developed which can be used for long runs.
Quality			
Layer Thickness	< 0.1-8 μm. Can give prints with variable film thickness.	0.04-2.5 μm. Constant film thickness.	Single monolayer thickness
Minimum Feature Size	75 μm	80 μm	Feature sizes as small as 5 μm are possible.
Registration	> 20	< 200	?
Flexibility			
	Variety of inks and substrates are possible.		Mainly for printing thiols on Au, Ag and Cu. Alkylsiloxanes on glass; of copper and polypyrrole on fluoropolymers has also been demonstrated.
Health & Environmental Impacts			
	Variety of waste outputs including chemicals for stamp production, inks, paper, etc.		Alkanethiols and dialkyl sulfides are irritants and have a strong odor. Health rating:2 Most etchants used are toxic

Chapter 4

Basic Principles of Web Handling

Web handling is a general term referring to the art and science of moving a web, i.e. a length of sheet or film, through a machine, typically at a fast rate, with minimal wastage. The handling of a web is considered a separate entity from that of converting or manufacturing. Web converting entails those activities which change the properties of the web such as printing, coating, laminating, etc. Web manufacturing typically refers to forming the web and includes such activities as extrusion, paper making, etc. The purpose of web handling is rather to *preserve* the properties of the web.

This chapter will cover the basic principles of web handling in typical roll-to-roll applications including roller design, web tension, nip interfaces, winding methods, and web guidance. The subject is vast and applied across many industries, from newspaper printing to electronics manufacturers to packaging companies and more. A great deal of research and knowledge is available to anyone concerned with this topic. This is by no means a comprehensive collection of web handling information; rather it covers the areas we found most useful to the design of our printing machine.

4.1 Rollers

Essentially, web handling is composed of rollers and the span of material between these rollers; they constitute the foundation of all web handling, converting, and

manufacturing. Rollers control many aspects of a machine's performance as well as many quality factors in the web: they change the tension, change the path, cause wrinkles and other defects, are a source of heat, and are oftentimes the foundation for converting processes (calendaring, coating, laminating, printing, etc.).

They are several key areas of interest in roller design and application. Following are the basic laws and rules-of-thumb.

4.1.9 Number of Rollers and Mounting Considerations

Deciding on the number of rollers in a machine is often a subjective matter. It is typically prudent to minimize the number of rollers; they cost money, take up space, increase maintenance responsibilities, make threading the web more difficult, can induce web defects like wrinkling or denting, and can increase tension due to bearing drag or inertia.

One key factor in deciding the number of rollers has to do with the unsupported span of material in between rollers. The optimum span is largely dependent on the width and thickness of the web. If it is too short, web alignment can be over-sensitive (see details of the Normal Entry Law in the following section), and if it is too long the web will tend to sag, flutter, or vibrate, causing interference with tensioning and/or guidance systems. At worst, these conditions can also lead to wrinkling and other defects. [22]

There are two general configurations for roller mounting, and several variants thereof. A live shaft consists of a roller with fixed ends that ride on a bearing fixed to the machine foundation. They are most often used where a drive motor must be attached. A dead shaft has bearings fixed to the roller itself and the shaft is mounted rigidly to the machine foundation. The shaft can be supported at each end, supported only at one end (cantilevered), or supported at several places along its width (for especially wide webs). Cantilever rolls are considered a more risky option and should only be used for narrow webs; typically less than 18". They must be designed with especially stout/precise bearing supports to resist excessive deflection. [23]

4.1.10 Alignment, Deflection, and Roundness

There are three key measurements of roller quality that affect the creation of a high quality, "flat" web. Rollers should be aligned, not bend excessively under normal machine conditions, and the diameter should not vary greatly [24].

Alignment is critical to minimize problems with web tracking, web contraction, and wrinkling. Out-of-plane alignment errors, when the centerlines of rollers are not parallel, are considered the most serious. According to the Normal Entry Law, a web enters a tracking roller at a right angle (see Figure 4-1). Therefore, a misaligned roller will steer a web in traction according to this law [23]. It is generally accepted that alignment on larger machines cannot be done with simple shop tools and must be aligned via optical or laser transit if accurate results are desired.

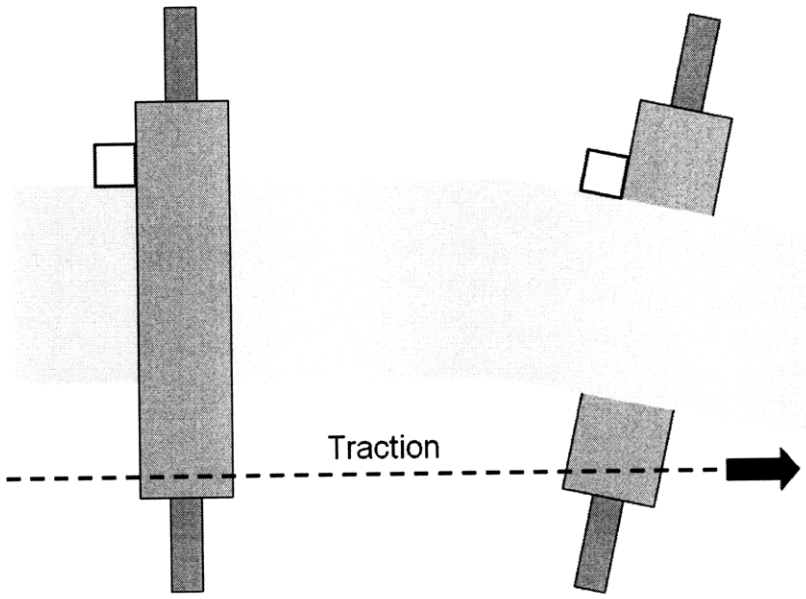

Figure 4-1: The web enters each roller at a right angle according to the Normal Entry Law [22]

Deflection is caused by external forces, namely tension, nip loads, and gravity. A general rule-of-thumb for deflection used by machine builders is to design rollers such that under the effects of gravity, nip load, and/or tension load, the roller should not deflect more than .00015 per inch of width. This is considered best practice to minimize the effects mentioned above [23].

Roundness (as well as balance, which is related) is the last key factors in roller performance. Out of round or unbalanced rollers cause tension variations, machine/web vibration, excessive nip loads, web wandering, bearing wear, noise, etc. Rollers should be designed and manufactured to minimize diameter variation and eccentricity [22]. Diameter variation is easy to check with a micrometer by measuring the roller at several places and noting the measurements. Runout can be done dynamically with a dial indicator to determine the Total Indicator Runout (TIR).

4.1.11 Substrate and Roller Interactions

The interaction between substrate and rollers is one of the key issues in web handling. Consideration for such factors as traction, slip and float are crucial for optimum machine performance.

4.1.11.1 Traction and Slip

Traction is the friction force that a roller can exert on a web. Without adequate traction, the web will tend to slip over the roller, and the machine will not be able to control its behavior. Traction is a function of wrap angle, web tension, and the friction coefficient of the roller and web (See Figure 4-2). If a web begins to slip on a roller, it is generally a sign that traction needs to be increased. This can be done by increasing tension, applying a high-friction surface coating to the roller, adding annular grooves, or by increasing the wrap angle [22].

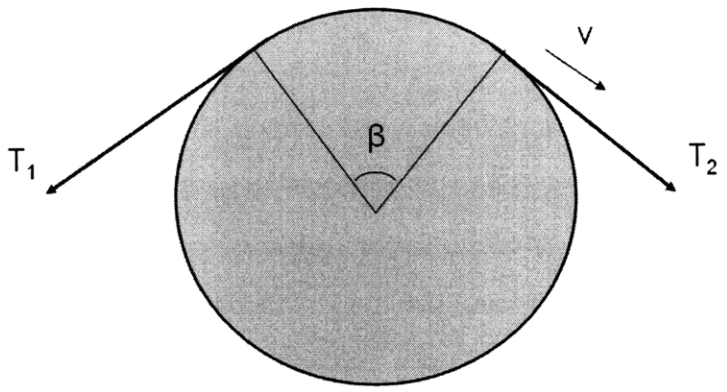

Figure 4-2: A schematic of wrap angle and tension of substrate on a roller

Increasing tension may not be the best option as the web may not respond well to the additional strain. Surface coatings tend to be less than ideal as they require additional costs both initially and for maintenance. Grooving only has an effect at low speeds. Increasing the wrap angle however, has no ill effects on the web or machine and provides a large increase in available traction [22]. According to belt friction theory, the opposing tension increases exponentially with contact angle (equation 4.1). This equation can then be reconfigured to calculate the minimum wrap angle to avoid slip (equation 4.2). The traction zone approaches its maximum as this ratio approaches 1.

$$T_2 = T_1 * e^{\beta\mu} \tag{4.1}$$

$$T_2 / T_1 < e^{\beta\mu} \tag{4.2}$$

4.1.11.2 Float

Web floatation is caused by the shear force between the substrate and the air. The effect tends to happen at faster line speeds in excess of 100 FPM and must be considered in high speed machinery. It effects tend to be especially noticeable with speeds in excess of 1000 FPM. Air entrapment is a function of roller radius, roller speed, substrate speed, tension, and kinematic viscosity by the relationship in Equation 4.3. [22]

$$H = .643r[6\,\mu(V_r + V_w)/T]^{2/3} \tag{4.3}$$

Where,

H = air film height

r = radius of roller

μ = kinematic viscosity

V_r = roller speed

V_w = web speed

T = tension

4.2 Web Tension

In web handling, tension is defined as the average machine direction (MD) web force expressed in force per unit web width (in the English system it is expressed as pounds per inch or PLI for short). Maintaining control over tension in web handling is essential for several reasons: to minimize bagginess and curl; maintain length, width, and thickness; maintain web path and registration; achieve good roll quality; avoid web breakage and/or wrinkling [22]. Web tension is affected by a variety of noise sources such as roller eccentricity, motor speed accuracy, substrate quality, roller drag caused by bearing friction, and others [23]. Therefore, it is imperative in web handling that tension is monitored and controlled in some way.

4.2.12 Tension Zones

Machines are typically broken up into tension "zones" (Figure 4-3). A tension zone is defined as the section of web between any two tensioning elements (typically motors, clutches, or brakes). One element in the system must act to control speed rather than tension. All other elements will control a tension zone either upstream or downstream from the master speed reference. The number of tension zones required in a given machine is a difficult question; too few will inhibit process optimization, while too

many will result in unnecessary cost and complexity. Steps to evaluate the number required include: evaluating process steps for tension sensitivity and group compatible processes; determining the driven elements; determining components such as undriven rollers that may affect tension by drag [13].

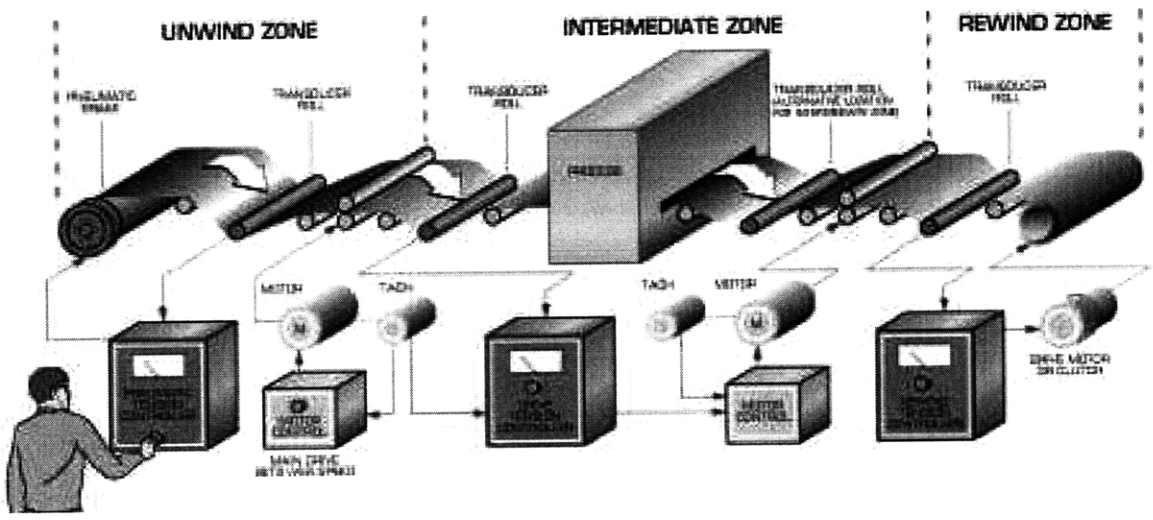

Figure 4-3: An example of a machine broken down into three tension zones [11]

4.2.13 Methods of Controlling Tension

There are three primary methods of setting tension. These are by no means the only ways of achieving tension, however they are the most basic and useful models. There are many hybrid solutions as well as advanced methods of controlling tension beyond the scope of this paper. Table 4-1 provides a description of each.

Table 4-1: an explanation of the basic tension control paradigms.

Type	*Best suited for*	*Description*
Load-cell/Brake	• Applications where tension is high enough to be measured with a load cell. • Control within 10% of the setpoint is required.	• Load cell measures the tension in the zone of concern and feeds back to the controller. • Controller compares value to the setpoint and adjusts the output torque of the unwind brake (typically pneumatic or magnetic particle) or intermediate driven roller.
Dancer	• Applications where tension does not need to be maintained within a narrow band • Tension errors around 50% are not uncommon.	• Idler roller mounted on a stage or pivot and counterbalanced by an adjustable air cylinder. • The position is detected by a potentiometer or encoder and fed back to the controller to adjust unwind torque. • Setpoint is not displayed as engineering units.
Draw	• Stretchy, extensible materials. • Tight speed tolerance req'd for inextensible materials • Applications where tension or strain is known.	• Tension is achieved by driving an upstream roller faster than a downstream roller. • Strain increases proportionally as the web passes over the downstream roller.

4.2.14 Load Cells

Load cells are the preferred method of measuring and controlling tension because their output can be converted directly into engineering units by calibration. In web handling, the load cell typically consists of an idler roll supported on one (cantilevered roller) or both ends by a bendable element with a strain gage that changes resistance as it is flexed [23]. The output can be calibrated to read out the normal force applied by the web by: 1) zeroing out the load cell amplifier with no load to offset the weight of the idler roll (analogous to hitting 'tare' on a scale); and 2) running a string through the web path and hanging a weight of known value and adjusting the output value (typically 0-10V or 0-20 mA) to correlate to this value. Because the normal force is determined by the orientation of the load cell and the wrap angle of the sub-

strate, vector mathematics must be used to determine the force seen by the sensor. The net force can be calculated using the following formula [11]:

$$N = \frac{4T\sin(B/2) - W\cos(A)}{2} \tag{4.4}$$

Where:

T = Tension,

N = Net Force,

B = Substrate wrap angle,

A = angle of normal force LOA from vertical

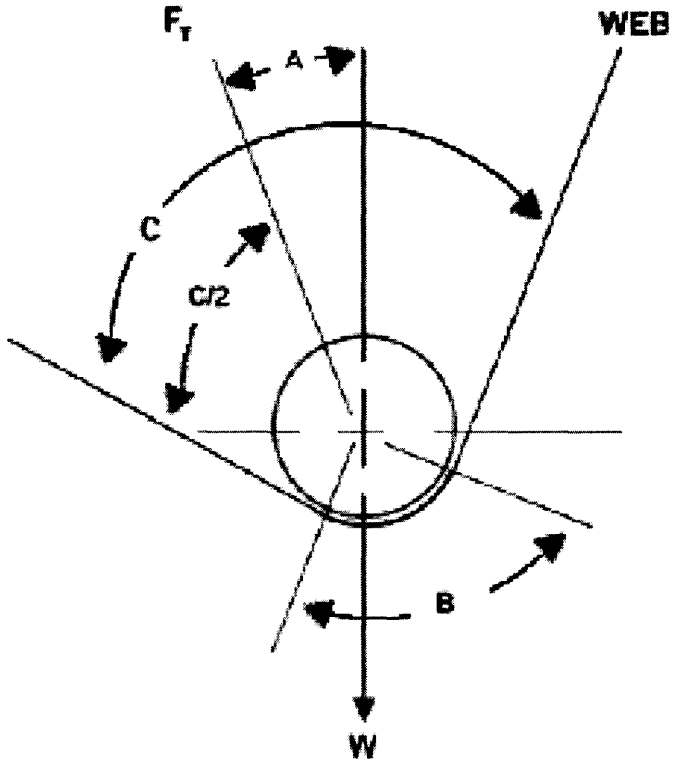

Figure 4-4: The critical dimensions for determining net force [11].

4.3 Nips

In terms of web handling, a nip is simply defined as a pinching force between two rollers. Nips are typically used to isolate tension zones, control wound-in tension in winders, apply pressure for printing, and a variety of other applications.

4.3.15 Hertzian contact

Nip stresses were first studied and modeled by Hertz in 1882 in response to spalling failure of railroad wheels. Hertz design equations for two parallel, elastic, isotropic cylinders can be used to calculate peak stresses, however it is not general enough to be applied to most web handling applications due to friction, anisotropic qualities, and the use of covers [23]. However, the model is useful for illustrating key concepts.

Additional work has been done in the study of nip interfaces. For example, G.J. Parish developed a number of equations to model the behavior of rubber covered rollers [26]. Although of interest to theorists, the application of these equations by themselves does not give a great deal of insight for the machine designer looking to expand his intuition. Instead, there are many empirical methods that provide sufficient results. One of the most useful is that of nip impressions and flexible sensors.

4.3.16 Nip Impression

Nip impression can be done both statically and dynamically. It is a good indicator of roller alignment, pressure distribution, roller geometry compatibility, and roller wear. Static impression is typically done with carbon-paper or similar material pressed in the nip at a predetermined load. Dynamic impression is more sophisticated and typically requires the use of flexible sensors that can pass through the nip while the machine is moving. These sensors can also be used for static impression. Figure 4-5 provides some basic diagnoses from static nip impressions.

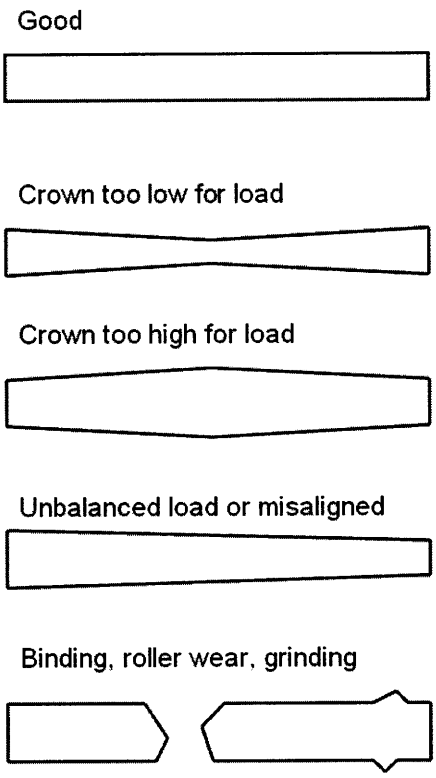

Figure 4-5: Typical shapes of nip impressions and their causes [22].

4.4 Other Topics in Web Handling

There are a plethora of other issues and considerations involved in web handling design that are beyond the scope of this paper. However, two further issues that deserve mention are winding and web guidance. Winding is a vast topic consisting of the mechanics behind winding substrates onto a spool at the last station of a roll-to-roll machine. Guidance is another important topic that refers to the maintenance of the web path while the machine is running.

4.4.17 Winding

Winding is generally accomplished by one of three methods. The simplest, called a center-wind, drives the roll completely by the core of the roll typically using a speed controlled motor. This method has the least amount of control over wound-in tension, and can only adjust within a narrow band. The next method, the surface wind, uses a

driven metal roller (termed the lay-on roller in industry) nipped against the outer surface of the winding roller (the drum roll). Either the lay-on roller or the drum roll moves as the roll grows, typically the former on larger machinery. By maintaining the nip load via pneumatic or hydraulics and web tension, this method has a good deal of control over wound-in hardness. The last method, the center-surface winder, differs only by the drum roll being driven as well. This provides control over nip load, tension, and torque differential. This gives even more control over wound-in hardness and is typically used for applications requiring very hard or very loose winds. [23]

4.4.18 Guiding

Web guidance is the act of centering and maintaining alignment of the web and rollers. It is especially important for registration, traction, and the reduction of defects such as wrinkling. It is accomplished either passively or actively.

In passive guidance systems, the rollers typically have geometry that either steers the web or prohibits it from wandering. Concave rollers cause the web to slip and slide into the low spot. Convex rollers, on the other hand, apply pressure to the center of the web and guide it on the high spot. End plates on a roller can also be used to restrict the web from wandering out of a specified region; however this method can lead to edge damage [22].

Active guidance uses sensors to feedback position info to a controller that can change the web position using an actuator. Sensors vary from mechanical switches to photo-eyes. There are a variety of mechanisms to guide the web, the most common being a roller that can pivot about an axis perpendicular to its centerline. There are a variety of variants of the pivoting roller, for example, the displacement guide. This system uses four rollers, where the two middle rollers that can pivot as a unit in the plane of the web run about the middle of the upstream roller and downstream fixed rollers. This displacement guide tends to stress the web less than the pivoting roller. [23]

Chapter 5

Machine Design

In its current state, microcontact printing is limited to lab scale testing with very low production rates. In 2007, a group of MIT engineers demonstrated that microcontact printing was feasible in a roll-to-roll continuous format [16].. Their machine demonstrated the feasibility of much higher production rates than the state of the art and made observations regarding key parameters necessary for a quality end product. This project expands on the knowledge gained from this group and further applies technologies borrowed from traditional roll-to-roll processes as well as creating new tools especially tailored to microcontact printing. In order to realize this, a prototype printing machine, continuous etching machine, and additional hardware were designed and built in order to further experiment with this new technology. The design process and details of the finished hardware are laid out in this chapter.

We will attempt to provide the reader with the concept generation and selection process, as well as a reasonable amount of details regarding the components of the various systems and subsystems in the tools we built.

5.1 Design Methodology

The design phase was critical in order to deliver a robust tool and optimize the quality of the output. It also needed to demonstrate the feasibility of manufacturing in a high-production environment. On the other hand, it was critical to build it in a timely fashion at minimum cost. As these goals were at odds of one another, a design strategy was developed to maximize utility and minimize time and cost. Following are the key points used to address these issues during the design phase:

- Modularity
    - Ability to adjust parameters quickly and easily
    - Flexibility for testing and optimization
    - Subassemblies can be built and tested outside the top-level system
    - Additional modules can be added or subtracted easily
- Use of existing subsystems and controls
    - Purchase of fully designed and tested units from manufacturers is much faster than developing new subsystems. For example, there are several manufacturers of tension control systems which have been used widely in industry.
    - Decreases design time, testing, and troubleshooting.
    - Cost offset by time saved in development
    - Support is available from applications engineers at the company.
- Design by part family
    - Similar parts are faster and cheaper to produce
    - Encourages modularity

5.2 Basic specifications

It was decided early on that the roll-to-roll paradigm was most suitable for fast production rates. This method has been proven to be extremely efficient for the majority of flexible substrate processing from printed goods, film coating, foil manufacturing, and a plethora of other techniques. The target specifications were that it be able to process up to 8" wide coated substrates up to 100 FPM. More specifically, the following concepts were decided as being the most critical in the design:

1. Synchronous drive system
2. Web tension control
3. Print pressure control and feedback
4. Robust stamp interface
5. Semi-automated inking of print roller
6. Process automation

In addition to the printing apparatus, it was also necessary to develop a new tool for manufacturing large area stamps. This was a critical path as the system relies heavily on the quality of the stamp to produce the end product. The stamp had to be able to be wrapped around a 5" diameter by 10" wide cylinder with minimal unprinted region. It was to be cast on a stainless steel backing using .005" sheetmetal.

Lastly, we were tasked to build a prototype rig for continuous etching. The key characteristic of this system was a solution to the low production rates inherent in the etching process. Because the etching process requires a variety of steps (etching, rinsing, drying), it needed to be somewhat modular in nature and had to be able to deliver variable process times at each step while still being a continuous process. It was also crucial that the process not affect the printed region in a negative way, such as by abrasion or smearing.

Solidworks 3D Computer Aided Design (CAD) software was used as the primary design tool. The ability to model individual components as well as assemble them in a virtual environment is extremely powerful in a complex machine. A great deal of

other data can also be embedded in the files, such as engineering drawings and specifications, manufacturing tolerances, part numbering and revisions, vendor part numbers, Bills of Material (BOM's), etc.

5.3 Microcontact Printing Machine

Final concept selection was made after several iterations. The final design was a fusion of open loop and closed loop tension control using clutches as well as motor draw (Figure 5-1).

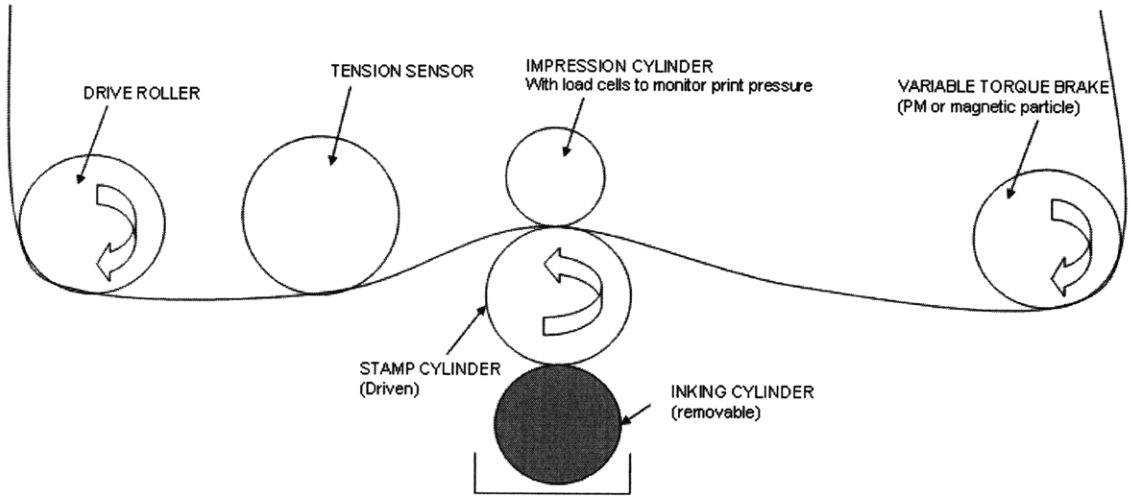

Figure 5-1: The proposed concept for the R2R μCP device

The design separates the three critical systems into modules (Figure 5-2), called the Supply Module (material handling for unwinding substrate from spool), the Print Module (inking, printing, and pressure application), and the Collect Module (material handling for rewinding substrate onto spool). Each system is discussed in the sections to follow.

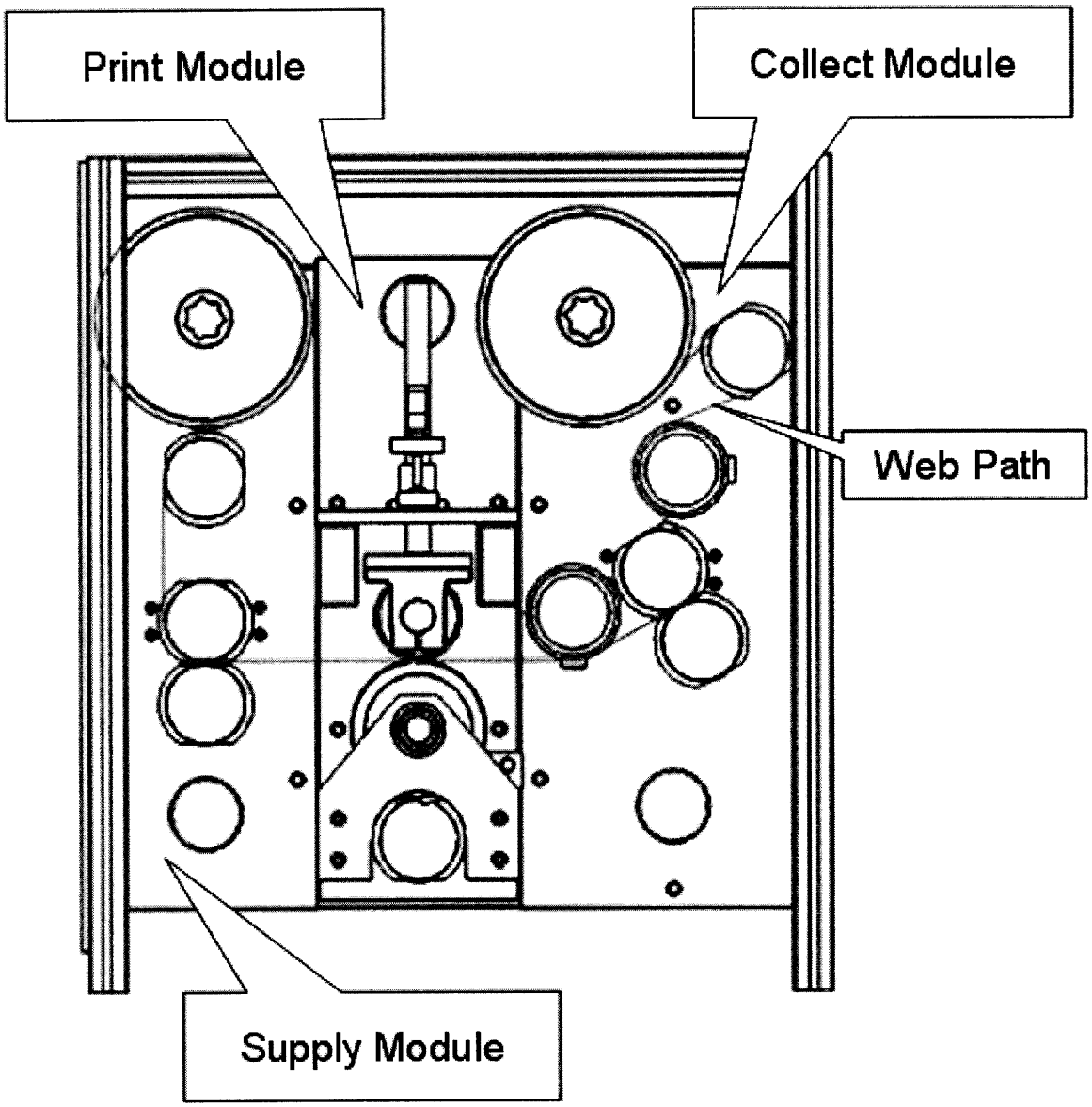

Figure 5-2: The three modules and path of the substrate.

The components of each module are mounted to a baseplate made from precision ground aluminum to ensure alignment of all components within the subassembly and with other modules. The three modules are mounted horizontally to a frame made from an extruded aluminum T-slot framing system; the material flows left to right. Cantilevered rollers allow easy access to the components. Similar components were used in each module to simplify design, assembly, part procurement, and maintenance. The control system uses a Programmable Logic Controller (PLC) to synchronize all movements, adjust parameters, and send data to a PC. Specifications for off-

the-shelf parts, engineering drawings of all custom components, as well as an overall Bill of Materials are included in Appendix A. Figure 5-3 shows the 3D model of the design with basic dimensions.

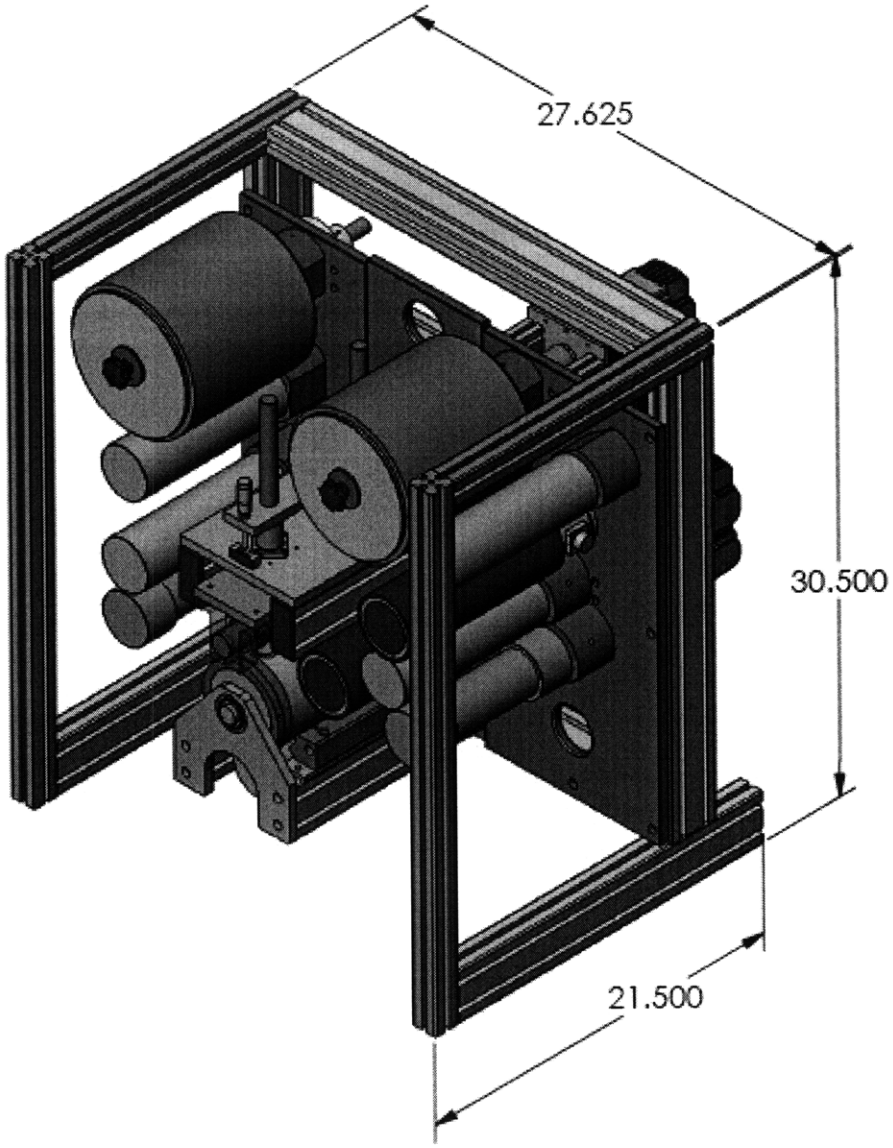

Figure 5-3: The 3D Solidworks model of the design.

5.3.19 Overview of Machine Functions

The machine uses a variety of mechanisms to achieve the primary parameters related to microcontact printing. Table 5-1explains how these are set and altered, as well as

the interactions with other settings. For further details, please see the following sections about the "Related Subassembly" listed in the table.

Table 5-1: An explanation of how each printing parameter is achieved by the settings on the machine.

Parameter	*Related Subassembly*	*Interactions*	*Description of Mechanism*
Printing Speed	Print Module	Noise (step pulse variations, EMI, motor characteristics)	Motor speeds are referenced from the printing roller speed, which is determined via a setting in the PLC program.
Web Tension	Supply Module, Collect Module	Noise (roller diameter variations, substrate defects, etc.)	Achieved via a friction clutch and a permanent magnet clutch in the first and second zone, respectively. The third and fourth zone are controlled by draw; changing the motor speeds from the reference speed (printing roller).
Wrap Angle	Print Module	Noise (roller diameter variations)	Changed by moving the print module vertically relative to the supply and collect modules.
Print Pressure	Impression Assembly	Speed, Wrap angle (only when negative), Contact width	The micrometer at the top of the assembly moves the roller vertically, compressing the roller covering. The displacement of the roller covering causes a force opposite the weight of the moving assembly. A load cell measures the force. Resultant force = mg – kx. Pressure is a function of force and contact area: P = F/A, where A = contact width * roller length
Contact Width	Stamp Roller Assembly, Impression Assembly	Print pressure, Stamp elasticity, Impression roll covering	As the impression roller is lowered, the roller covering is compressed and the contact width increases (graph of force vs. width vs. pressure)
Contact Time	Stamp Roller Assembly, Impression Assembly	Print pressure, Wrap angle, Speed	Dependent on the substrate speed, the width of the contact, and the wrap angle around the stamp (for negative wrap angles).

5.3.20 Supply module

The supply module (Figure 5-4) consists of the substrate unwinding and tension control functions. As with all the modules, the main component is a base-plate machined from Mic-6 precision ground aluminum. The flatness specification of .005" (over 4' x 8' stock) of this plate ensures that all components are well aligned, roller centerlines parallel, and other modules aligned to this assembly. There are no powered rollers in this module; all tension control and handling is done passively.

The spool of substrate is placed on the spool roll using the adapters that fit a 6" core. Tension in the first zone is maintained using a custom made friction clutch that uses a plastic pressure plate with a spring washer. A basic clutch of this nature was chosen

because the tension in this zone is not critical and did not justify the use of a hysteresis clutch, or other high-cost component. However, a permanent magnet clutch (Figure 5-5) is used in the next zone. This type of clutch uses high energy, multi-pole magnets to establish lines of magnetic force that retard the motion of the center rotating disc. They are ideal for precise torque in relatively low tension applications (.14 – 50 lbs). It is run open loop; all adjustments are made by adjusting the position of the internal magnets. The roller in this position is covered with 1/16" neoprene to provide traction and prevent slip. In addition, a nip roller is engaged tangentially that provides radial force to avoid slipping.

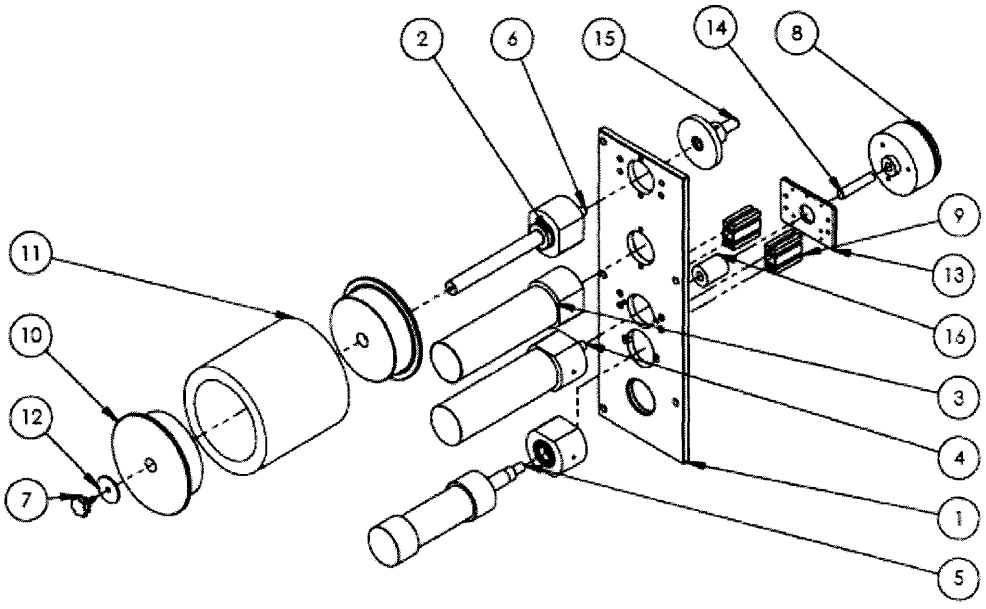

ITEM NO.	DESCRIPTION	QTY.
1	MODULE PLATE, SUPPLY	1
2	BEARING BLOCK ASSY	4
3	IDLER ROLLER	1
4	IDLER ROLLER	1
5	BONE ROLLER	1
6	SPOOL ROLLER	1
7	KNOB	1
8	PM CLUTCH	1
9	MOTOR STANDOFF	2
10	SUBSTRATE SPOOL END	2
11	SUBSTRATE	1
12	WASHER, SPOOL	1
13	MOTOR MOUNT PLATE	1
14	CLUTCH SHAFT	1
15	FRICTION CLUTCH ASSY	1
16	COUPLING	1

Figure 5-4: An exploded view of the Supply Module.

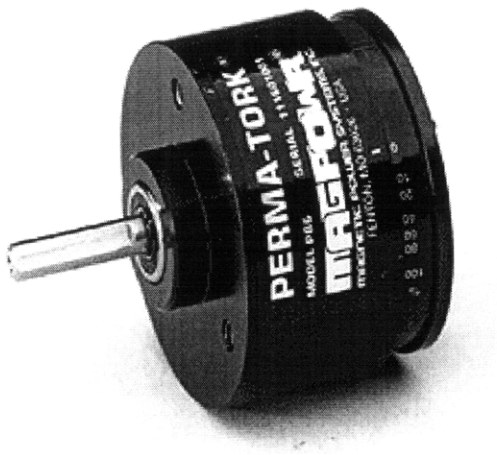

Figure 5-5: The Magpowr permanent magnet clutch used for tensioning the substrate in the tension zone before printing [13]

5.3.20.1 Bearing Block Assembly

One of the other critical subassemblies used in this module, as well as the others, is the bearing block assembly (Figure 5-6). All rollers in the machine, with the exception of the impression roller and tension sensors, ride on this assembly. It consists of a set of preloaded deep-groove Conrad bearings, spaced 2" apart by an aluminum sleeve, and mounted in an aluminum housing. Bearing preload is an important factor as it affects all aspects of bearing performance, especially stiffness. It is accomplished by forcing all the elements into contact by displacing one race axially with respect to the other. It results in greater accuracy, repeatability, and stiffness; however, at the cost of increased friction [9]. A light preload was chosen as it is a good compromise between axial stiffness and friction; it is achieved by a nut that engages two spring washers. Preloading was done primarily by feel; however I estimated the preload force to be about 5lbs based on the spring constant stated by the manufacturer and the compression from the nut. The factor of safety for the loading capacity was approximately 2.5 based on C10 load life calculations (for 5000 hrs and 1000RPM) and the dynamic load capacity stated by the bearing manufacturer. If anything, this was a conservative estimate because such high speeds were used in the calculation. Runout was

measured at several points along the printing roller; maximum runout was approximately .0015" TIR at the end farthest from the bearing block.

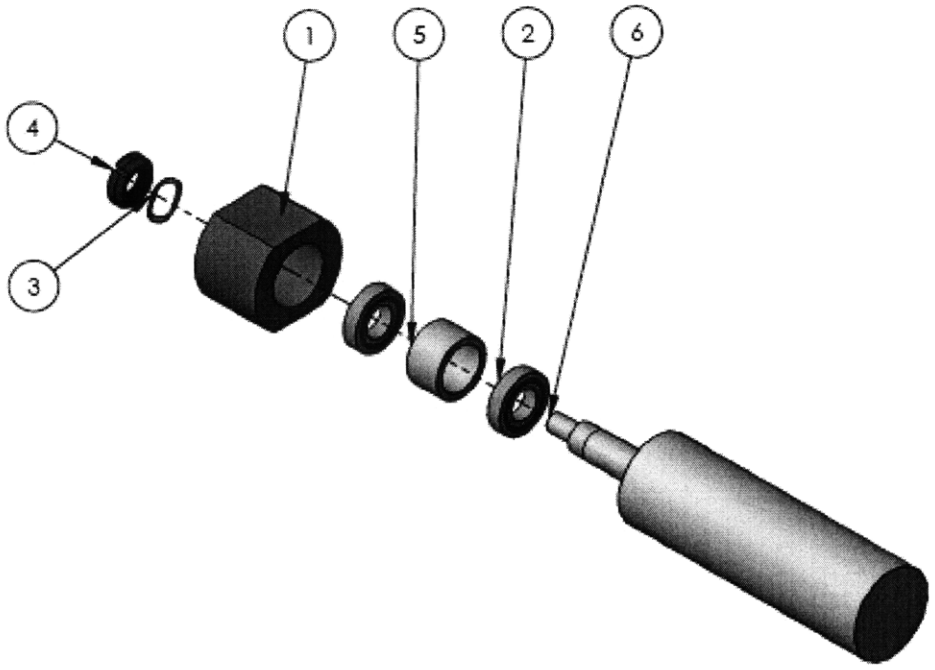

ITEM NO.	DESCRIPTION	QTY.
1	BEARING BLOCK	1
2	BALL BEARING, 1" ID 2" OD	2
3	WAVE WASHER	1
4	BEARING LOCKNUT	1
5	BEARING SPACER	1
6	IDLER ROLLER	1

Figure 5-6: An exploded view of the bearing block assembly

5.3.21 Printing module

The printing module (Figure 5-7) is the most critical assembly of this system. It encompasses all of the most important functions: stamp mounting, printing speed, printing load, substrate-stamp wrap angle, and inking. Our system consists of several subassemblies. The print roller subassembly includes the main stepper-motor-powered roller that drives the stamp against the substrate. A novel method for mounting steel backed stamps to cylinders is employed. A PDMS covered roller below the stamp roller can be lifted and engaged to ink the stamp and an air-knife used to blow nitro-

gen on the rotating cylinder. The impression roller assembly consists of a stage that the impression roller rides on. The impression roller is a foam covered roller that applies pressure to the substrate as it rides over the Stamp Roller. A pair of load cells is used to measure the force applied.

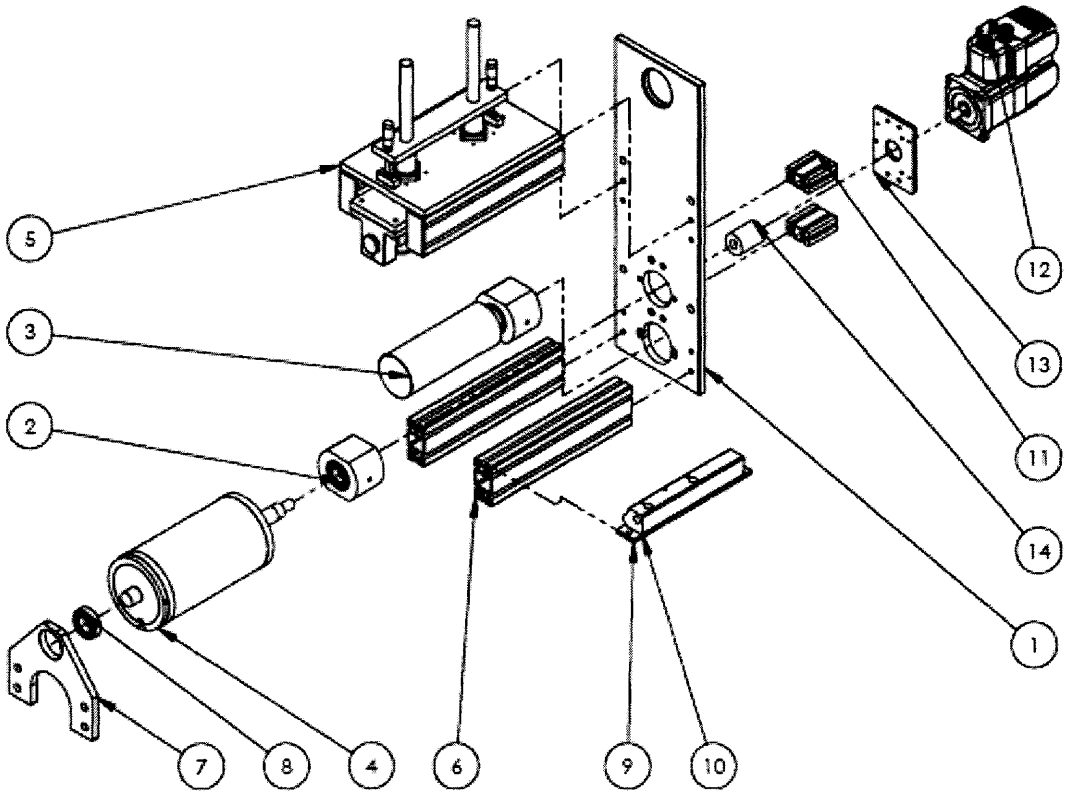

ITEM NO.	DESCRIPTION	QTY.
1	MODULE PLATE, PRINT	1
2	BEARING BLOCK ASSY	2
3	INKING ROLLER	1
4	STAMP ROLLER ASSY	1
5	IMPRESSION ROLLER ASSY	1
6	8020 STANDOFF	2
7	BEARING PLATE, PRINT	1
8	BALL BEARING, 1" ID 2" OD	1
9	AIR KNIFE MTG PLATE	1
10	AIR KNIFE	1
11	MOTOR STANDOFF	2
12	STEPPER MOTOR NEMA34	1
13	MOTOR MOUNT PLATE	1
14	COUPLING	1

Figure 5-7: An exploded view of the Printing Module. Subassemblies are detailed in the following sections.

5.3.21.1 Stamp Roller Assembly

This assembly consists of all the parts that comprise the stamp mounting and rotating components (Figure 5-8). It rides on a bearing block as well as an additional front bearing (See Figure 5-7) to minimize deflection and vibration. The accuracy and repeatability of this assembly has a huge affect on the printing quality as all the most critical processes occur at this station. Stamp mounting flatness, shaft eccentricity, vibration, and a number of other factors contribute greatly to the performance of the machine.

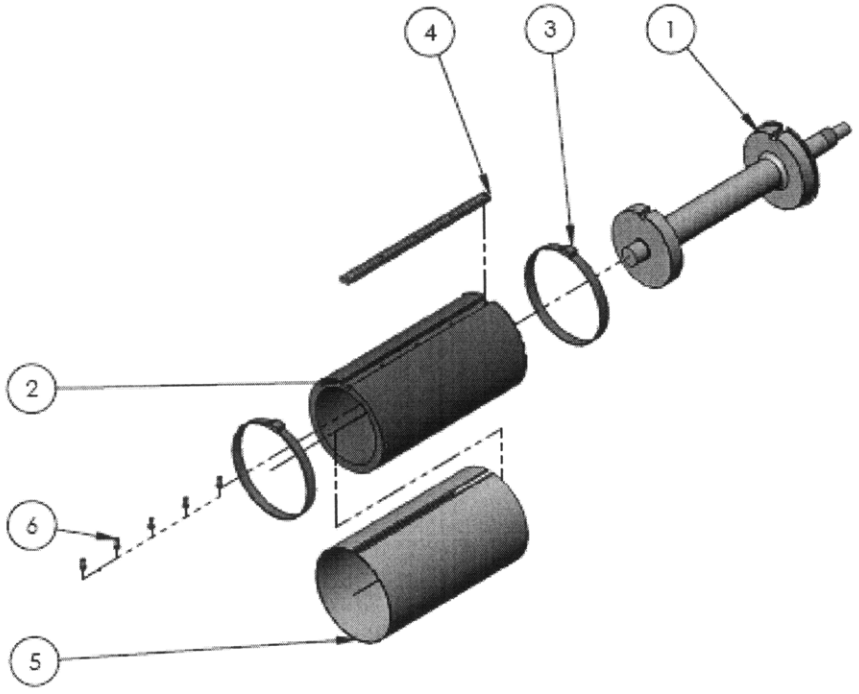

ITEM NO.	DESCRIPTION	QTY.
1	PRINT ROLLER	1
2	STAMP TUBE	1
3	HOSE CLAMP	2
4	STAMP RETAINER BAR	1
5	STEEL MOUNTED STAMP	1
6	8-32 X .375 SHCS	5

Figure 5-8: An exploded view of the Stamp Roller Assembly.

There is an inherent risk of distortion with wrapping a stamp around a cylinder. While an infinitely large diameter cylinder is the ideal solution, it is obviously not practical or possible. We chose the largest stamp cylinder that could be accommodated by the machine (while also accounting for feasibility for stamp manufacturing) to minimize the arc that the stamp must be stretched around. We planned to study the effects of this in the experimentation stage, and hypothesized that the distortion effect would be isotropic.

The stamp is mounted to the Stamp Tube and slid onto the Print Roller and secured with two bolts. This composite design makes the removal and exchange of tooling very fast, an essential characteristic for a production environment. The PDMS stamp is cast on a .005" thick 302 stainless steel backplane of dimension 9.25" x 15.35". This is then wrapped around the Stamp Tube and the ends inserted into a groove in the Retainer Bar (Figure 5-9). The groove is machined such that the ends of the steel stamp backplane enter it tangentially. The .020" left protruding from the inscribed circle of the backing is below the surface of stamp's inscribed circle (providing that a thick enough stamp is being used). Two large hose clamps are then installed to provide additional radial and axial clamping. This method does not take up a substantial area of printable space (approximately 15 degrees) and holds the stamp and backing in very close contact with the outer surface of the roller. It requires that the stamp be cast in a rectangle smaller than that of the stamp to allow clamping to the tube. The bolts that secure the Retainer Bar fit through a radial relief in the Print Roller.

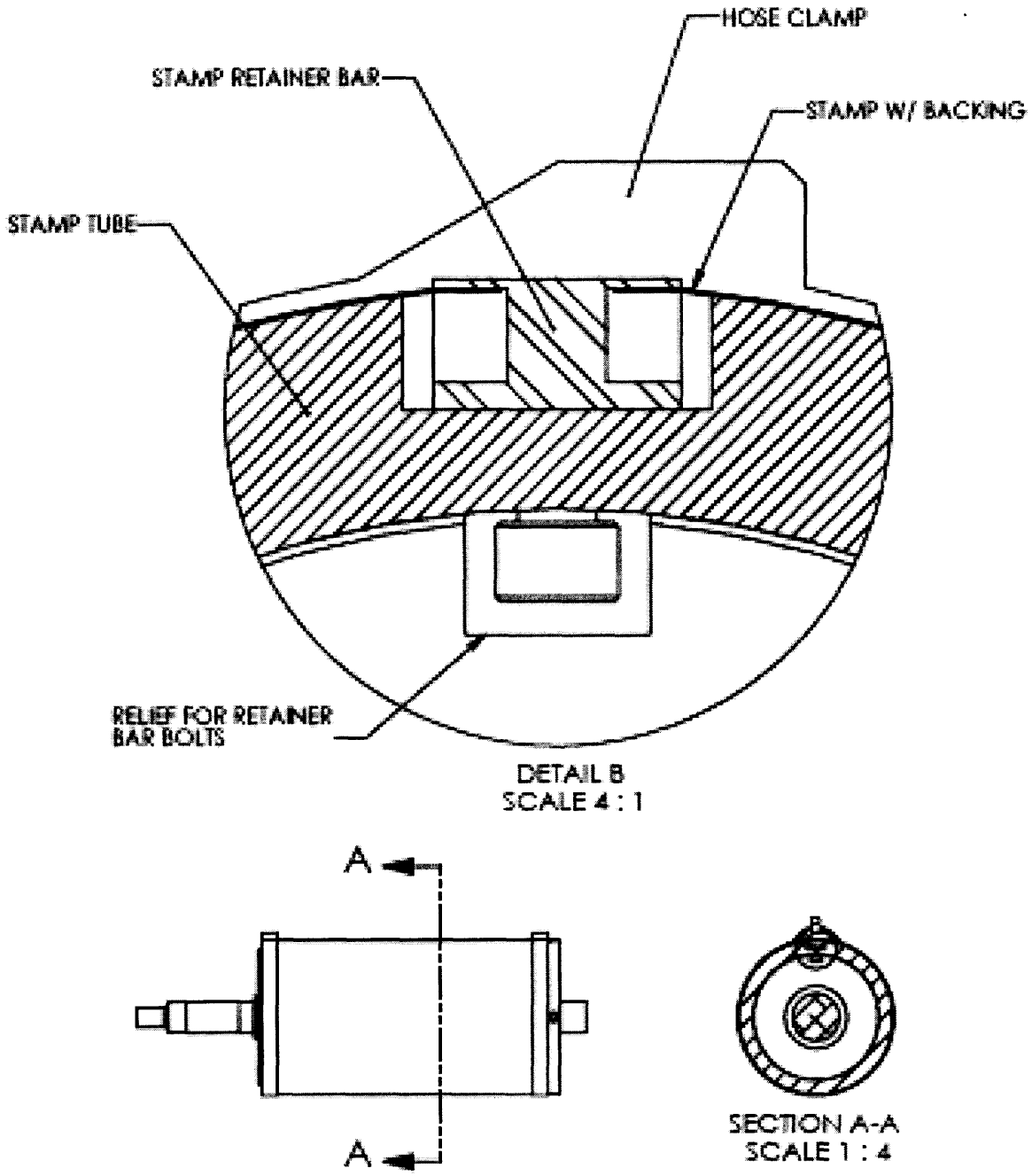

Figure 5-9: A section view of the stamp-roller interface.

5.3.21.2 Drive Motors

Stepper motors were chosen to drive all powered rollers due to their simplicity, low-cost, and ease-of-setup. Although they do not provide the most ideal smooth motion

and response, the benefit of quick and easy setup far outweighed their weaknesses. The identical motor was used on all three powered rollers. It is a NEMA 34 frame motor, with peak holding torque of 406 oz-in (Figure 5-10). These particular motors can be powered on 120VAC and only require step and direction signals from a controller; they have a built in power supply and driver. The driver is capable of 20 different microstep settings with a maximum microstep/step of 256. Torque requirements were calculated based on roller diameter and target system speed. Maximum speed is an important factor in any motor application, but is especially important in a stepper system due to the relationship between speed and torque. Step motors lose torque with increasing speed due to limitations caused by winding inductance; therefore a speed-torque curve (supplied by the manufacturer) must be consulted when selecting a motor (Figure 5-11). With a target line speed of 300 feet per minute, our maximum forecasted speed was 240 RPM for the print roller and 400 RPM for the drive roller. At this speed, the motor still has approximately 400 oz-in of torque (25 in-lbs), which is enough to tension the PET to more than 10 lbs; more than sufficient for our system.

Figure 5-10 The IMS NEMA 34 stepper motor with integrated power supply and driver was used to drive the print roller, drive roller, and collect roller. This model only required the user to attach 120VAC power and IO; both which were supplied via cables from the manufacturer.

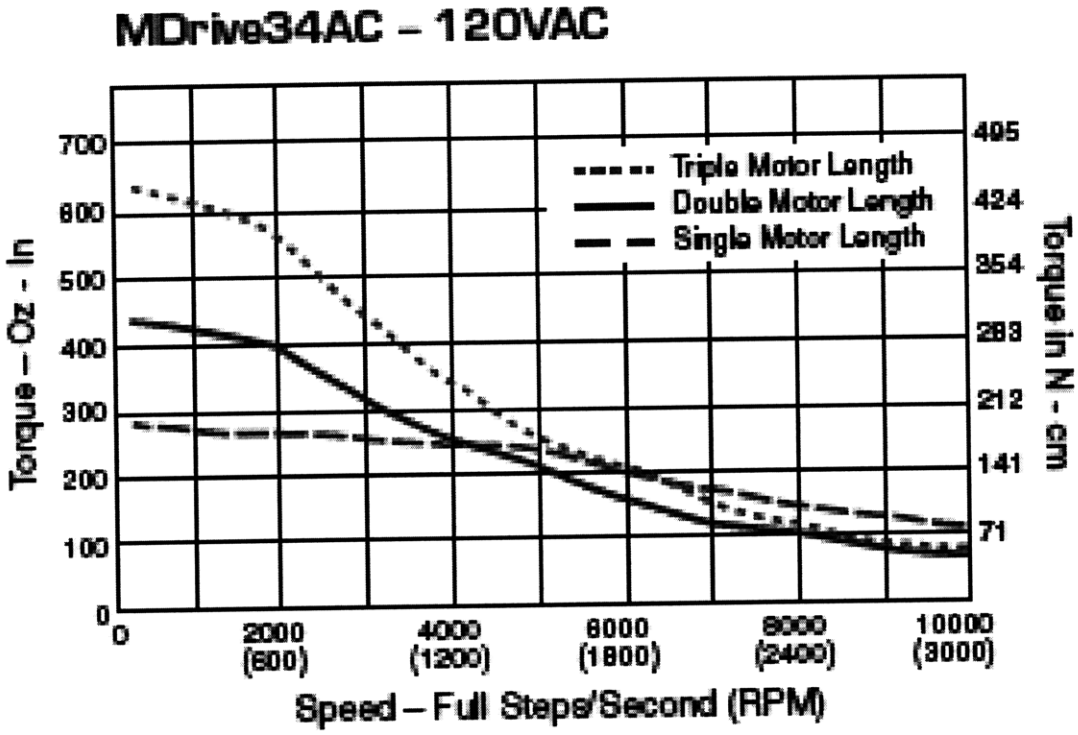

Figure 5-11: The speed-torque relationship for the stepper motor from IMS. The motor we used is represented by the blue line.

In order to attach the motor to the shaft of each roller, an Oldham flexible coupling was selected (Figure 5-12). This style of coupling uses a nylon disc in between two aluminum hubs. The compliant nylon compensates for any misalignment between the shafts and also acts to dampen motor vibrations. The damping properties are especially beneficial to this system as vibration could translate into printing defects. It also makes for a quieter, smoother system.

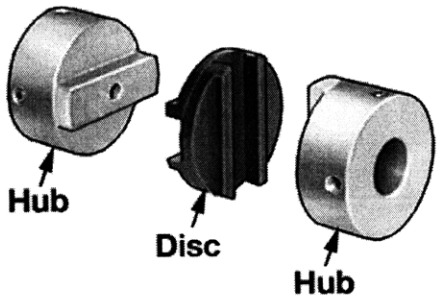

Figure 5-12: An Oldham style coupling used to interface the motors and clutch with various rollers [12]

5.3.21.3 Impression assembly

The impression assembly (Figure 5-13) consists of a stage that can be adjusted up and down to vary printing load. The roller is covered in 1/8" of cellular silicone foam to create a compliant layer. Micrometers on top are used to compress the foam to create a spring force. 0-10 lb load cells under the micrometers monitor how much weight is resting on the print roller. Early on, these load cells were accidentally broken by exceeding their capacity and a single cantilever load cell was used in their place. Also, it should be noted that the load cells only provide information about force, not the actual pressure distribution at the print-impression interface.

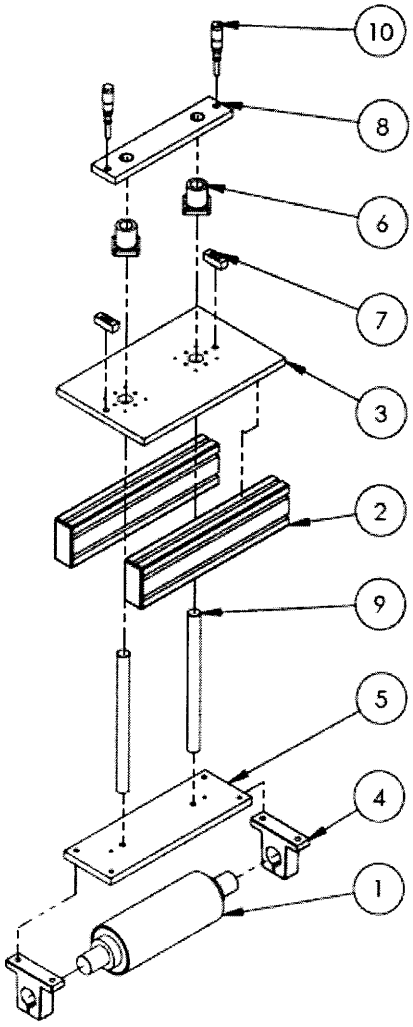

ITEM NO.	DESCRIPTION	QTY.
1	IDLER ROLLER ASSY	1
2	8020 STANDOFF	2
3	IMPRESSION FIXED PLATE	1
4	SHAFT MOUNT	2
5	SHAFT SUPPORT PLATE	1
6	LINEAR BALL BEARING	2
7	LOAD CELL	2
8	PRESSURE PLATE	1
9	LINEAR SHAFT, .750"	2
10	MICROMETER	2

Figure 5-13: An exploded view of the Impression Assembly. Modifications were later made to this assembly to accommodate another type of load cell. Details are in the following chapter.

The printing load is determined by the spring constant of the foam and the weight of the moving assembly depending on the setting of the micrometers. A schematic of the interface is provided in Figure 5-14 the relationship graphed in Figure 5-15. The pressure distribution about the contacted arc of the stamp is determined by:

- applied force
- stamp compliance
- foam compliance
- position of the micrometer (translates into center-to-center distance for rollers)
- tension of the substrate
- roller runout (noise)
- vibration (noise)
- alignment of the impression roller to the printing roller (noise)

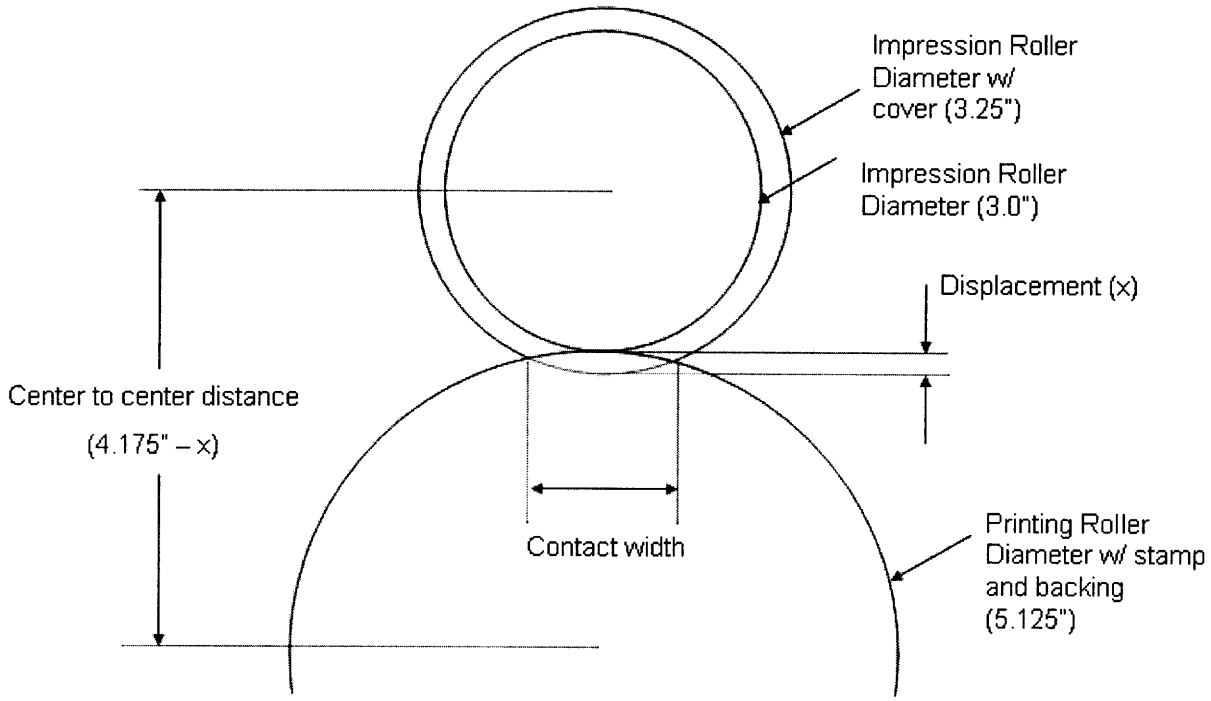

Figure 5-14: Critical dimensions at the Impression-Print roller interface.

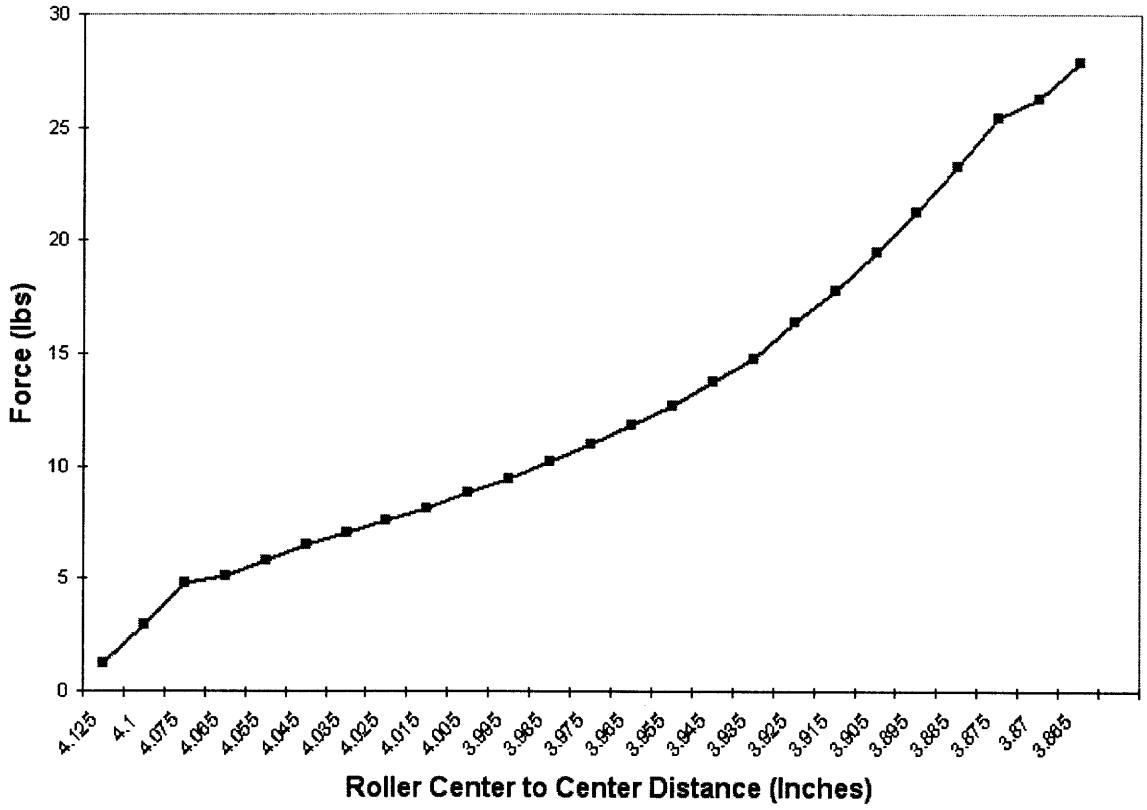

Figure 5-15: The relationship between the impression roller displacement and the force, determined empirically.

5.3.21.4 Inking method

Ink is applied by one of two methods. The first is by removing the stamp from the cylinder and wet inking it with octadecanethiols. The thiols last for many prints, so this method was used for testing purposes, but it is more labor-intensive because the stamp must be removed. The other method uses an inking roller with a layer of PDMS on its surface that can be raised into contact with the stamp roller and transfer thiols directly. This same roller can be reconfigured to serve as a cleaning roller by attaching double-sided tape to it to clean the surface of the stamp during printing. Because we did not have enough time to perfect the method of applying a layer of PDMS to the roller, we were not able to adequately test this system.

5.3.21.5 Wrap angle adjustment

The entire Print Module can be slid up and down via the T-slots it is mounted to on the machine frame. The angle (α) that the substrate contacts the stamp roller at can be varied both positively (wrap angle around the impression cylinder) and negatively (wrap angle around the print roller) or left to contact the roller tangentially, as illustrated in Figure 5-16. This characteristic was especially useful during initial testing of the machine.

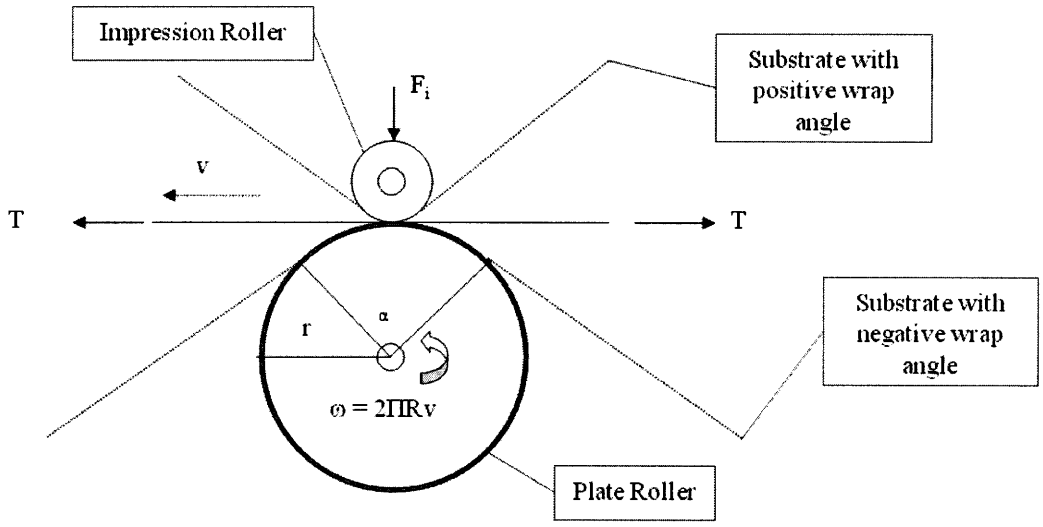

Figure 5-16: A schematic showing the critical dimensions for wrap angle adjustment.

5.3.22 Collect module

Substrate winding and tension control are the main functions of the Collect Module (Figure 5-17). There are two powered rollers in this system, one to drive the substrate from the printing area, and another to wind printed substrate. Differential speeds of these motors are used to control tension, while a load-cell based tension sensor (Figure 5-18) is employed in each zone to feedback tension information. Cantilevered tension rollers were selected based on performance and form factors. They were laid out in the design to have the maximum amount of wrap angle (and thus the strongest signal) while still fitting in the confines of the module. Idler rollers were also placed to ensure that the sensor wrap angle did not change. Inserts had to be added to the

second sensor to allow the printed side to run on the roller without contacting the middle of the print (similar to the "Bone Roller" used for nips) and causing defects; this was a compromise to save space. The inserts were two 1.5" long Teflon thin-walled tubes, which slid over the roller and were secured at the front and back with approximately 6" between them (not included in the assembly drawing).

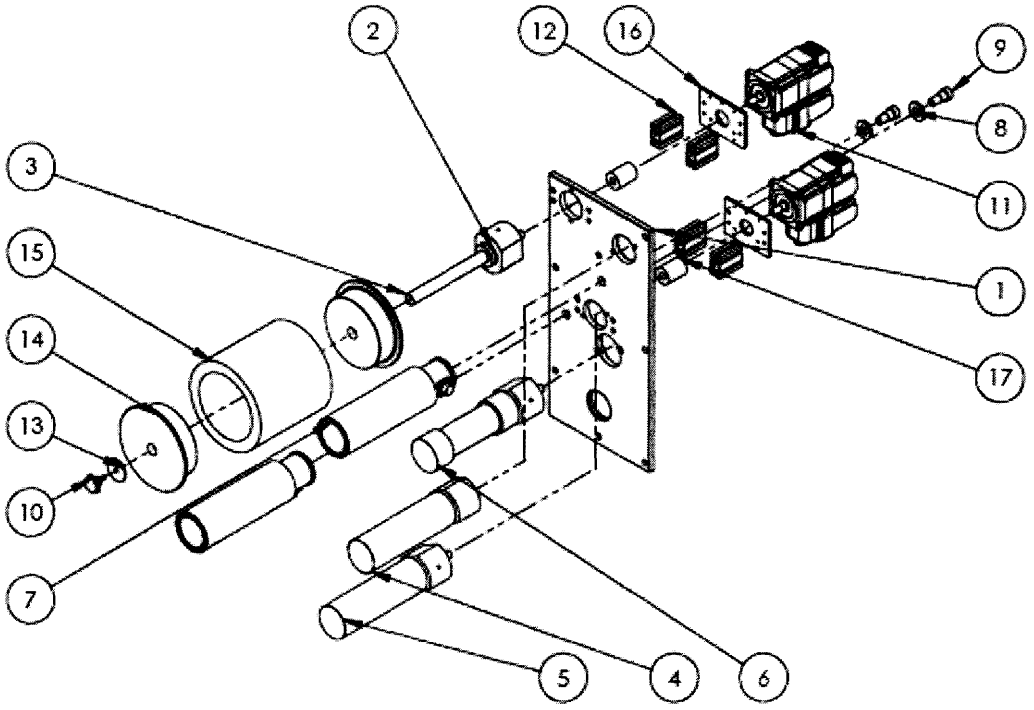

ITEM NO.	DESCRIPTION	QTY.
1	MODULE PLATE, COLLECT	1
2	BEARING BLOCK ASSY	4
3	SPOOL ROLLER	1
4	IDLER ROLLER	1
5	IDLER ROLLER	1
6	BONE ROLLER	1
7	TRANSDUCER ROLL	2
8	WASHER, .750" ID	2
9	SHOULDER BOLT, .625"	2
10	KNOB	1
11	STEPPER MOTOR NEMA34	2
12	MOTOR STANDOFF	4
13	WASHER, SPOOL	1
14	SUBSTRATE SPOOL END	2
15	SUBSTRATE	1
16	MOTOR MOUNT PLATE	2
17	COUPLING	2

Figure 5-17: An exploded view of the Collect Module

Figure 5-18: The cantilevered "Narrow Web" transducer from Dover Flexo Electronics [10]

5.3.23 Electrical and Control System

The electrical system consists of high voltage distribution (110VAC), a 24V power supply and distribution, a Programmable Logic Controller (PLC), several buttons, an Emergency Stop relay (a motor contactor), sensor amplifiers for the load cells and tension amplifiers, and stepper motors (described in previous section). The whole system is assembled in an electrical enclosure to prevent harm to man and machine. A schematic is provided in Figure 5-19.

High voltage enters the system and is current limited to 20A by a circuit breaker. Ground and neutral are distributed via a terminal block. Power for the motors goes through a contactor which is engaged via a button on the enclosure and disengaged via an Emergency Stop button mounted on the front of the machine. In the case of an emergency stop, all power is removed from the stepper motors. The PLC, PLC Input/Output (IO), sensor amplifiers, and Emergency Stop system are powered by 24V. All analog signals are 0-10VDC and are fed into an expansion module in the PLC. The earth ground is connected to machine ground in one point only to prevent ground loops that may cause disturbances in the analog signals. 24V Return is also grounded

to prevent noise and ease machine troubleshooting (a multimeter's negative probe can be touched to bare metal anywhere on the machine frame).

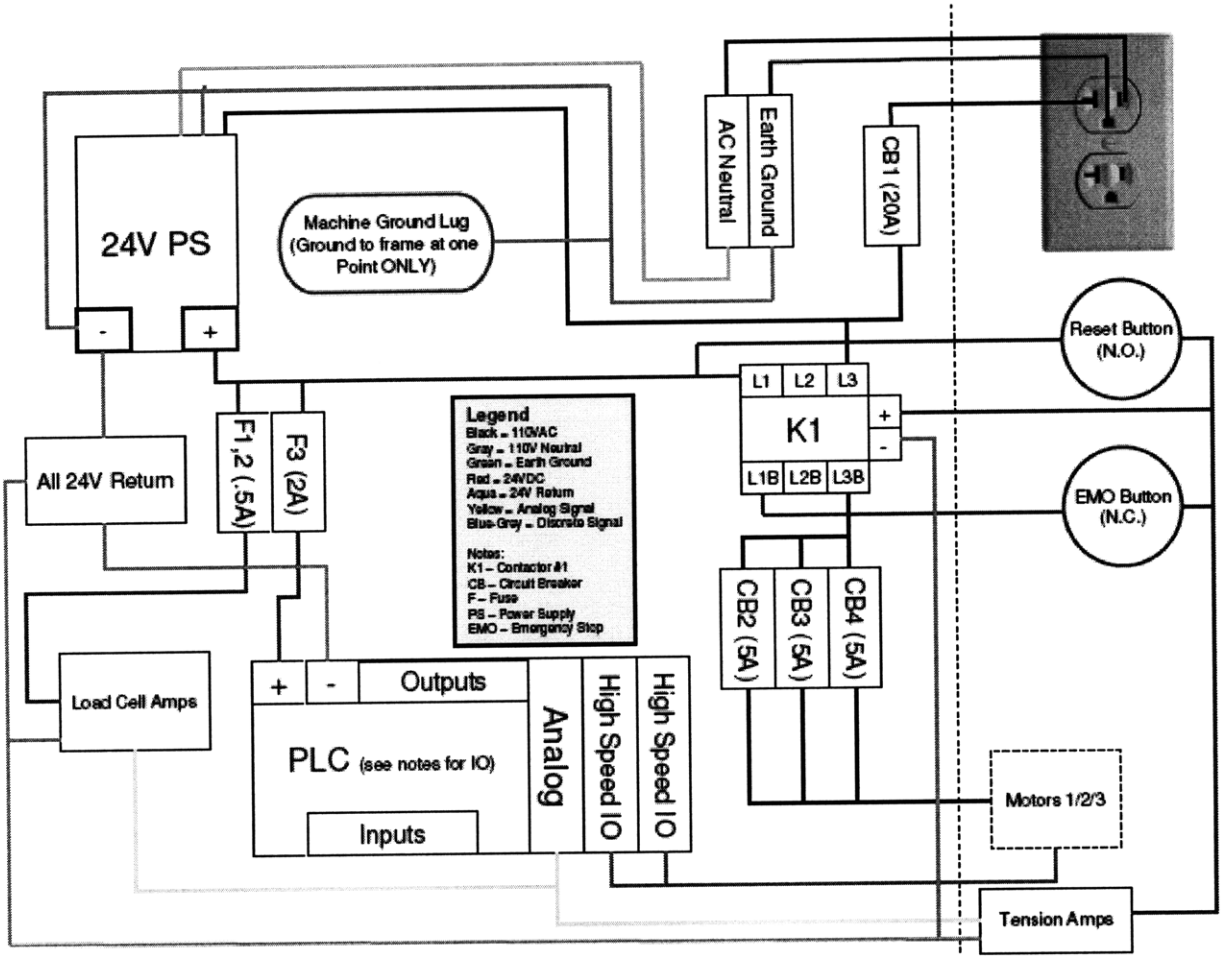

Figure 5-19: A basic schematic of the electrical system.

The main controller in this system is an Automation Direct PLC, programmed with ladder logic using DirectSoft 5.0. Three expansion modules were added: an analog IO unit and two high speed IO (HSIO) modules. The HSIO is used to provide step and direction signals to the drive and print stepper motors up to 25 KHz. The PLC has the ability to output at 10 KHz on the base unit, but is limited to only one signal. The collect motor runs on this output (and must be microstepped to a more coarse resolution to achieve the desired speed).

The program makes decisions based on tension data, programmed schemes and equations, and inputs from buttons. It outputs motor instructions (step and direction), discrete operator alerts, and ascii text for data collection. Two PID loops are used in the

program to control the tension of the substrate. Figure 5-20 provides a basic flowchart of the program. More details regarding the control scheme can be found in Shawn Shen's thesis [25].

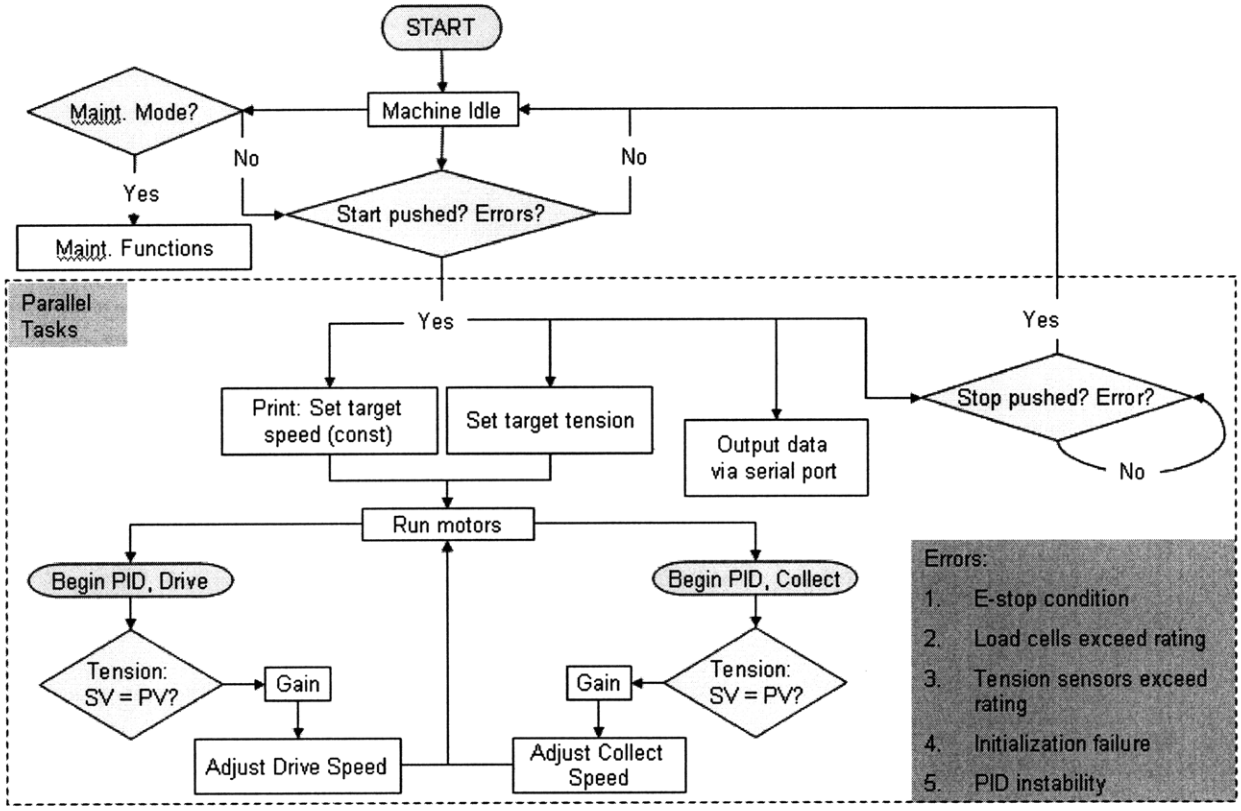

Figure 5-20: Control system flowchart.

Tension, load, and speed data is sent out the PLC serial port to a remote laptop every 1/32 of a revolution of the printing cylinder. Hyperterminal, a Windows communication program is used to capture incoming text. The PLC program formats the data into a string of the form "Tension1, Tension2, Force, Adjusted_force, command_speed, PID_adjusted_speed". The "Capture text" function in Hyperterminal allows a text file to be created from any incoming data. This data can then be opened in Excel by using the commas in the string as delimiters.

5.4 Stamp Fabrication Fixtures

5.4.24 Scope and purpose

This part of the project was essential to the success of the printing process. Making large area PDMS stamps is not a trivial task. In previous research at NanoTerra, small stamps were made with no backing and attached directly to a roller by hand. This resulted in a large number of problems in the process and end product including distortions, thickness non-uniformity caused by stretching, and problems with adherence to the backing. Our challenge was to create a stamp with a printable region of 6" wide minimum by 15" long. Critical parameters include flatness of the stamp, flatness of the steel backing, uniformity of features, and minimization of defects (particulate matter, bubbles caused by air trapping).

5.4.25 Concept selection

There are a variety of ways to realize these goals. The old method of gluing pre-made stamps to a backing was discarded due to the problems mentioned before. We decided to try two methods, one that has been used before and another which has been used before but not at this scale. The method that NanoTerra had in its tool library was a very basic injection mold with a 12" wafer as the master. The wafer sits under a square border and a vacuum plate with the backing attached is bolted to the bottom part of the mold. PDMS is injected into a port until it comes out a port at the opposite side. This method worked well in the past and results in stamps with little or no air trapping. However, we were limited to only a 12" long region, which would result in wasted space on our print roller. This was not ideal, but was considered as a backup if the other method did not work.

The other method (Figure 5-21) was to pour PDMS over a tray with a 2 x 6 array of square wafers (cut from 6" wafers). A vacuum chuck above holds the substrate flat

and is lowered onto the PDMS. Spacers at the corners determine stamp thickness. The ability to place an array of wafers in the tray has benefits for research, because a variety of patterns can be tested using one stamp. This idea can be scaled up, by placing larger wafers in the tray. We chose 6" wafers because the MTL shop at MIT only had the capability to process this size.

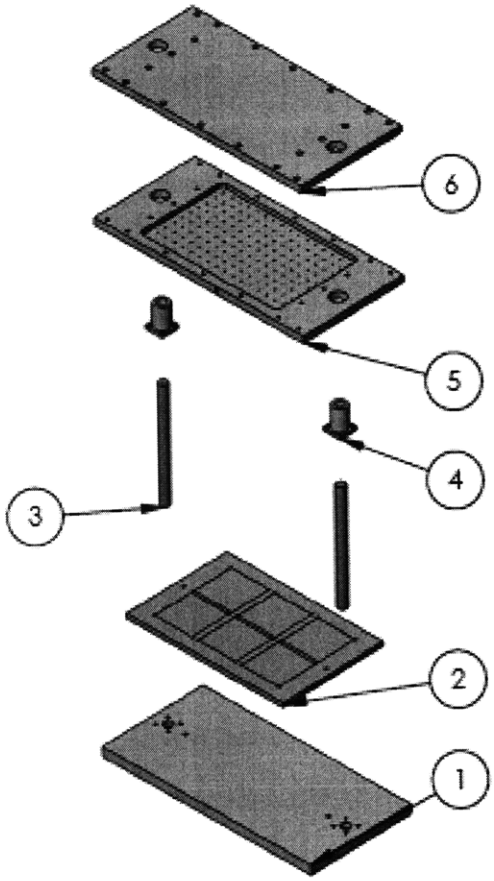

ITEM NO.	DESCRIPTION	QTY.
1	STAMP FIXTURE BASE	1
2	WAFER TRAY	1
3	BEARING SHAFT	2
4	LINEAR BEARING BLOCK	2
5	VAC PLATE	1
6	VAC BACKING PLATE	1

Figure 5-21: An exploded view of the stamp making jig. The Wafer Tray accommodates an array of six wafers, allowing a variety of patterns to be printed at once.

5.4.26 Stamp Fabrication

The fixture was used to fabricate a number of stamps. Unfortunately, air trapping occurred under all conditions tried, and we decided to forego this method. Instead, the injection-molding fixture at NanoTerra was used to fabricate stamps. The fixture was based on a 12" wafer and could make stamps with an area of 8" by 8" by injecting PDMS into a cavity covered by the steel backing and supported with a vacuum plate. Although this did not optimize the stamp area on our cylinder, the stamps produced were of good quality.

5.5 Continuous Etching machine

5.5.27 Scope and Purpose

We were also tasked with creating a system that could etch substrate continuously in order to keep up with the speed of printing. This is essential in industry, because etching would be the obvious bottleneck in the process. Our task was to create a scalable prototype that could be used to do basic testing of the principle operation. As this subproject was largely outside the main scope of our project, it received less of our energies and is mentioned only briefly in this paper.

5.5.28 Specifications

There were essentially three main concept specifications. First, the machine should be able to operate at a line speed capable of keeping pace with printing while not taking up an unreasonable amount of space. Second, if there is multiple stations in the process (as in some Nanoterra proprietary techniques, where there is a total of three dipping steps and two drying steps), each process time should be alterable without affecting the line speed. Third, it should not create additional defects compared to the state of the art (etching by hand is the most common method at NanoTerra).

5.5.29 Concept selection

We chose a modular approach to this problem. Figure 5-22 shows the 3D model of the finished design. The substrate is run through a variety of rollers that allow it to pass into tanks with the appropriate chemicals. Effectively the material is batched into a smaller tank rather than having to have very long or deep tanks. Modules can be added simply by bolting another one on and running the substrate through both (Figure 5-23). Additional wheels can be added to guide the substrate vertically or horizontally, depending on the desired configuration of the machine. The printed side is guided only by the outermost 1" strip on each side by individual wheels to avoid contacting the printed pattern. The rollers that guide the substrate into the tank are on linear bearings, which allow them to move up and down, making it possible to change the process time of each station.

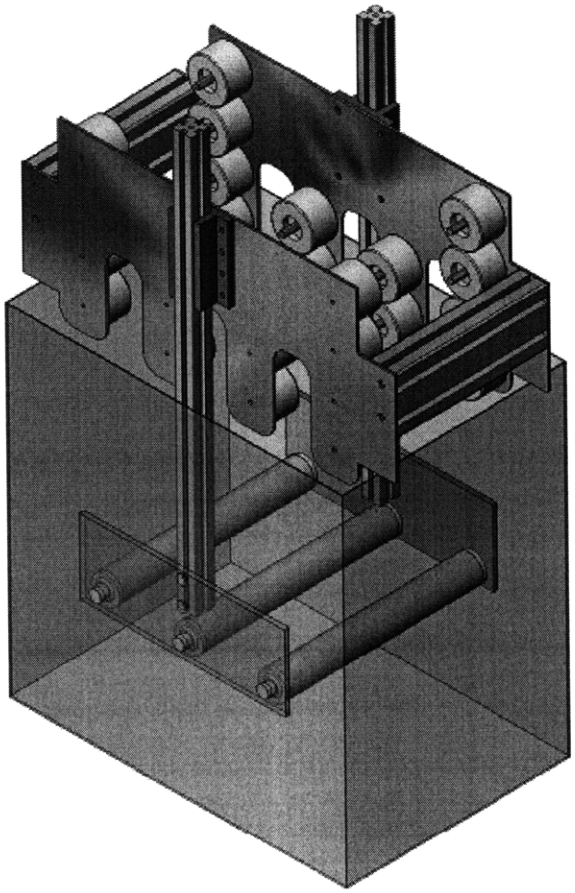

Figure 5-22: A Solidworks model of the Etching Module.

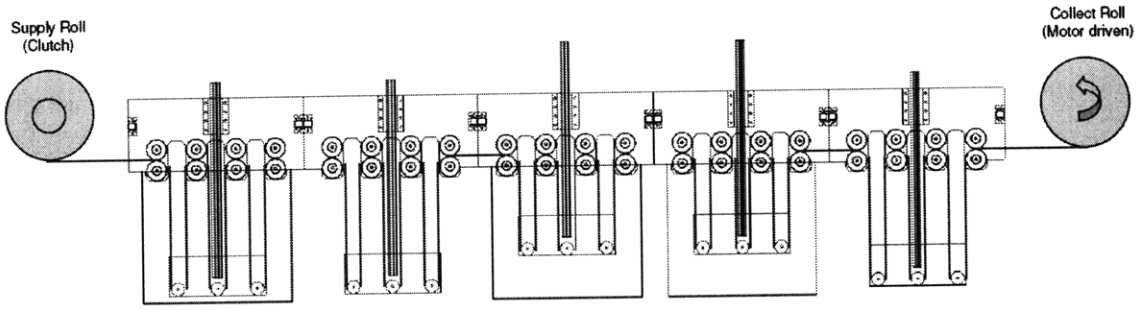

Figure 5-23: A schematic of the modular nature of the design. Additional processing steps can be added by attaching more modules.

In order to run the system at speeds comparable to that of printing, which would be necessary in a manufacturing environment, this concept can be scaled. This can be accomplished by adding more rollers and making the tank longer or allowing the bottom rollers to be adjusted farther down and making the tank deeper. We wrote a spreadsheet that calculates these parameters based on line speed. The user inputs the line speed, roller diameters, individual process times, and tank depth; the spreadsheet outputs the required number of rollers (Figure 5-24).

Roller Diameter (D)	2	(in)
Line Speed (v)	100	(fpm)

	Max Time (sec)	Sub. Depth (in)	Sub. Length (Lt)	min # rollers (n)
Backfilling	50	24	1000	24
Drying 1	50	24	1000	24
Etching	30	24	600	14
Rinse	30	24	600	14
Drying 2	45	24	900	21
Total substrate length in process (inches)			4100	
(feet)			341.7	

Figure 5-24: A design spreadsheet used to calculate the number of rollers.

5.6 Hardware Manufacturing and Assembly

Most custom components were manufactured by a local machinist or by one of our team at the MIT LMP machine shop. Figure 5-25 is a typical drawing used to have the parts manufactured. Electronic components were generally off-the-shelf components, with some exceptions like custom made cables. Most components only needed basic power and logic wiring. Figure 5-26 thru Figure 5-28 show the completed machines.

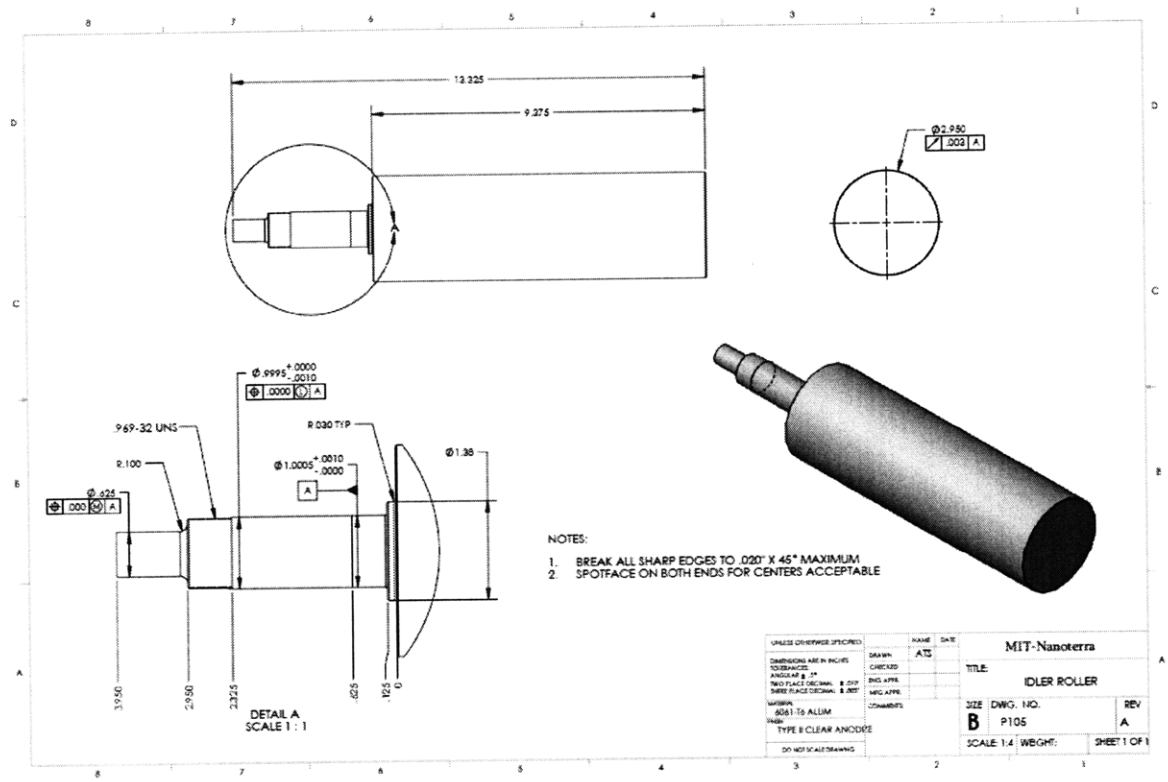

Figure 5-25: A typical engineering drawing used in this project for communicating part dimensions to machinists. Geometric and linear tolerancing was used to communicate critical dimensions and characteristics. The rest of the part drawings can be found in Appendix B.

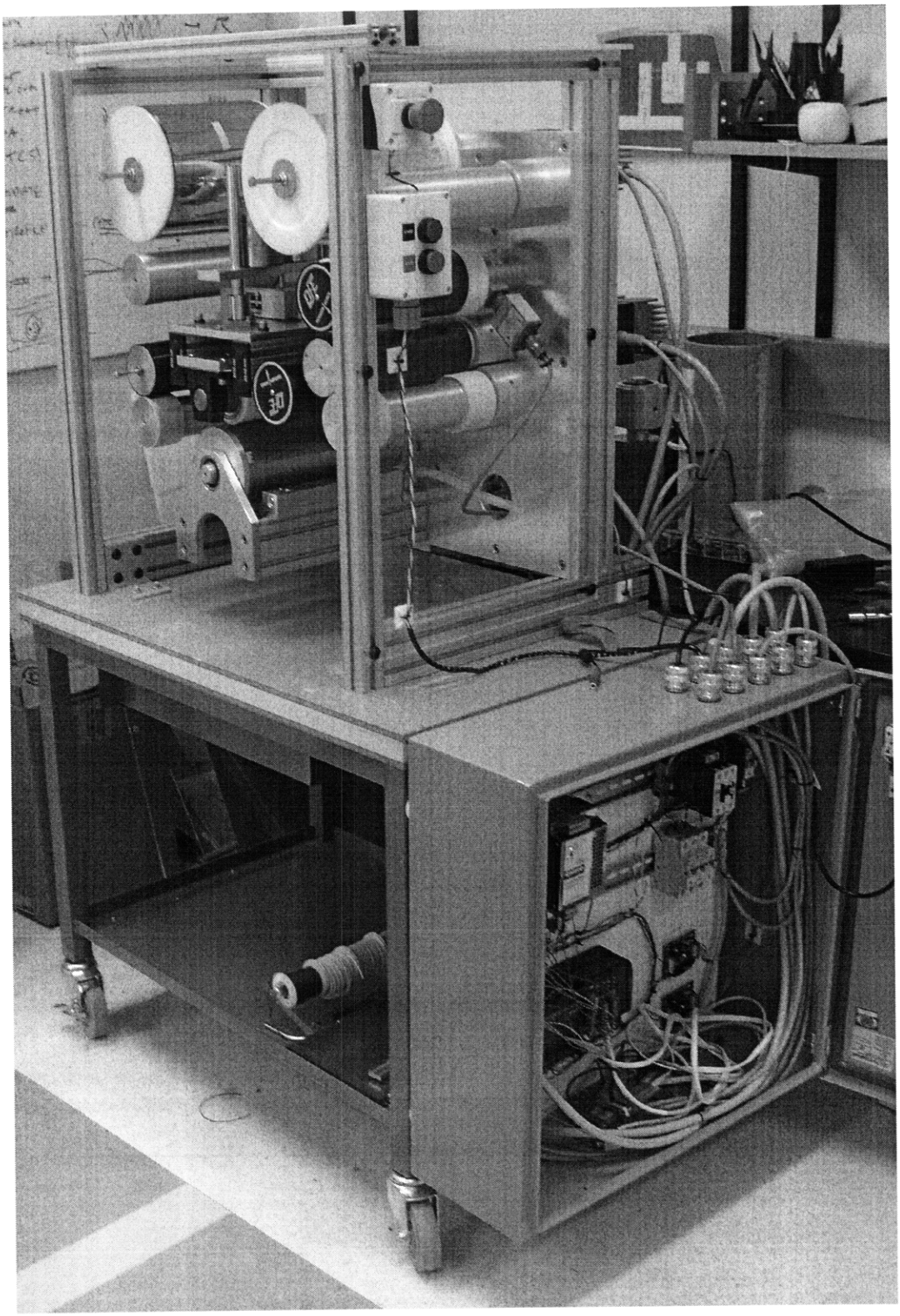

Figure 5-26: The assembled printing machine and electronics enclosure. The majority of custom components were manufactured by a local machinist and assembled by us at the NanoTerra facility.

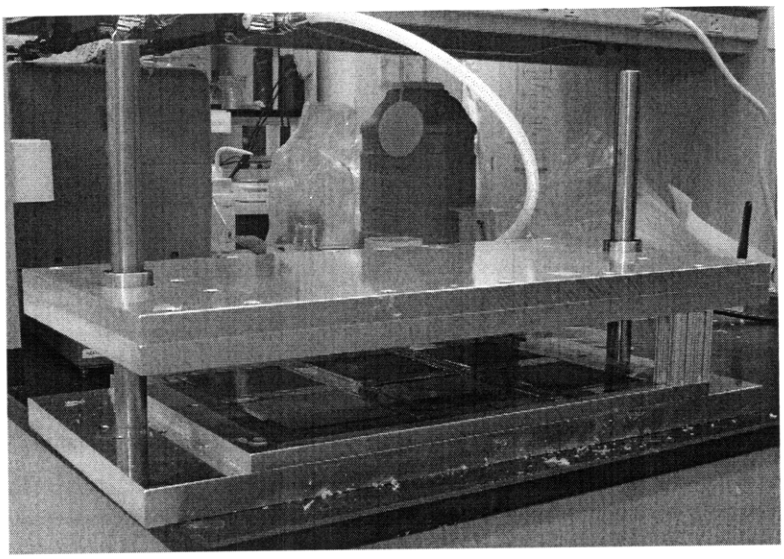

Figure 5-27: The assembled stamp jig. The large plates were manufactured by a local machinist from MIC-6 precision ground aluminum.

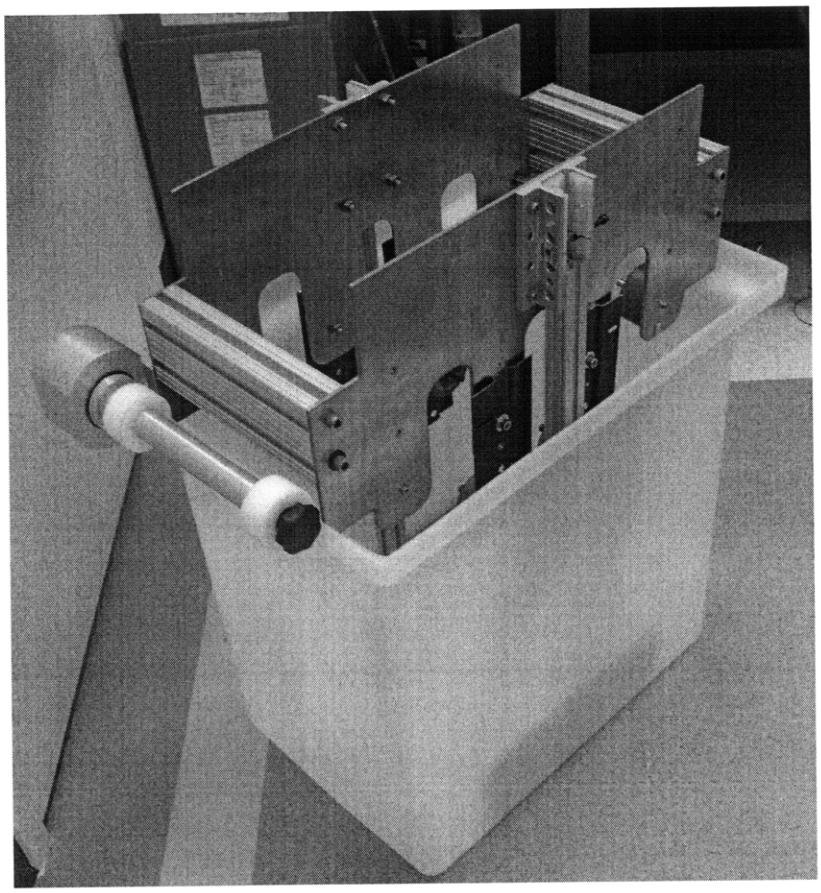

Figure 5-28: The assembled etching machine prototype with some minor modifications to reduce etchant volume. Most of the parts for were manufactured at the MIT LMP shop using a CNC waterjet cutter, milling machines, and lathes.

Chapter 6

Experimental Methodology

This chapter discusses the methodology for experimentation including the overall process model, characteristic measurements, design of experiments (DOE), measurement techniques, as well as preliminary experimentation. For more detailed information, please refer to Kanika Khanna's thesis [15].

6.1 Process Model for Roll-to-Roll μCP

Following is a brief explanation of the process model for control of roll-to-roll μCP (Figure 6-1) developed by Kanika Khanna [15] based on research by Dr. David Hardt [20]. It is especially of interest for experimental design and analysis of manufacturing systems.

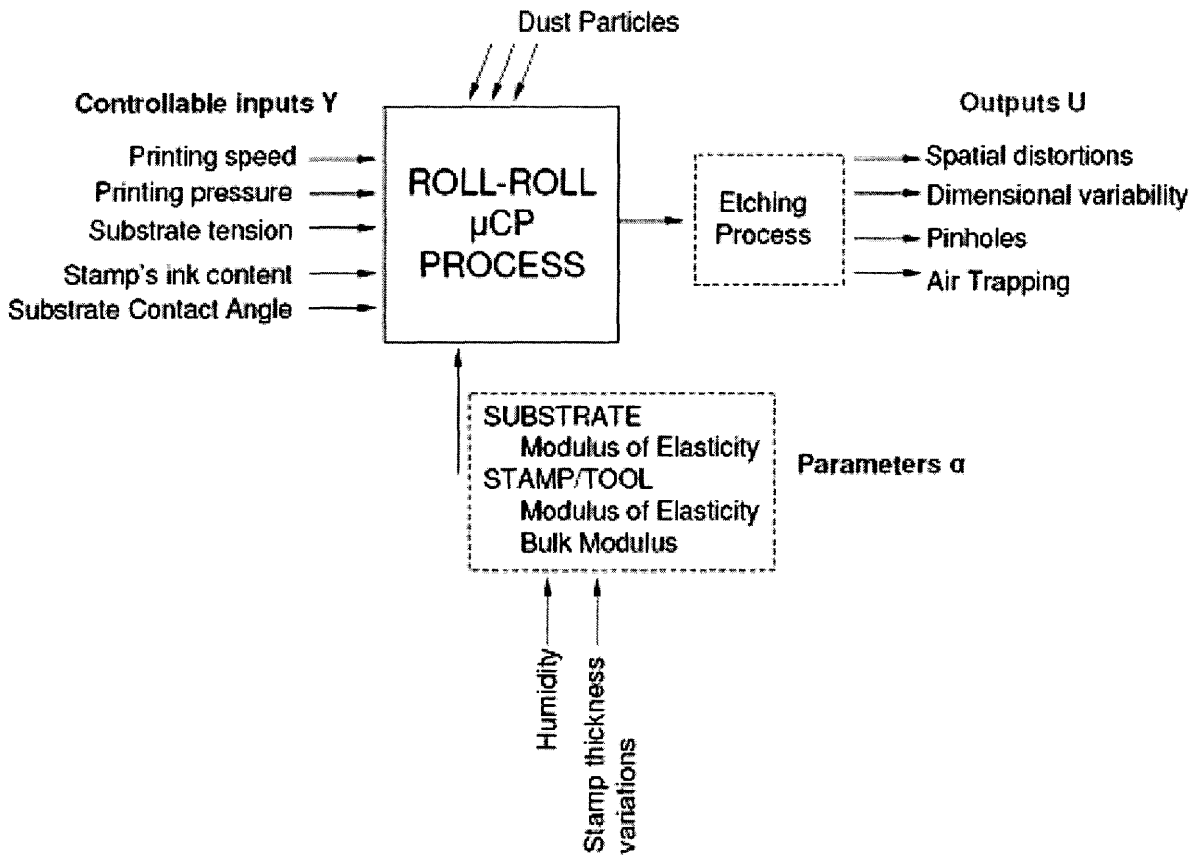

Figure 6-1: A process model of roll-to-roll MCP inputs and outputs [15]

The outputs of primary interest in μCP are: 1) yield or percentage of area printed; 2) the dimensions of local features typically represented as lengths, widths, diameters, etc.; and 3) the location of features with respect to a fixed point and generally referred to as spatial distortion.

Material parameters of interest comprise the properties of the Au-PET substrate, especially its modulus of elasticity. The primary equipment parameters of interest are the states and properties of the stamp and machine tool. Of key importance is the stamp wrapping method on the printing cylinder and the impression roller cover.

The controllable inputs are listed in Figure 6-1. Mechanical and program-driven controls are detailed in Chapter 5. Ink content is controlled via frequent inking to ensure that the amount in the stamp is kept fairly constant. Finally, geometrical properties of the stamp also affect the output and are determined via the stamp fabrication process.

Determining the type of interaction for a continuous process is interesting. When viewing the process perpendicular to the MD (i.e. along the contact length), the process would be considered parallel. Therefore, contact width and pressure distribution are of primary interest. However, when viewed along the MD (i.e. along the direction of printing), the process would be considered to be serial. Viewed like this, printing speed as a function of time and printing pressure as a function of time are of primary interest.

6.2 Quality Measurements

We chose yield, dimensional variation, and spatial distortion as our key quality measures are they are considered the fundamental measures of printing quality; NanoTerra uses these frequently in their research. The pattern is an alternating array of rectangular and triangular pixel arrays with a 1.5mm pitch. The rectangular pixels were chosen for measurements as they are easier to define and measure and are affected less by etching. Also, they are composed of more pixels on the screen, so a greater accuracy can be achieved when measured. The critical dimensions are shown in Figure 6-2.

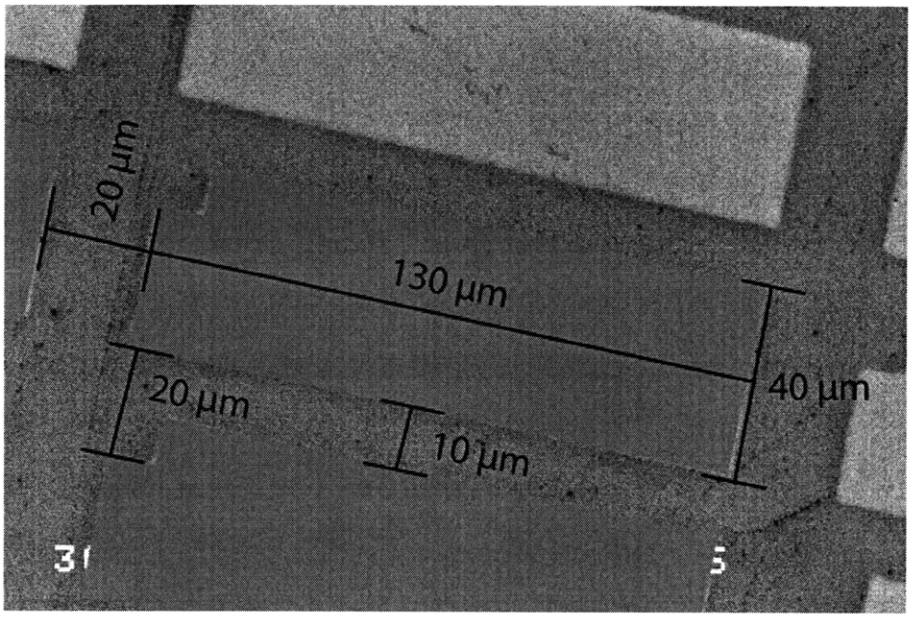

Figure 6-2: Critical pixel dimensions. Note: the area in green is the etched region and the darker area the printed resist region.

6.3 Design of Experiments

Two sets of experiments were designed. The first is a 2^2 full factorial (Figure 6-3) to test the effects of printing force (pressure is indirectly controlled and discussed in a following section) and printing speed on yield, dimensional variation, and spatial distortion. Tension was minimized and kept constant as it tends to stretch the substrate and cause distortion. From this we wished to extract information regarding how the process outputs responded to changes in these two inputs. The second experiment is a 1-dimensional scan (Figure 6-4) of the effect of speed, especially the effects of speeds in excess of 100 fpm. Printing force and tension are kept constant.

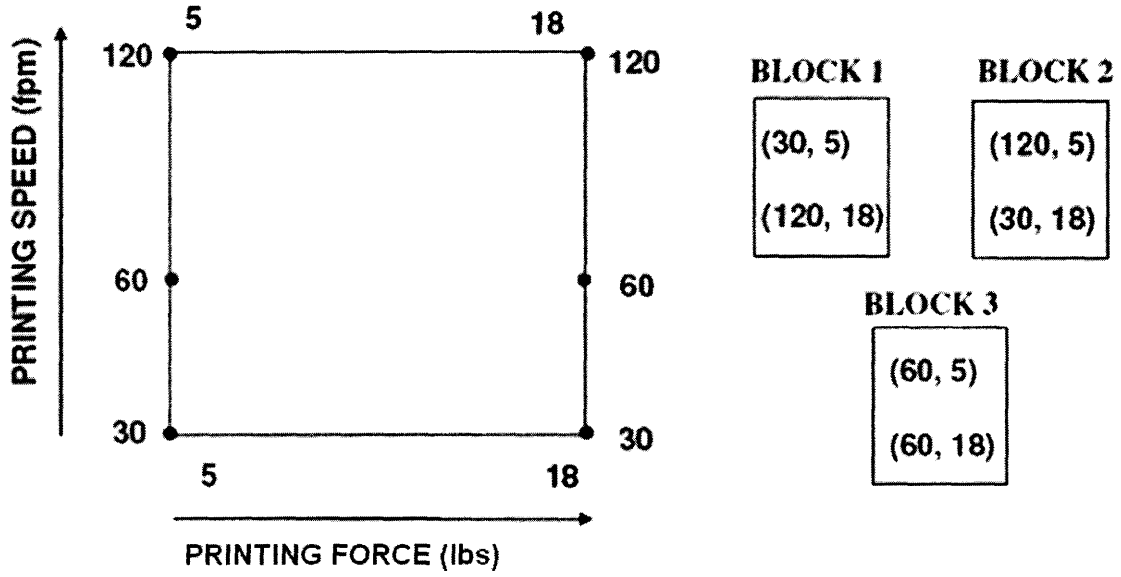

Figure 6-3: The 2^2 full factorial design with printing force and speed. [15]

SPEED (fpm)	30	60	120	240	400
CONTACT TIME (ms)	63	32	16	8	5

Figure 6-4: Conditions for the 1-D scan of speed effects. [15]

10mM octodecanethiol was used as the ink in all experimentation. It was applied to the stamp off the machine by dripping ink on the patterned surface and allowing 10 minutes for the thiols to diffuse into the stamp (essentially the same as immersive ink-

ing). A blast of nitrogen was then used to remove any excess alcohol. 3M Scotch tape was used before and after inking to remove any particles.

Etching was done using thiourea ferric nitrate. The etchant comprised 1.14 grams of thiourea and 4 grams of ferric nitrate added to 500ml of water at about 40 degree C and mixed vigorously. The print was then cut into 8" x 8" squares, submerged in the etchant bath, and manually agitated. The unprinted gold was etched in 3-4 minutes and rinsed using deionized water. Etchant typically lasted about a half hour before it had to be replaced. The etching module mentioned before was only used for one long print in order to prove its usefulness.

6.4 Measurement Techniques

Measurement was done using high-powered microscopes that had the ability to capture digital images. These images could then be manipulated via a MATLAB program. Local dimensions were measured at 50X. An image of a pixel (refer to Figure 6-2) was captured at 25 regions on the print, and the length and width measured using a MATLAB program.

Distortions are the general large scale change in the printed pattern as compared to the stamp. The amount by which a single pixel is distorted is the distance between the position where it was intended to be and the position where it actually is printed. Distortions are quantified by fixing one point and pivoting the reference grid at that point and then calculating the relative displacements of pixels from their intended positions in the grid [7]. A Nikon Veritas microscope with an XY stage was used to capture a grid of images for distortion analysis. MATLAB was used to measure and fit the data. Refer to Kanika Khanna's thesis for a detailed explanation of measurement techniques [15].

The accuracy of each measurement is as follows (established by NanoTerra):

- *Distortions*: Standard NT technique, accuracy: ± 4 μm. (42 points per print).
- *Dimensions*: Optical measurements, accuracy: ± 250 nm. (25 points per print).

6.5 Preliminary Experimentation

In order to get a sense of the machine, the effects of input parameters, and to determine sampling sizes, a variety of preliminary experiments were carried out.

The first task was to get the machine running properly; especially the tension control system. Plain PET was used to tune the PID parameters and get a sense of the mechanics of the machine. The first problem encountered was that the substrate tended to stick and slip off the stamp and subsequently wreak havoc on the tension control loop as the wrap angle on the tension sensor changed with respect to time. This resulted in the first set of load cells being overloaded due to the substrate being jerked through the system and the impression stage jumping up and down. Our first solution was to add idler rollers after the printing process to keep the wrap angle on the tension roller constant (see Figure 6-5). These were later removed when the PID loop was further tuned; however, we believe it is a good improvement for further work to avoid programming difficulties.

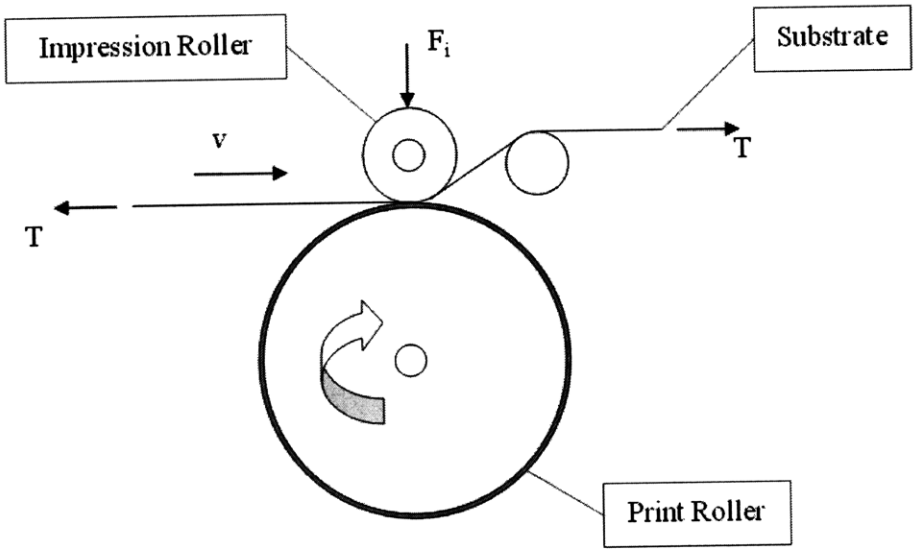

Figure 6-5: Idler rollers were added after the printing cylinder to maintain the wrap angle on the tension sensor.

Our first round of prints was printed on AU-PET using 10mM octadecanethiols, etched with thiourea ferric nitrate, and analyzed according to NanoTerra's standard

procedures. We observed a diamond-shaped distortion pattern (Figure 6-6) in all the prints that we attributed to misalignment of the stamp along the print direction coupled with wrapping around a cylinder. Because it was found to be a systematic effect attributable to a known cause, a MATLAB program was written that accounted for it in all subsequent tests.

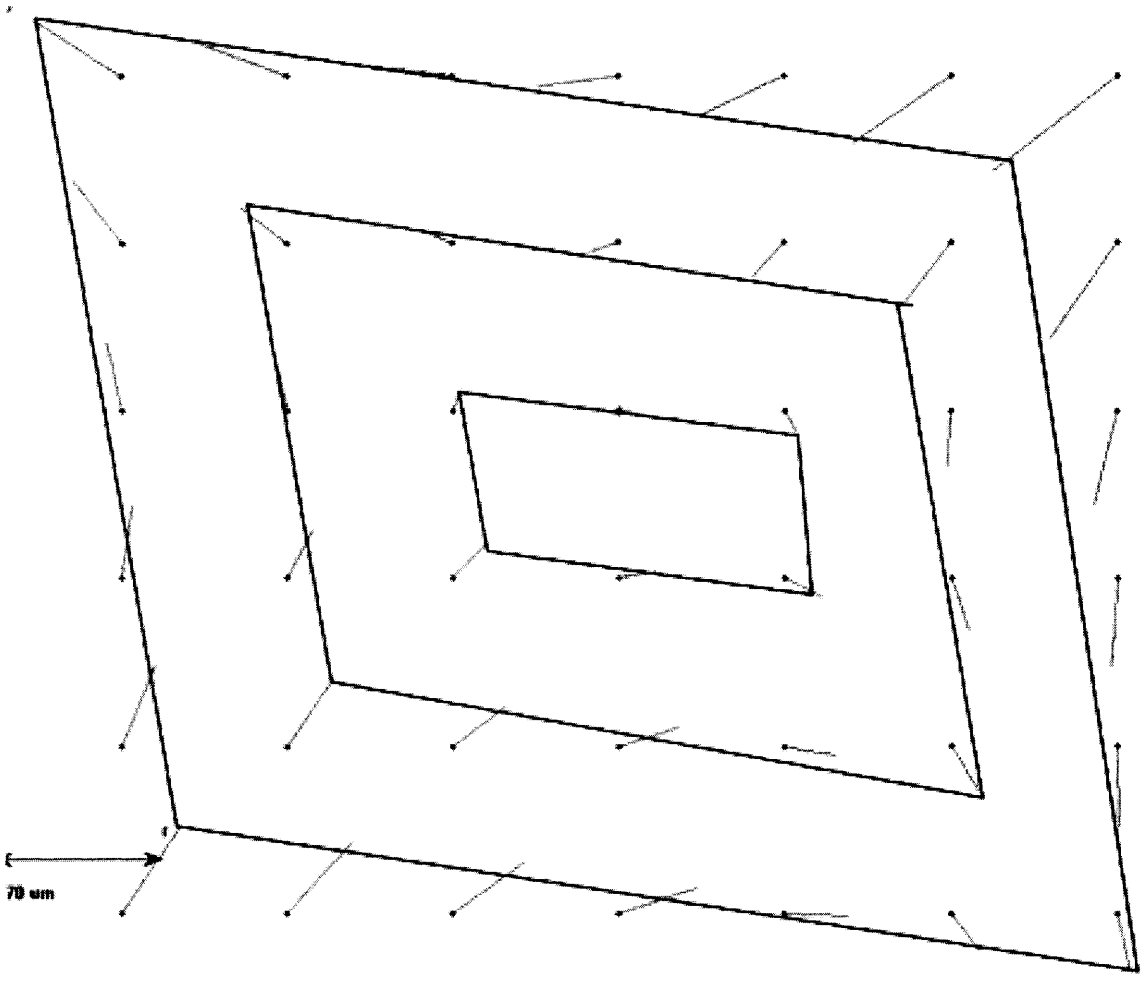

Figure 6-6: The recurring diamond-shaped distortion pattern observed in all of our prints. The black dots represent the reference grid and the red lines are the feature shift from the reference grid scaled by a factor of 300. Note: the diamond shapes were added for emphasis.

In order to determine the optimum sample size for dimensional variation, we sampled a large number of pixels from our initial prints and calculated the relevant statistics for length and width (Table 6-1).

Table 6-1: A summary of the initial dimensional results [15]

Sample size= 70		
	Length	Width
Average	132.57	40.04
Standard Deviation	0.57	0.36
COV	0.00	0.01
Standard Error	0.07	0.04

For a 100(1-α) % confidence interval:

$$x - t_{\alpha/2,n-1}\, s/\sqrt{n} \leq \mu \leq x + t_{\alpha/2,n-1}\, s/\sqrt{n} \qquad (6.1)$$

where x is the mean and s is the standard deviation of the sample, μ is the mean of the population and n is the sample size. Thus for the population mean to lie within a maximum of +/-d microns of the sample mean with 100(1- α) % confidence, the sample size is determined by:

$$n = (t_{\alpha/2,n-1}\, s / d)^2 \qquad (6.2)$$

Therefore, with a sample size of 25, the mean and width should lie within +/-.26 microns and +/-.16 microns of the population mean with 95% confidence, respectively. A sampling size of 25 was therefore a fair compromise between accuracy and effort (the measurement process is quite time consuming). For the remainder of measurements, a 5 x 5 grid was used to determine measurement regions.

6.5.30 Determination of Contact Width and Pressure

Values for the printing force and speed were determined after initial experiments to determine an acceptable range. The contact areas were determined at different forces using a piece of gold substrate and an inked stamp. The force was set, impression roller lifted, and the gold advanced between the stamp-impression interface. The impression roller was then set down (light tension was maintained by hand) for ap-

proximately 5 sec to allow thiols to transfer and the substrate was subsequently etched. The print was then measured with a caliper and the approximate area calculated based on the shape of the impression. The nip impressions are shown in Figure 6-7. From these numbers, the average pressure can then be calculated and used as a rough reference. Because we were unsure of the actual pressure distribution at the nip, we used the applied force as our parameter for experimentation. See Table 6-2 and Figure 6-8 for the relationship between force and contact width, as well as force and pressure.

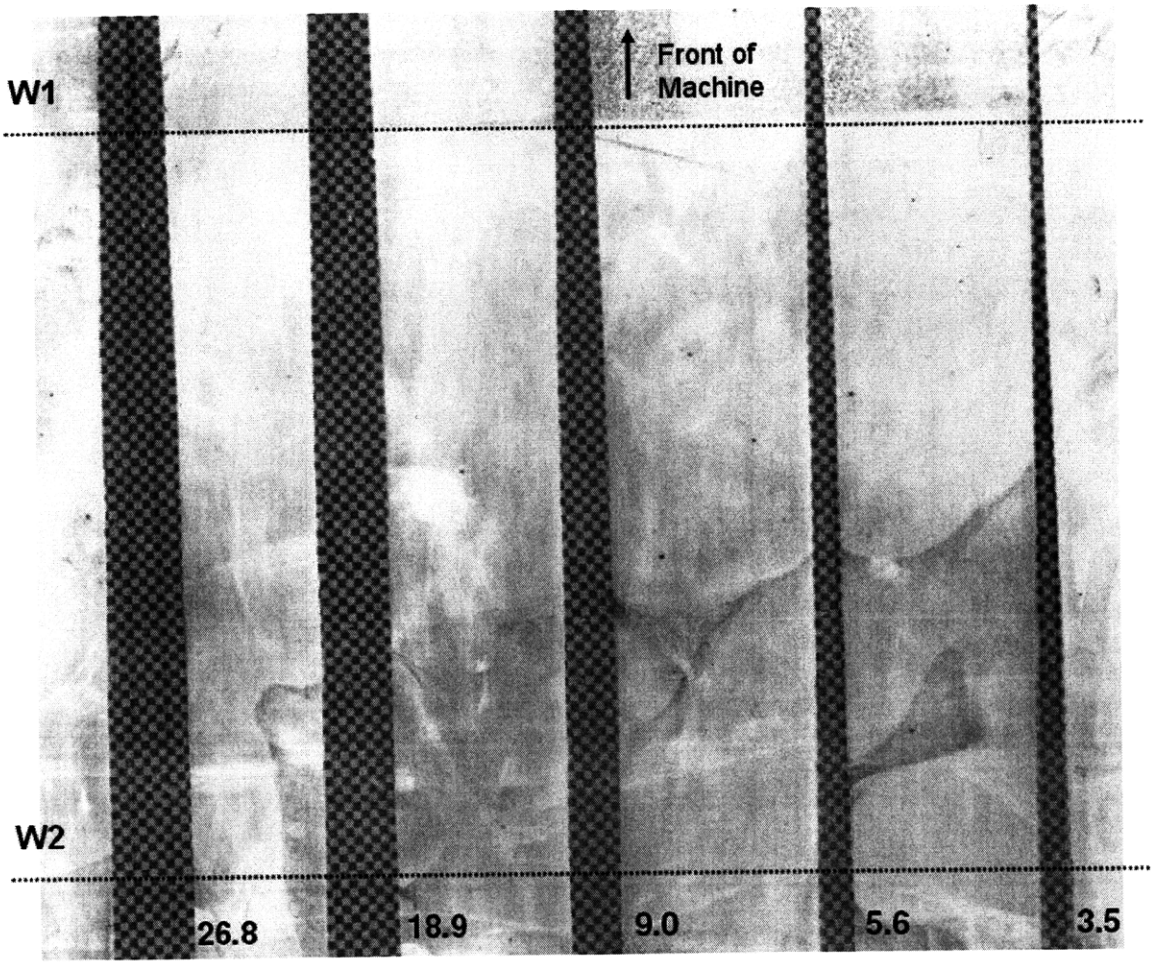

Figure 6-7: Nip Impressions demonstrating the change in contact width with varying load. The corresponding load (in lbs) is shown at the bottom of each print. Their shape implies that there is some misalignment in the system (shims under the roller mounts could improve the alignment); however no systematic effects attributable to this were observed in our results.

Table 6-2: Printing pressure and contact area calculated from nip impressions. Note: the "calculated width" is the width back-calculated from the area and 8" stamp length and represents the ideal width if the contact was perfectly uniform.

Force (lbs)	*W1 (in)*	*W2 (in)*	*Contact Area (in2)*	*Pressure (psi)*	*(Kpa)*	*Calculated Width*
3	0.09	0.23	1.52	2.0	13.6	0.19
5	0.14	0.25	1.75	2.9	19.7	0.22
9	0.27	0.35	2.62	3.4	23.7	0.33
18	0.46	0.52	4.02	4.5	30.9	0.50
27	0.49	0.59	4.49	6.0	41.4	0.56

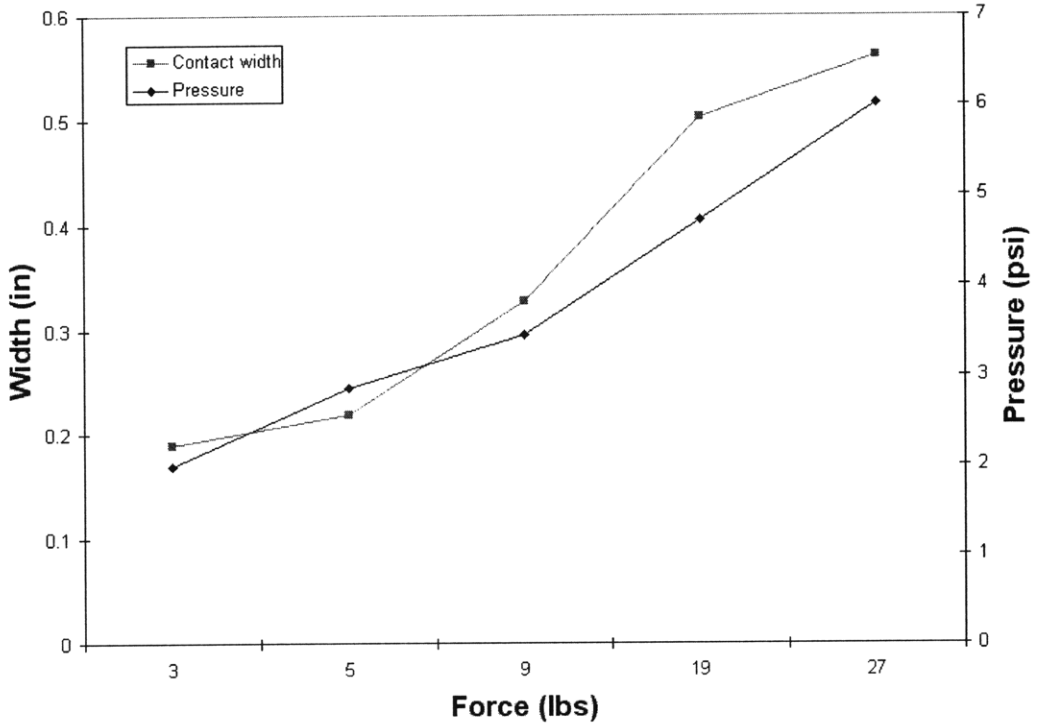

Figure 6-8: This graph depicts the relationship between force and pressure and force and average contact width. Because the contact width increases with force, the pressure is not proportional to force, nor does it increase linearly. It should be noted that the pressure depicted here is only theoretical and represents the average pressure over contact area. The actual pressure distribution may be quite different. The area was calculated using nip impressions, Figure 6-7.

6.5.31 Stamp Dimensions

The dimensions of the stamp were measured to determine their effect on the finished print. Because we did not have the equipment to measure the stamp while mounted to the cylinder, we measured it while flat using a vacuum chuck on the Veritas measuring machine. Note: the measurements were based on the Veritas images, which are less accurate than the Nikon microscope images. The results are as follows:

Table 6-3: Results from stamp measurement

	Mean (μm)	Max (μm)	95th percentile (μm)
Distortions	5.7	13.7	10.7
Dims (width)	39.1 ± .27	-	-
Dims (length)	129.7 ± .21	-	-

Chapter 7

Results

This chapter reports the results from our designed experiments and machine/process performance. Both qualitative and quantitative results are presented.

7.1 Summary of Results

The experiments we conducted revealed a variety of new insight into continuous microcontact printing. Those results of the greatest interest are:

- Neither printing pressure nor speed was found to have a significant effect on spatial distortions and pattern dimensions in the range of settings we used.
- The variation in pattern dimensions was small (C.O.V ~0. 5%) and randomly distributed across the prints.
- Achieved ~100% pattern transfer (yield) on all prints without double-printing or smudging.
- It is possible to print a robust etch-resisting SAM at very high speeds (400 ft/min, unit area contact time ~ 5ms).
- At very high speeds (400ft/min), some systematic air trapping was observed
- Confirmed that PDMS is a very durable stamp material (all prints were made with the same stamp as well as run over plain PET for ~20,000 revolutions).

- The alignment of the stamp on the backing may have a significant effect on distortion patterns.

7.2 Results from 2^2 full factorial DOE

7.2.32 Analysis of dimensional variation

We used a program in MATLAB to compute the overall dimensional variation from the microscope images (Figure 7-3). The results are as follows in Table 7-1:

Table 7-1: Dimensional results from full factorial experiments.

Dimensions, Length

		Speed (fpm)				
		120	60	30		
Force (lbs)	5	133.17	133.03	133.09	Mean	All units in µm
		0.34	0.28	0.36	StDev	
		133.85	133.65	133.85	Max	
	18	132.76	133.13	133.22	Mean	
		0.23	0.37	0.29	StDev	
		133.27	134.04	133.85	Max	

Dimensions, Width

		Speed (fpm)				
		120	60	30		
Force (lbs)	5	40.39	40.27	40.40	Mean	All units in µm
		0.29	0.26	0.24	StDev	
		40.96	40.58	40.77	Max	
	18	40.21	40.38	40.43	Mean	
		0.30	0.28	0.32	StDev	
		40.77	40.77	40.96	Max	

Dimensional variation was found to be small and similar for all the conditions we tested under. The coefficient of Variation was less than .35% under all conditions. The average length and width was larger than the stamp dimensions, which was expected due to stamp stretching and minor over-etching. There also appeared to be no system-

atic effects; the size was evenly distributed throughout the print, as can be seen in the colorbar chart in Figure 7-1 and Figure 7-2.

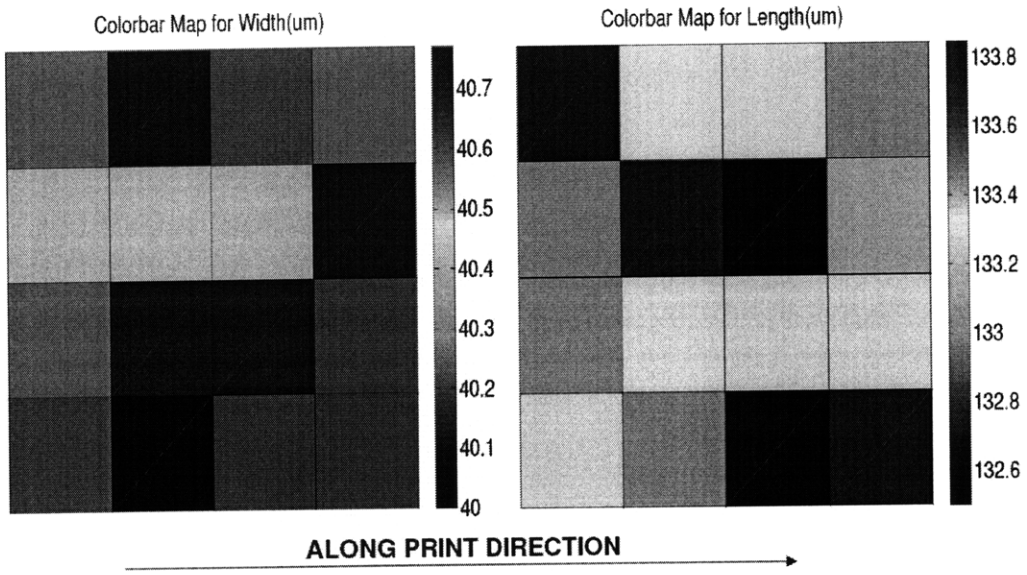

Figure 7-1: A colorbar of the feature length (left) and width (right) at 30fps and 5lbs. The feature size seems to be evenly distributed throughout the print; no systematic effects appear to exist.

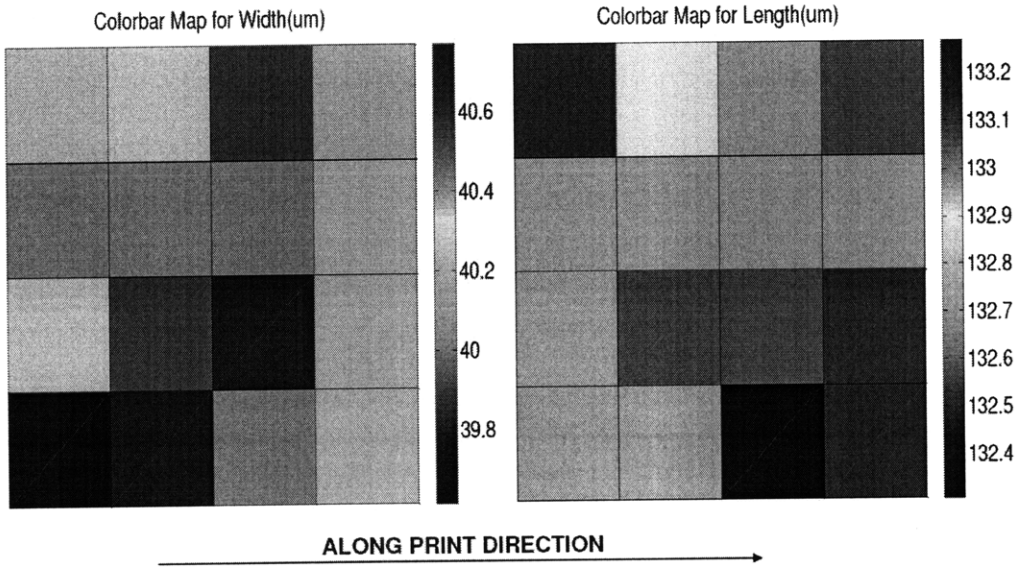

Figure 7-2: Colorbar for 120 fpm, 18 lbs.

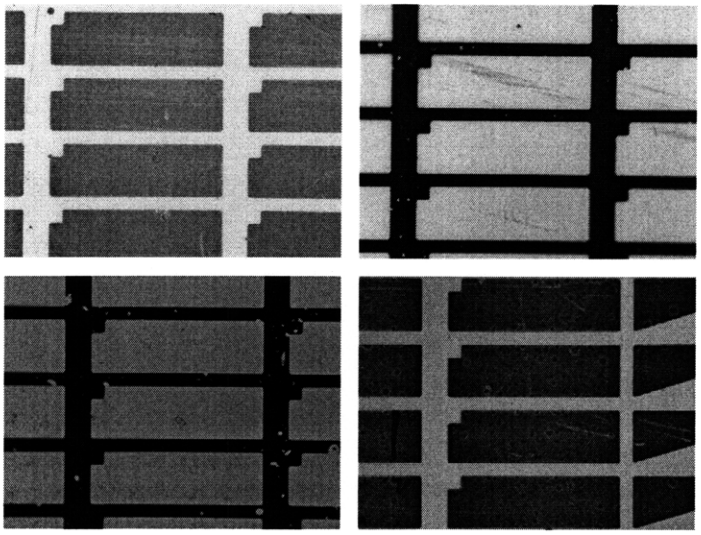

Figure 7-3: Typical images taken on the Nikon microscope. The print on the bottom left was taken later in the experimentation and has various defects that we attributed to stamp deterioration.

An ANOVA analysis was also performed to quantify the effects from printing force (load) and speed (Table 7-2). No significant effects on dimensions or distortions were found in the operating region we tested in as the F-value was found to be less than F-critical. Although, this was somewhat surprising, it is proof that this process is very robust. It would be useful to confirm this in future work by testing under a wider operating range.

Table 7-2: ANOVA results for dimensions (Two-factor without replication)

Mean Pixel Length

Source of Variation	*SS*	*df*	*MS*	*F*	*F crit*	*P-value*
Speed	0.037537	2	0.018768	0.40894	19.00003	0.709753
Load	0.005086	1	0.005086	0.11082	18.51276	0.77087
Error	0.091791	2	0.045895			
Total	0.134414	5				

Mean Pixel Width

Source of Variation	*SS*	*df*	*MS*	*F*	*F crit*	*P-value*
Speed	0.014568	2	0.007284	0.60801	19.00003	0.621887
Width	0.000247	1	0.000247	0.020655	18.51276	0.898896
Error	0.023959	2	0.01198			
Total	0.038774	5				

7.2.33 Analysis of spatial distortions

Distortion analysis was carried out using the Veritas microscope. MATLAB was used to measure and assemble a vector map and other statistics. The results at each setting are summarized in the following table:

Table 7-3: Distortion results from full factorial experiments

Distortions

Force (lbs)	Speed (fpm) 120	60	30		All units in µm
5	21	26	13	Mean	
	51	65	32	Max	
	49	60	28	95%ile	
18	11	19	15	Mean	
	30	64	37	Max	
	37	47	45	95%ile	

As was mentioned before, a diamond shaped pattern was observed in all prints. Because the effect was found in all prints and believed to be caused by stamp misalignment, an algorithm was written in MATLAB to ignore this effect when fitting the grid. The vector map before and after fitting is shown in Figure 7-4.

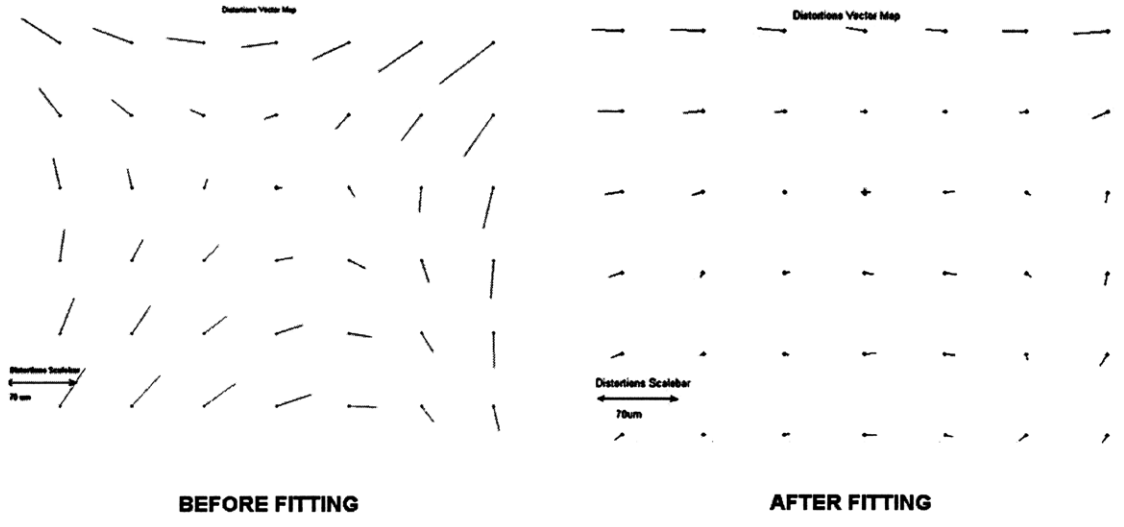

Figure 7-4: The vector map before and after fitting to ignore the effects of stamp misalignment.

An ANOVA analysis was also performed to determine the effects of load and speed on spatial distortion. Like the analysis for dimensional variation, no effect was found on spatial distortion at the operating range we used, indicated by the F-statistic being smaller than F-critical (See Table 7-4). Again, this was a surprise, but was more proof that the process is robust to variations in operating parameters. It is also further support for high-speed microcontact printing.

Table 7-4: ANOVA results for distortion (Two-factor without replication)

95%ile Distortions

Source of Variation	*SS*	*df*	*MS*	*F*	*F crit*	*P-value*
Speed	547.7158	2	273.8579	2.642816	19.00003	0.274513
Load	44.75454	1	44.75454	0.431896	18.51276	0.578578
Error	207.2471	2	103.6235			
Total	799.7174	5				

7.3 Results from 1-D scan of speed

Even at high speeds up to 400fpm, we observed almost 100% pattern transfer with the exception of some systematic air trapping. The pixel dimensions were found to be tightly distributed and did not follow a systematic trend based on increasing speed (Figure 7-5 and Figure 7-6). Distortion results were slightly different, however. We were only able to measure distortions at 240fpm and found the maximum value to be 66 μ m and the 95 percentile of 65.77 μm. These larger distortions could be attributable to the tension being more difficult to control or perhaps a magnification of the alignment effects observed before. The vector map (Figure 7-7) seems to show that the edges are being tensed differently than the middle of the web, perhaps due to the use of "bone rollers" at the drive roller and clutch roller nips.

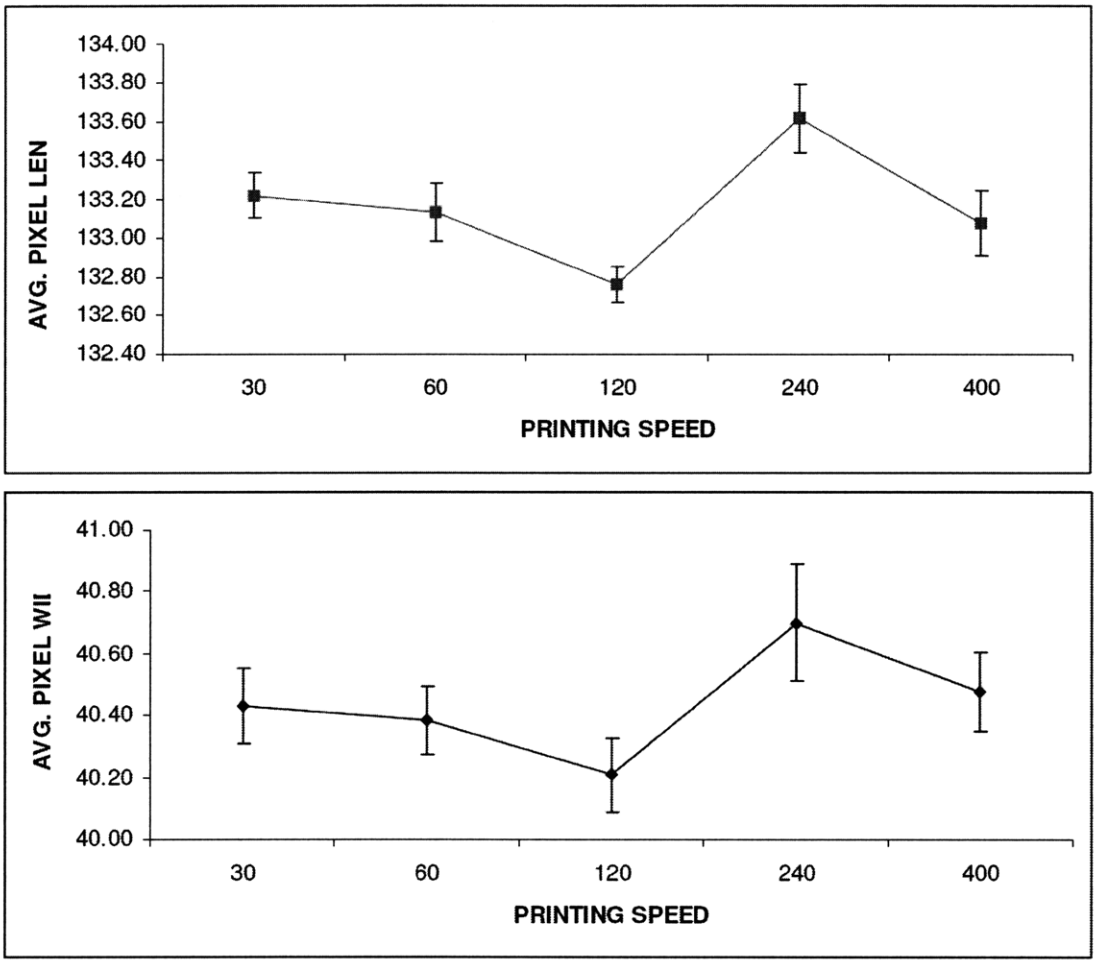

Figure 7-5: 95% confidence intervals on the average pixel lengths as a function of printing speed

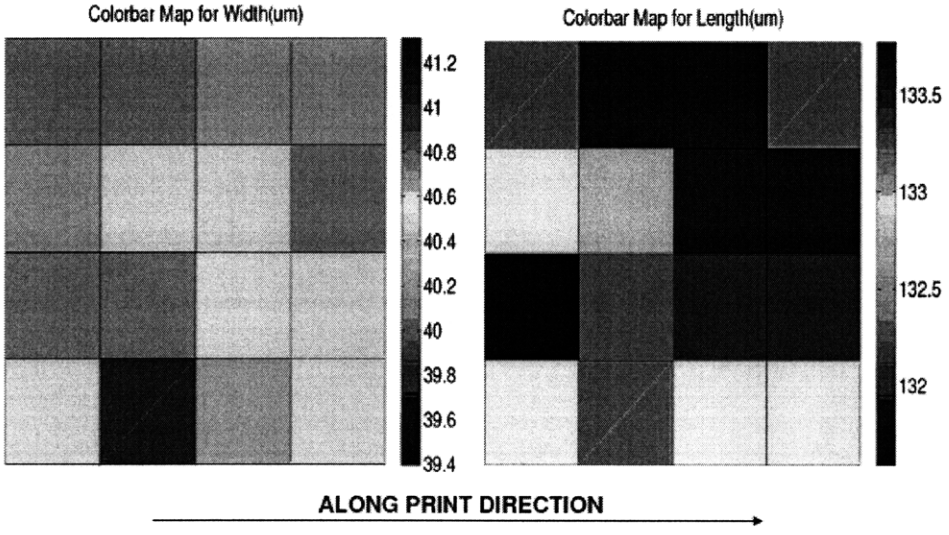

Figure 7-6: Colorbar for 400fpm and 18lbs.

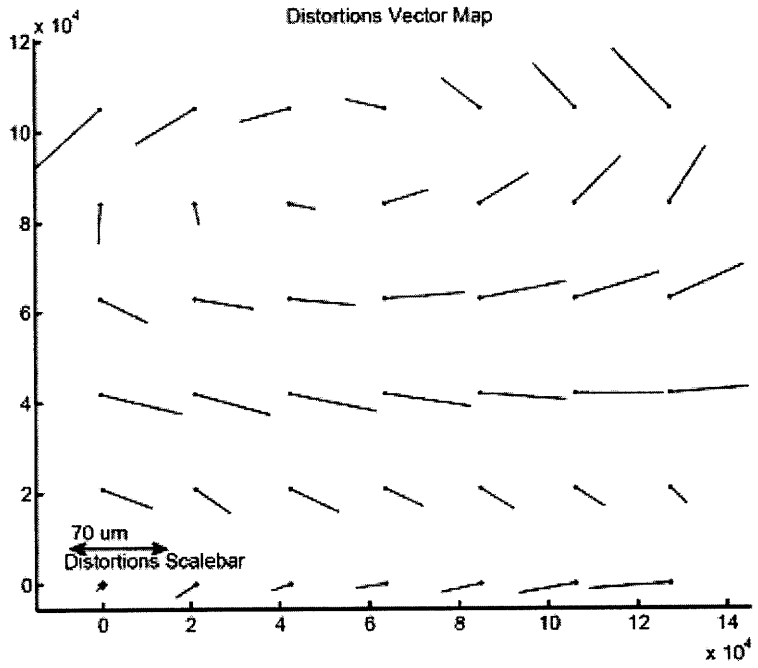

Figure 7-7: Vector map of 240fpm, 18lbs. There appears to be different effects at play at higher speeds from what we observed in previous tests.

The only significant effect we observed at high speed was a very consistent pattern of dots under the triangular pixels (Figure 7-8). They were also observed at 240fpm, but its effects were especially apparent at 400 feet per minute (Figure 7-9). We believe this problem is due to air being trapped between the stamp and substrate in larger areas. Because the contact time is so short (see Table 7-5) the air does not have time to escape and causes a small bubble that inhibits the transfer of thiols in that region. Higher printing forces may be able to alleviate the problem; however we did not have enough time to test that theory. If no other solution can be found, design rules for high speed printing may also have to be applied to limit large print areas where air trapping is most likely to occur.

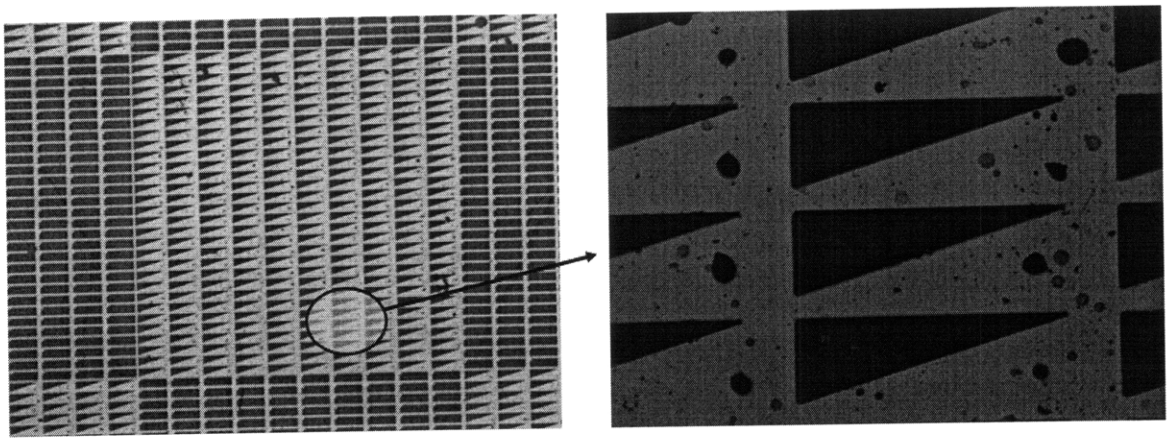

Figure 7-8: Print at 400 fpm. The black dots under each triangular pixel are areas where thiols did not print and were probably caused by air getting trapped between the stamp and substrate.

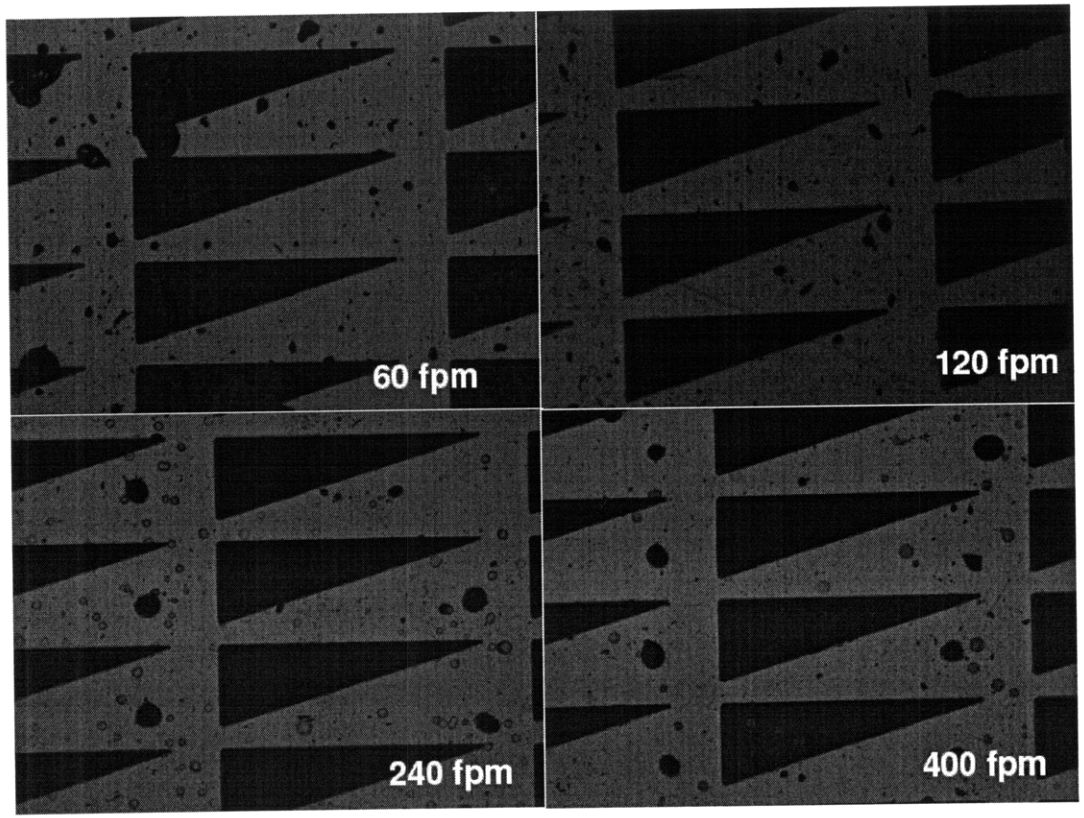

Figure 7-9: Side-by-side comparison of air-trapping at increasing speeds [15]

Table 7-5: The effective contact times for each run calculated from speed and contact width (average contact width determined empirically, see Section 6.5.30).

Speed (fpm)	*Force (lbs)*	*Contact Width (in)*	*Contact Time (ms)*
30	18	0.50	84
60	18	0.50	42
120	18	0.50	21
200	18	0.50	13
400	18	0.50	6

7.4 Continuous Etching Results

A 48" print was made with the printing machine and attached to a leader and follower of plain PET. The web was fed through a tank of thiourea ferric nitrate at approximately 2 fpm (it could be run faster by increasing the number of rollers or depth of tank). Agitation was done manually by moving the tank. The print was etched satisfactorily and proved that continuous etching is possible even with a slow etchant such as thiourea. By scaling the size of the modules up and using faster etchants, it is feasible that etching could be done at rates comparable to printing.

7.5 Machine Performance Results

Several aspects were used to determine the overall performance of the machine:

- *Printing force accuracy and precision*: load cell data from the PLC was collected from the serial port during each run and analyzed to verify that printing force did not vary greatly during the print. By observing patterns in the data, we extracted the regions from the actual print (Figure 7-10) and confirmed that printing force varied little during most prints (~1.5% COV).

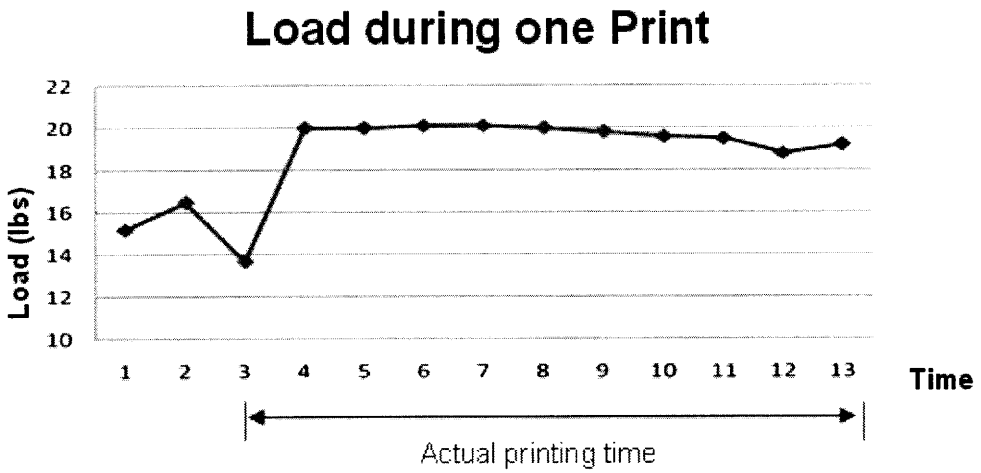

Figure 7-10: Load cell data from one print, extracted from the overall data set from the entire run.

- *Tension control precision*: tension data from the first sensor was collected from the PLC via the serial port during each run and analyzed to verify that it was in control (Figure 7-11). It typically never varied more than 0.50 pounds during most runs. There was a settling period after each seam, however, that caused most of this variation. By covering the seam with foam or PDMS, the effect could probably be reduced. Nevertheless, the tension control system worked quite well and was able to maintain a very light tension, even at high speeds. More information regarding the control system performance can be found in Shawn Shen's thesis [25].

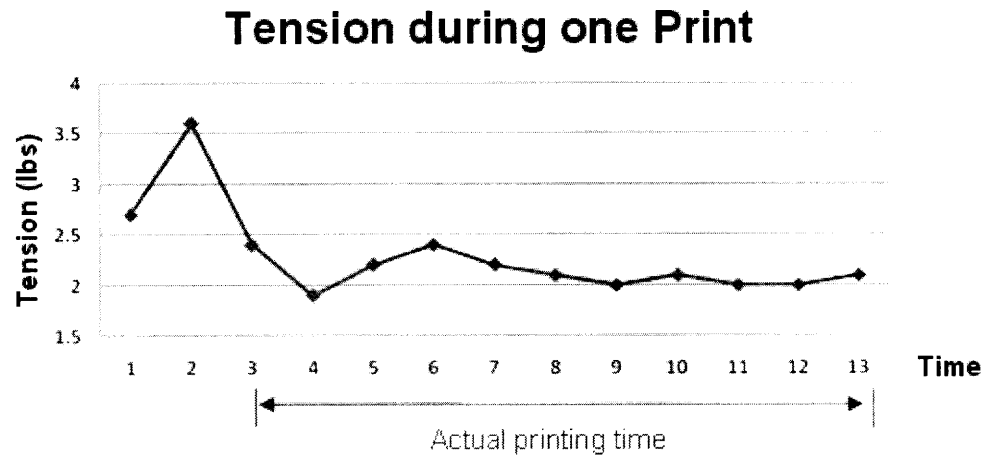

Figure 7-11: Tension data (from the first sensor) from one print, extracted from the overall data set from the entire run.

- *Control system robustness*: the control program on the PLC and PLC hardware worked very well. Even under varying conditions, the PID parameters only needed moderate tuning.
- *Appearance of the web*: with proper alignment of the substrate, the web flowed through the machine very smoothly, with no bagginess or wrinkling. Nip pressure at the drive roller and clutch roller also proved to be critical. By attaching foam around the bone roller, we were able to make this setting less sensitive.
- *E-stop function*: the emergency stop relay worked well and cut off power to the motor drives quickly. Fortunately, it was never needed, but is an important feature of any automated system.
- *Effectiveness of stamp mounting*: mounting the stamp was fast and effective; however it took some experimentation to perfect the technique. The best method was to loosen the Stamp Retainer Bar (SRB); stand the Stamp Tube on end; insert one end of the stamp and temporarily tape it in place to the SRB; carefully wrap the stamp around and insert the other end into the groove on the SRB; loosely place the hose clamps on each end; tighten down the SRB; and finally tighten the hose clamps slightly. Tightening the hose clamps too much tends to cause bulges. Better hose clamps that can exert pressure all the way around would be ideal.

Chapter 8

Conclusions and Future Work

A working roll-to-roll machine was developed that demonstrated the ability to perform microcontact printing at high speeds and sufficient quality. The machine demonstrates that the integration of traditional printing hardware and techniques with microcontact printing is feasible. Also, it is a step in a positive direction for a technology that has been done primarily in a manual fashion in a laboratory setting.

Two sets of experiments were designed to assess quality based on input factors. In the first, printing pressure and speed were varied and the quantitative effects on dimensional variation and distortion were evaluated. In the other experiment a 1-dimensional scan of the effect of high speed was evaluated. The following conclusions were reached based on these experiments:

- 100% pattern transfer occurred at all settings used. Double-printing and/or slip was never observed.
- Neither printing pressure nor speed was found to have a significant effect on spatial distortions and pattern dimensions. The variation in pattern dimensions was small (C.O.V ~0. 5%) and randomly distributed across the prints.
- Producing a high-quality, etch resistant SAM is possible even at high speeds (400 fpm). Air trapping does tend to occur after about 200 fpm, however. It appears that high speeds are mainly limited by contact time, mechanical constraints, and aerodynamics.

- PDMS is a highly durable stamp material. The stamp was used for 1000's of prints during machine testing and during experimentation. It imprinted on plain PET many 1000's of times while the machine was first being tested.
- Injection molding is the preferred method of producing large area stamps. We were not able to achieve good results by other methods.
- Our method and apparatus for wrapping stamps around cylinders appeared to be a robust solution that could be used in a production environment.
- The machine that we developed is robust, easy to operate, and produces good results, both in terms of printing and web handling.

There is a great deal of additional work to be done to gain further insight into roll-to-roll μCP for mass production. Following is a list of the areas we think are most critical:

- *SEM analysis of edge roughness*: This metric was not used during analysis, but could provide further insight.
- *Standardized 1-d scan on printing speed*: because our method was not fully standardized during this test, we had some results that we believe could have been better, had a stricter protocol been followed. This could include: a more consistent inking process, using fresh etchant of the same temperature and time for each print, as well as other factors.
- *Effect of stamp thickness and alignment*: these may be a key factor in distortion.
- *High speeds at larger wrap angles*: Wrap angle could help the transfer of SAM's during high-speed printing and perhaps reduce the effects of air trapping.
- *Reduction of pinholes caused by dust particles*: Higher quality prints can be made if dust can be eliminated from the environment. Static caused by the PET was a major issue that seemed to attract large amounts of dust.
- *Better estimation of stamp life and durability*: Although we observed long stamp life, it was never measured. A quantitative analysis would be valuable.

- *Continuous Inking*: As we did not have enough time to test this system and it would contribute greatly to commercialization of continuous μCP, this may be an area of great interest.
- *Printing Pressure*: Actual printing pressure should be measured to evaluate effects and machine performance. A flexible sensor or other similar method should be used.
- *Impression Assembly Improvements*: the load cells should be placed directly above the pillow blocks. A lower friction bearing system should also be in place; perhaps using a flexure or a pivot/counterbalance system.
- *New Stamp Manufacturing Methods*: The injection molding technique seemed to work very well, however other methods should be developed to produce high-quality stamps. A larger injection mold with two large wafers could be made that can maximize stamp area on the printing cylinder. The stamp is truly the heart of the machine and it needs more attention.

Appendix A

Engineering Drawings

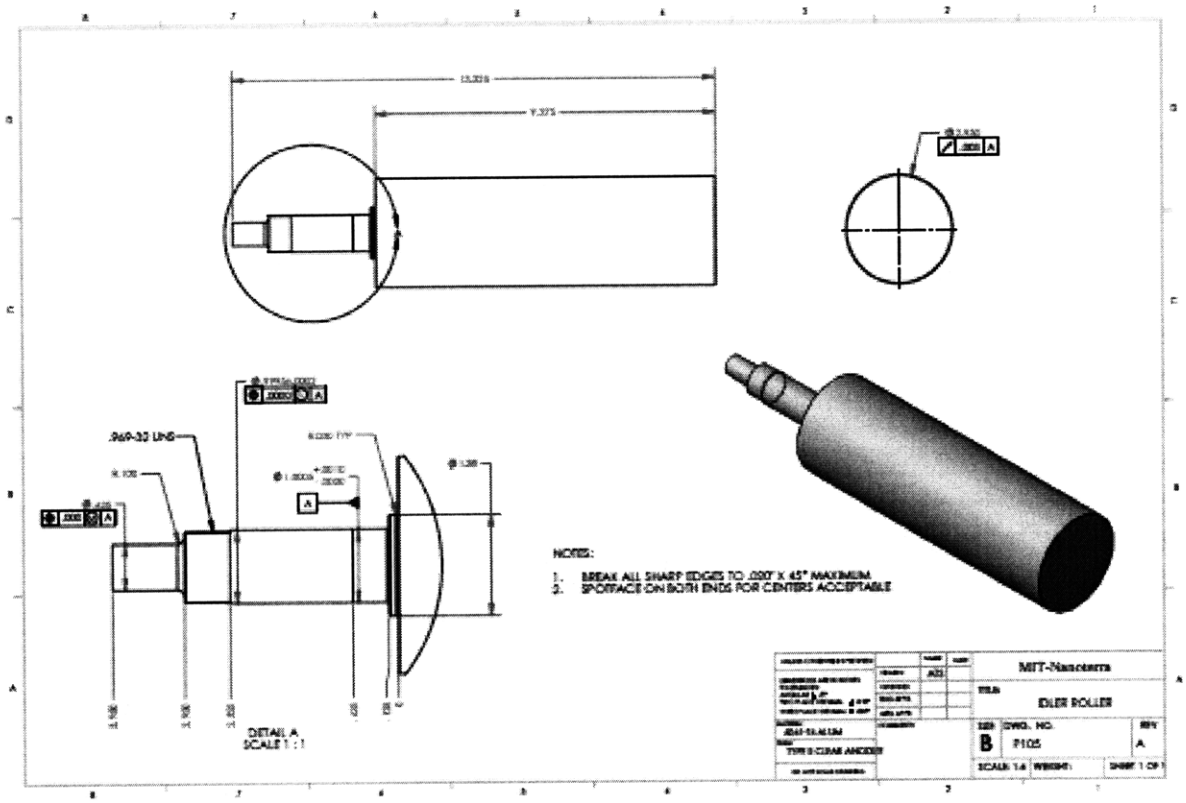
.969-32 UNS
DETAIL A
SCALE 1 : 1
NOTES:
1. BREAK ALL SHARP EDGES TO .020" X 45° MAXIMUM
2. SPOTFACE ON BOTH ENDS FOR CENTERS ACCEPTABLE
MIT-Nanoterra
IDLER ROLLER
B
P105

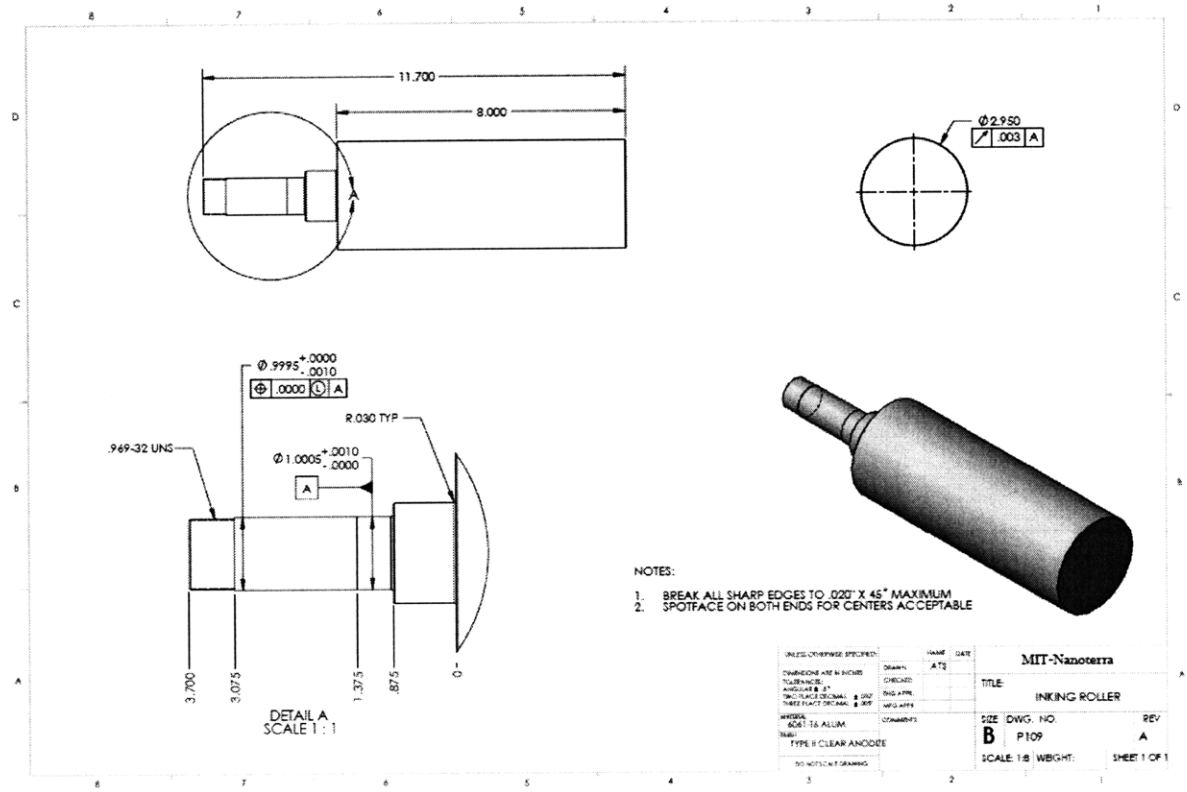
11.700
8.000
Ø2.950
.003 A
.969-32 UNS
R.030 TYP
3.700
3.075
1.375
.875
DETAIL A
SCALE 1 : 1
NOTES:
1. BREAK ALL SHARP EDGES TO .020" X 45° MAXIMUM
2. SPOTFACE ON BOTH ENDS FOR CENTERS ACCEPTABLE
MIT-Nanoterra
INKING ROLLER
B
P109
A

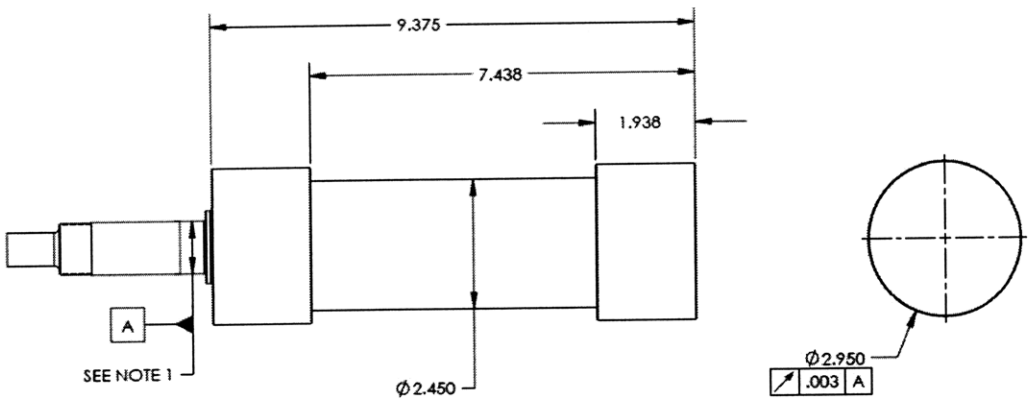

NOTES:

1. REFER TO DRAWING NO. P105 DETAIL-A FOR ADD'L SHAFT DIMENSIONS
2. BREAK ALL SHARP EDGES TO .020" X 45° MAXIMUM
3. SPOTFACE ON BOTH ENDS FOR CENTERS ACCEPTABLE

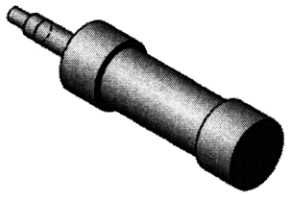

UNLESS OTHERWISE SPECIFIED:		NAME	DATE
DIMENSIONS ARE IN INCHES	DRAWN	ATS	
TOLERANCES: ANGULAR ± .5° TWO PLACE DECIMAL ± .010" THREE PLACE DECIMAL ± .005"	CHECKED		
	ENG APPR.		
	MFG APPR.		
MATERIAL: 6061-T6 ALUM	COMMENTS:		
FINISH: TYPE II CLEAR ANODIZE			
DO NOT SCALE DRAWING			

MIT-Nanoterra

TITLE: BONE ROLLER

SIZE A | DWG. NO. P106 | REV A

SCALE: 1:8 | WEIGHT: | SHEET 1 OF 1

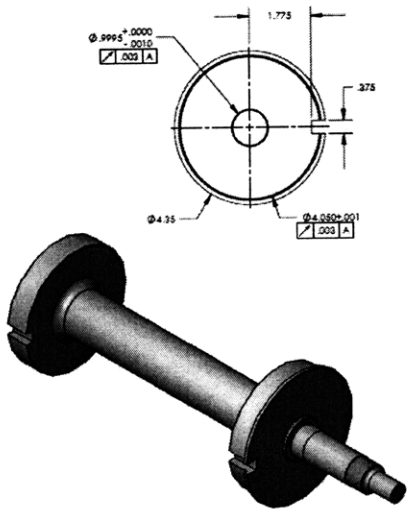

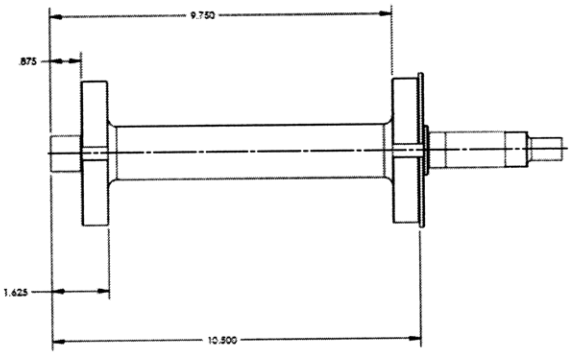

NOTES:

1. REFER TO DRAWING NO. P105 DETAIL-A FOR ADDITIONAL SHAFT DIMENSIONS
2. BREAK ALL SHARP EDGES TO .020" X 45° MAXIMUM
3. SPOTFACE ON BOTH ENDS FOR CENTERS ACCEPTABLE

UNLESS OTHERWISE SPECIFIED:		NAME	DATE
DIMENSIONS ARE IN INCHES	DRAWN	ATS	
TOLERANCES: ANGULAR ± .5° TWO PLACE DECIMAL ± .010" THREE PLACE DECIMAL ± .005"	CHECKED		
	ENG APPR.		
	MFG APPR.		
MATERIAL: 6061-T6 ALUM	COMMENTS:		
FINISH: TYPE II CLEAR ANODIZE			
DO NOT SCALE DRAWING			

MIT-Nanoterra

TITLE: PRINT ROLLER

SIZE B | DWG. NO. P108 | REV A

SCALE: 1:4 | WEIGHT: | SHEET 1 OF 1

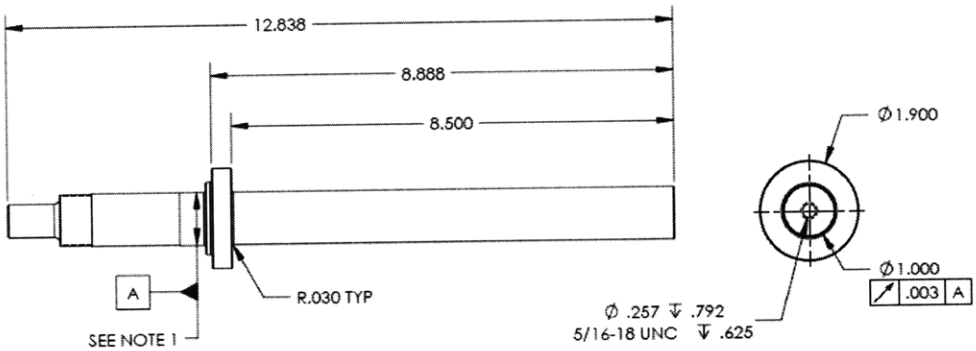

NOTES:

1. REFER TO DRAWING NO. P105 DETAIL-A FOR ADD'L SHAFT DIMENSIONS
2. BREAK ALL SHARP EDGES TO .020" X 45° MAXIMUM
3. SPOTFACE ON BOTH ENDS FOR CENTERS ACCEPTABLE

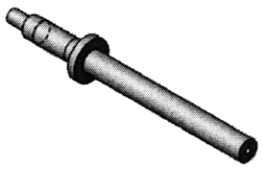

UNLESS OTHERWISE SPECIFIED: DIMENSIONS ARE IN INCHES. TOLERANCES: ANGULAR ± .5° TWO PLACE DECIMAL ± .010" THREE PLACE DECIMAL ± .005"		NAME / DATE	MIT-Nanoterra
	DRAWN	ATS	
	CHECKED		TITLE: SPOOL ROLLER
	ENG APPR.		
	MFG APPR.		
MATERIAL: 6061-T6 ALUM	COMMENTS:		SIZE: A — DWG. NO.: P107 — REV: A
FINISH: TYPE II CLEAR ANODIZE			SCALE: 1:8 — WEIGHT: — SHEET 1 OF 1
DO NOT SCALE DRAWING			

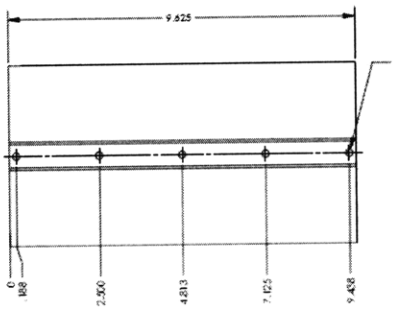

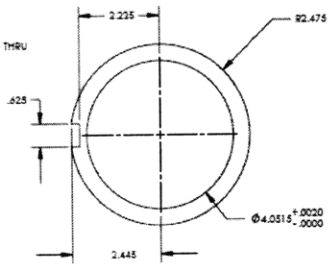

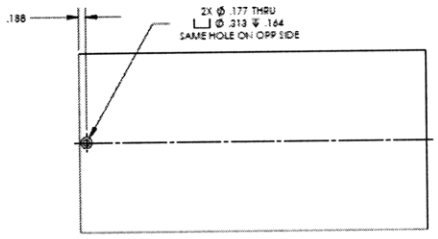

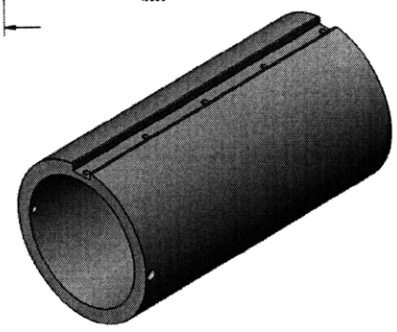

NOTES:

1. BREAK ALL SHARP EDGES TO .020" X 45° MAXIMUM

UNLESS OTHERWISE SPECIFIED: DIMENSIONS ARE IN INCHES. TOLERANCES: ANGULAR ± .5° TWO PLACE DECIMAL ± .010" THREE PLACE DECIMAL ± .005"		NAME / DATE	MIT-Nanoterra
	DRAWN	ATS	
	CHECKED		TITLE: STAMP TUBE
	ENG APPR.		
	MFG APPR.		
MATERIAL: 6061-T6 ALUM	COMMENTS:		SIZE: B — DWG. NO.: P112 — REV: A
FINISH: TYPE II CLEAR ANODIZE			SCALE: 1:2 — WEIGHT: — SHEET 1 OF 1
DO NOT SCALE DRAWING			

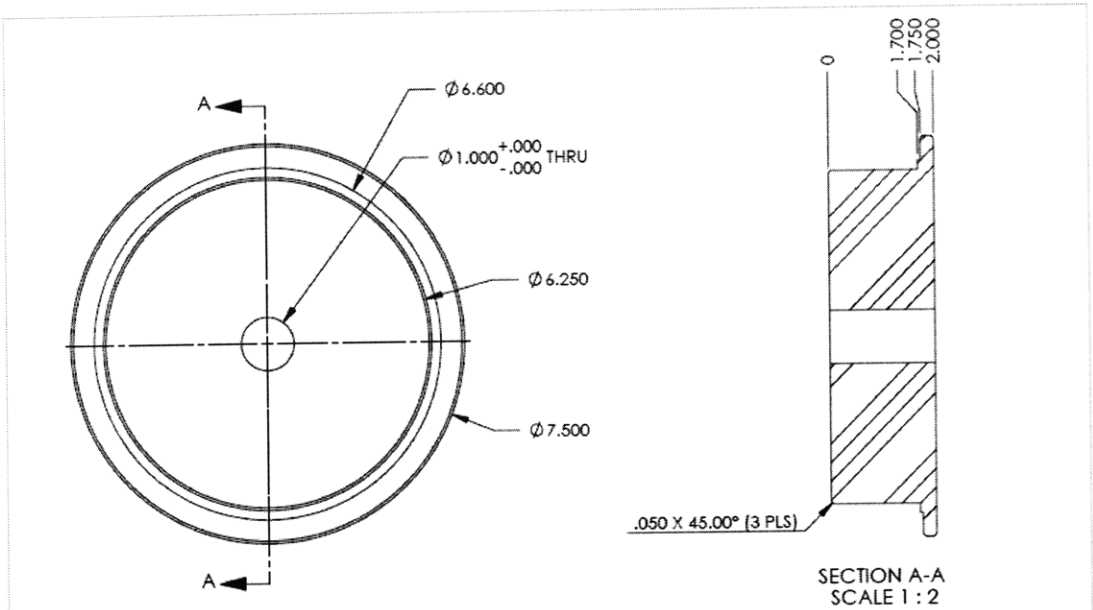

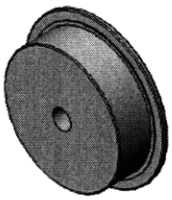

UNLESS OTHERWISE SPECIFIED:		NAME	DATE
DIMENSIONS ARE IN INCHES TOLERANCES: ANGULAR ± .5° TWO PLACE DECIMAL ± .010" THREE PLACE DECIMAL ± .005"	DRAWN	ATS	
	CHECKED		
	ENG APPR.		
	MFG APPR.		
MATERIAL: NYLON	COMMENTS:		
FINISH			
DO NOT SCALE DRAWING			

MIT-Nanoterra

TITLE: SUBSTRATE SPOOL END

SIZE	DWG. NO.	REV
A	P117	A

SCALE: 1:4 WEIGHT: SHEET 1 OF 1

5 4 3 2 1

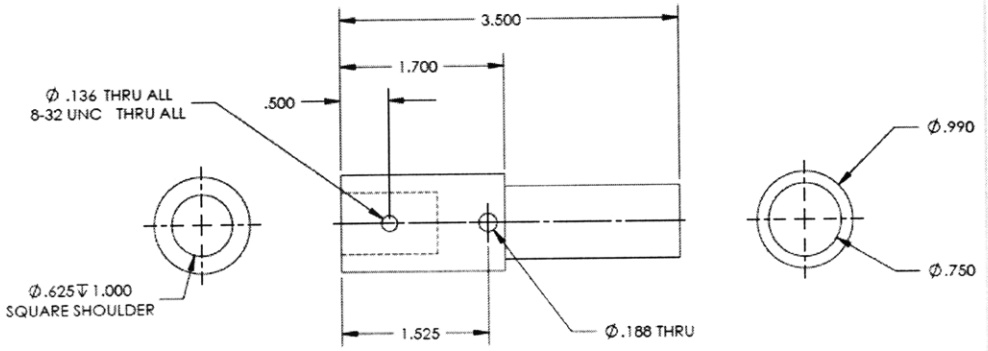

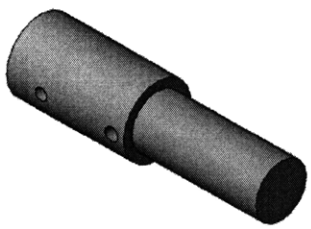

UNLESS OTHERWISE SPECIFIED:		NAME	DATE
DIMENSIONS ARE IN INCHES TOLERANCES: ANGULAR ± .5° TWO PLACE DECIMAL ± .010" THREE PLACE DECIMAL ± .005"	DRAWN	ATS	
	CHECKED		
	ENG APPR.		
	MFG APPR.		
MATERIAL: ALUM	COMMENTS:		
FINISH			
DO NOT SCALE DRAWING			

MIT-Nanoterra

TITLE: ADAPTER SHAFT

SIZE	DWG. NO.	REV
A	P202	A

SCALE: 1:2 WEIGHT: SHEET 1 OF 1

5 4 3 2 1

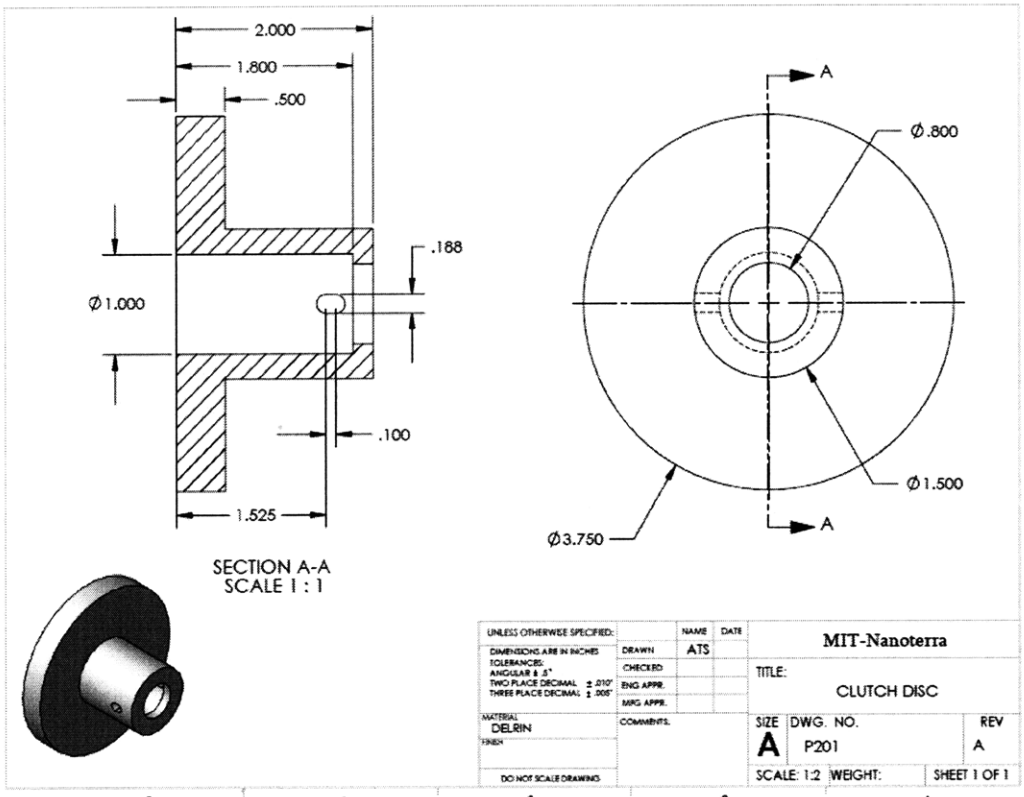
2.000
1.800
.500
.188
Ø1.000
.100
1.525
SECTION A-A
SCALE 1 : 1
A
Ø.800
Ø1.500
Ø3.750
A
UNLESS OTHERWISE SPECIFIED:
DIMENSIONS ARE IN INCHES
TOLERANCES:
ANGULAR ± .5°
TWO PLACE DECIMAL ± .010"
THREE PLACE DECIMAL ± .005"
DRAWN
CHECKED
ENG APPR.
MFG APPR.
COMMENTS:
NAME
DATE
ATS
MIT-Nanoterra
TITLE:
CLUTCH DISC
MATERIAL
DELRIN
FINISH
DO NOT SCALE DRAWING
SIZE
A
DWG. NO.
P201
REV
A
SCALE: 1:2
WEIGHT:
SHEET 1 OF 1

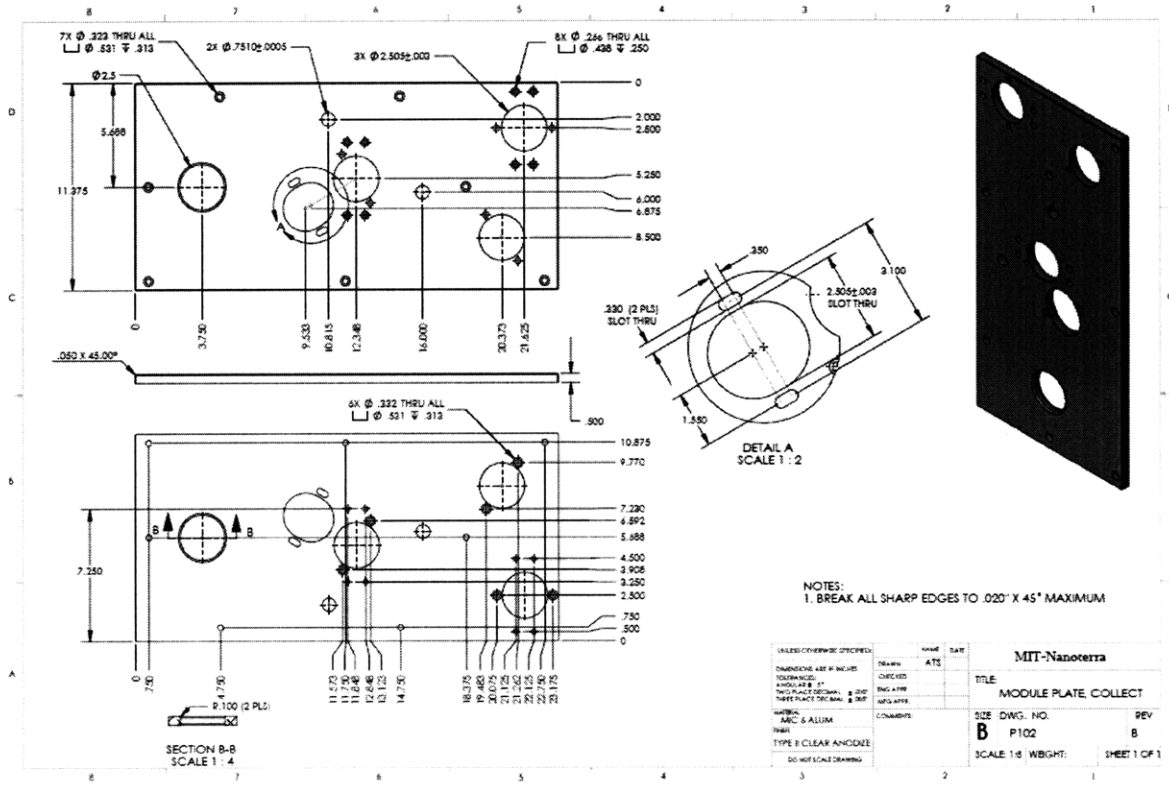
7X Ø .323 THRU ALL
⌴ Ø .531 ↧ .313
2X Ø.7510±.0005
3X Ø2.505±.003
8X Ø .266 THRU ALL
⌴ Ø .438 ↧ .250
Ø2.5
5.688
11.375
0
2.000
2.800
5.250
6.000
6.875
8.500
3.750
9.533
10.815
12.348
16.000
20.375
21.625
.050 X 45.00°
.500
6X Ø .332 THRU ALL
⌴ Ø .531 ↧ .313
10.875
9.770
7.220
6.592
5.688
4.500
3.908
3.250
2.500
.750
.500
0
7.250
B
B
.750
1.750
11.750
12.846
13.125
14.750
18.375
19.485
20.075
21.125
21.262
22.125
22.230
23.175
R.100 (2 PLS)
SECTION B-B
SCALE 1 : 4
.350
3.100
.330 (2 PLS)
SLOT THRU
2.505±.003
SLOT THRU
1.550
DETAIL A
SCALE 1 : 2
NOTES:
1. BREAK ALL SHARP EDGES TO .020" X 45° MAXIMUM
UNLESS OTHERWISE SPECIFIED:
DIMENSIONS ARE IN INCHES
TOLERANCES:
ANGULAR ± .5°
TWO PLACE DECIMAL ± .010"
THREE PLACE DECIMAL ± .005"
DRAWN
CHECKED
ENG APPR.
MFG APPR.
COMMENTS:
NAME
DATE
ATS
MIT-Nanoterra
TITLE:
MODULE PLATE, COLLECT
MATERIAL
MIC 6 ALUM
FINISH
TYPE II CLEAR ANODIZE
DO NOT SCALE DRAWING
SIZE
B
DWG. NO.
P102
REV
B
SCALE: 1:4
WEIGHT:
SHEET 1 OF 1

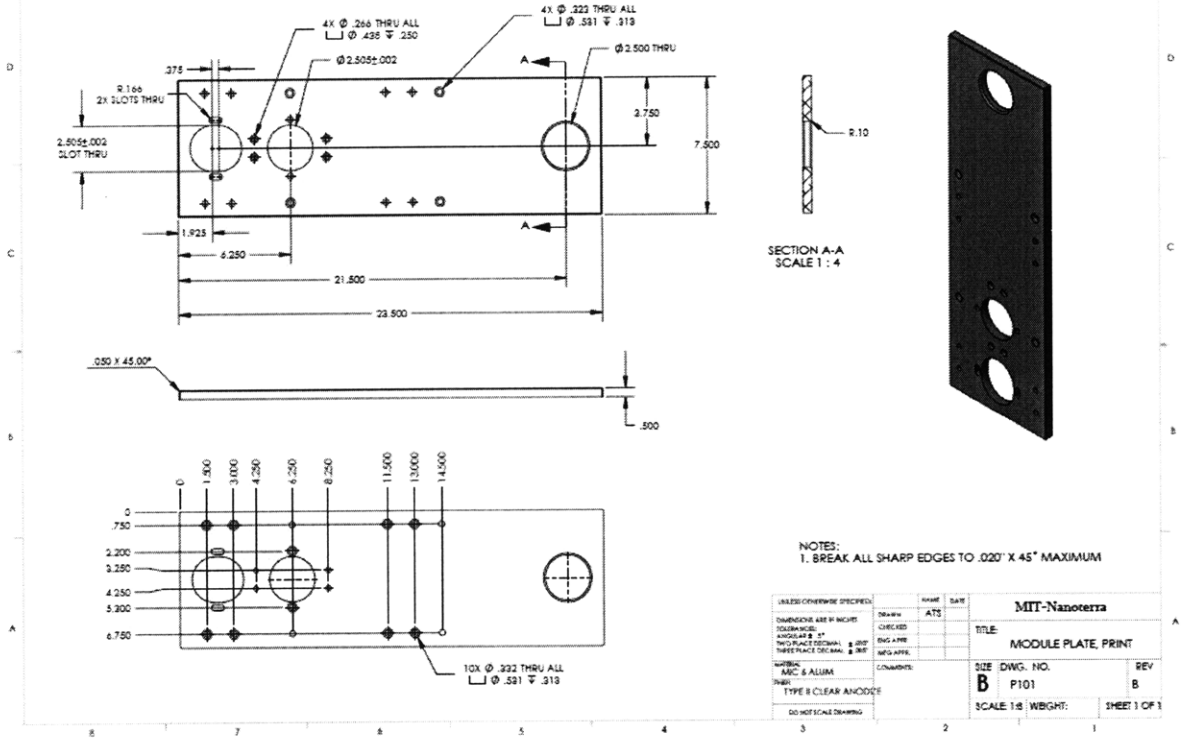
4X Ø .266 THRU ALL
⌴ Ø .438 ↧ .250
4X Ø .322 THRU ALL
⌴ Ø .531 ↧ .313
Ø2.500 THRU
Ø2.505±.002
.375
R.166
2X SLOTS THRU
2.505±.002
SLOT THRU
2.750
7.500
1.925
6.250
21.500
23.500
A
A
R.10
SECTION A-A
SCALE 1 : 4
.050 X 45.00°
.500
0
1.300
3.000
4.250
6.250
8.250
11.500
13.000
14.500
0
.750
2.200
3.250
4.250
5.300
6.750
10X Ø .322 THRU ALL
⌴ Ø .531 ↧ .313
NOTES:
1. BREAK ALL SHARP EDGES TO .020" X 45° MAXIMUM
UNLESS OTHERWISE SPECIFIED:
DIMENSIONS ARE IN INCHES
TOLERANCES:
ANGULAR: ± .5°
TWO PLACE DECIMAL ± .010"
THREE PLACE DECIMAL ± .005"
MATERIAL
MIC 6 ALUM
FINISH
TYPE II CLEAR ANODIZE
DO NOT SCALE DRAWING
NAME
DATE
DRAWN
ATS
CHECKED
ENG APPR.
MFG APPR.
COMMENTS:
MIT-Nanoterra
TITLE:
MODULE PLATE, PRINT
SIZE
B
DWG. NO.
P101
REV
B
SCALE: 1:8
WEIGHT:
SHEET 1 OF 1

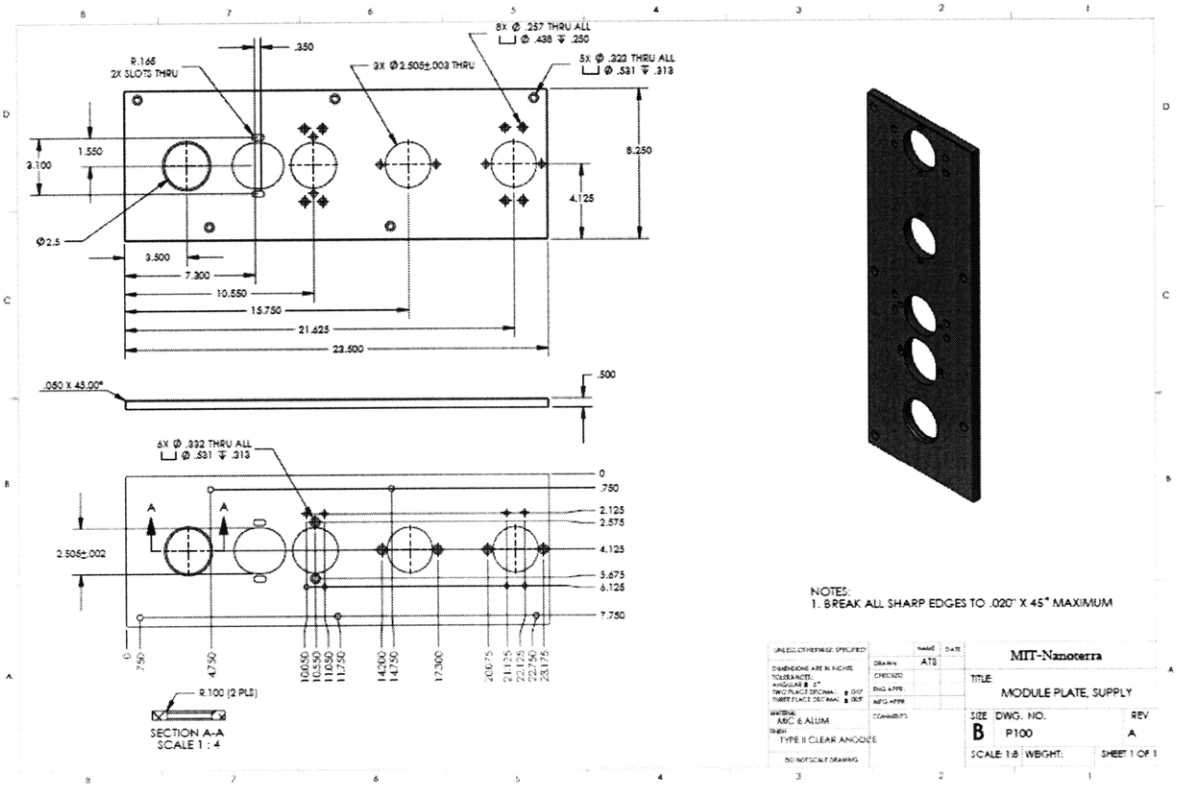
8X Ø .257 THRU ALL
⌴ Ø .438 ↧ .250
5X Ø .322 THRU ALL
⌴ Ø .531 ↧ .313
3X Ø2.505±.003 THRU
R.166
2X SLOTS THRU
.350
3.100
1.550
8.250
4.125
Ø2.5
3.500
7.300
10.550
15.750
21.625
23.500
.050 X 45.00°
.500
6X Ø .322 THRU ALL
⌴ Ø .531 ↧ .313
2.505±.002
A
A
0
.750
2.125
2.575
4.125
5.675
6.125
7.750
0
.750
4.750
10.050
10.550
11.050
11.750
14.300
14.750
17.300
20.075
21.125
22.125
22.675
23.175
R.100 (2 PLS)
SECTION A-A
SCALE 1 : 4
NOTES:
1. BREAK ALL SHARP EDGES TO .020" X 45° MAXIMUM
UNLESS OTHERWISE SPECIFIED:
DIMENSIONS ARE IN INCHES
TOLERANCES:
ANGULAR: ± .5°
TWO PLACE DECIMAL ± .010"
THREE PLACE DECIMAL ± .005"
MATERIAL
MIC 6 ALUM
FINISH
TYPE II CLEAR ANODIZE
DO NOT SCALE DRAWING
NAME
DATE
DRAWN
ATS
CHECKED
ENG APPR.
MFG APPR.
COMMENTS:
MIT-Nanoterra
TITLE:
MODULE PLATE, SUPPLY
SIZE
B
DWG. NO.
P100
REV
A
SCALE: 1:8
WEIGHT:
SHEET 1 OF 1

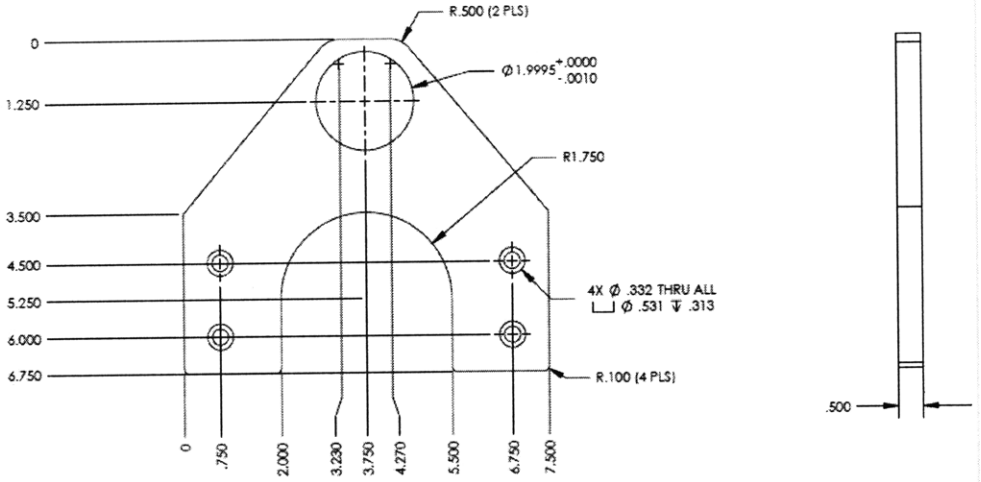

NOTE:
1. BREAK ALL SHARP EDGES TO .020" X 45° MAX

UNLESS OTHERWISE SPECIFIED: DIMENSIONS ARE IN INCHES TOLERANCES: ANGULAR ± .5° TWO PLACE DECIMAL ± .010" THREE PLACE DECIMAL ± .005"		NAME / DATE	MIT-Nanoterra
	DRAWN	ATS	TITLE: BEARING PLATE, PRINT
	CHECKED		
	ENG APPR.		
	MFG APPR.		
MATERIAL: MIC 6 ALUM FINISH: TYPE II CLEAR ANODIZE	COMMENTS:		SIZE: A — DWG. NO. P111 — REV: A
DO NOT SCALE DRAWING			SCALE: 1:4 — WEIGHT: — SHEET 1 OF 1

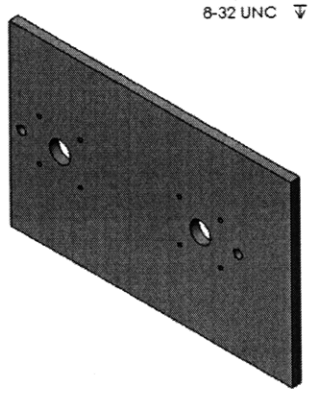

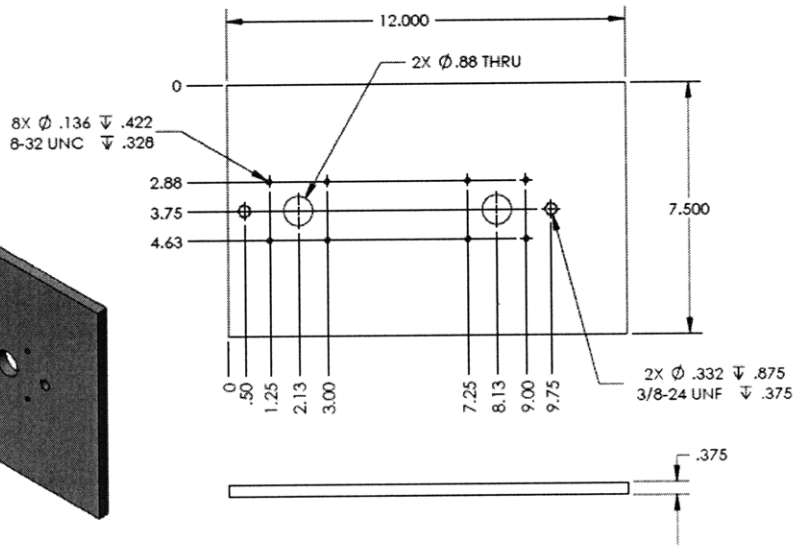

NOTE:
1. BREAK ALL SHARP EDGES TO .020" X 45° MAX

UNLESS OTHERWISE SPECIFIED: DIMENSIONS ARE IN INCHES TOLERANCES: ANGULAR ± .5° TWO PLACE DECIMAL ± .010" THREE PLACE DECIMAL ± .005"		NAME / DATE	MIT-Nanoterra
	DRAWN	ATS	TITLE: IMPRESSION FIXED PLATE
	CHECKED		
	ENG APPR.		
	MFG APPR.		
MATERIAL: MIC 6 ALUM FINISH: TYPE II CLEAR ANODIZE	COMMENTS:		SIZE: A — DWG. NO. P116 — REV: A
DO NOT SCALE DRAWING			SCALE: 1:8 — WEIGHT: — SHEET 1 OF 1

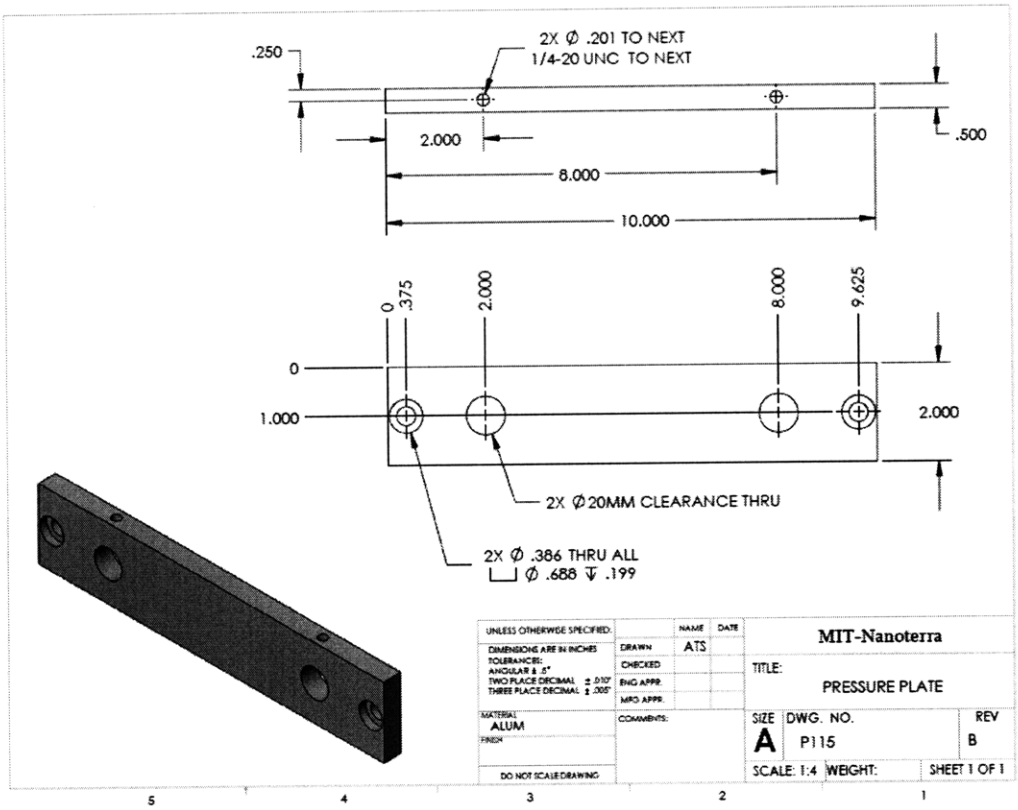

UNLESS OTHERWISE SPECIFIED:		NAME	DATE
DIMENSIONS ARE IN INCHES	DRAWN	ATS	
TOLERANCES:	CHECKED		
ANGULAR ± .5°	ENG APPR.		
TWO PLACE DECIMAL ± .010"	MFG APPR.		
THREE PLACE DECIMAL ± .005"			
MATERIAL: ALUM	COMMENTS:		
FINISH			
DO NOT SCALE DRAWING			

MIT-Nanoterra

TITLE: PRESSURE PLATE

SIZE	DWG. NO.	REV
A	P115	B

SCALE: 1:4 | WEIGHT: | SHEET 1 OF 1

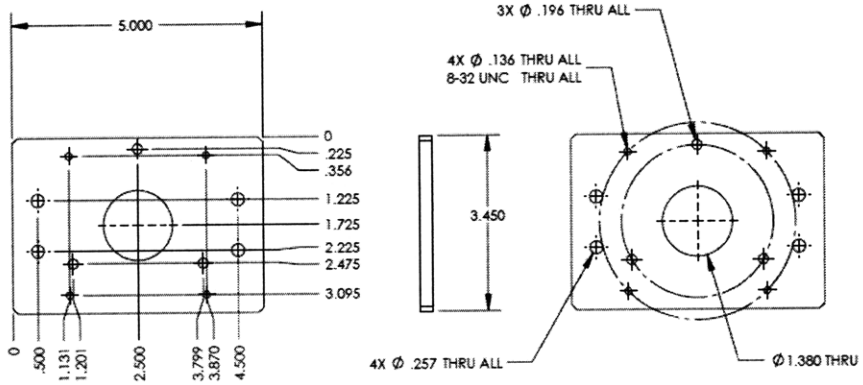

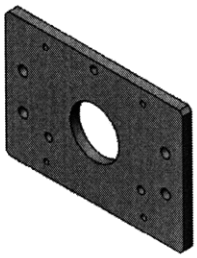

UNLESS OTHERWISE SPECIFIED:		NAME	DATE
DIMENSIONS ARE IN INCHES	DRAWN	ATS	
TOLERANCES:	CHECKED		
ANGULAR ± .5°	ENG APPR.		
TWO PLACE DECIMAL ± .010"	MFG APPR.		
THREE PLACE DECIMAL ± .005"			
MATERIAL: ALUMINUM	COMMENTS:		
FINISH			
DO NOT SCALE DRAWING			

MIT-Nanoterra

TITLE: MOTOR MOUNT PLATE

SIZE	DWG. NO.	REV
A	P110	B

SCALE: 1:2 | WEIGHT: | SHEET 1 OF 1

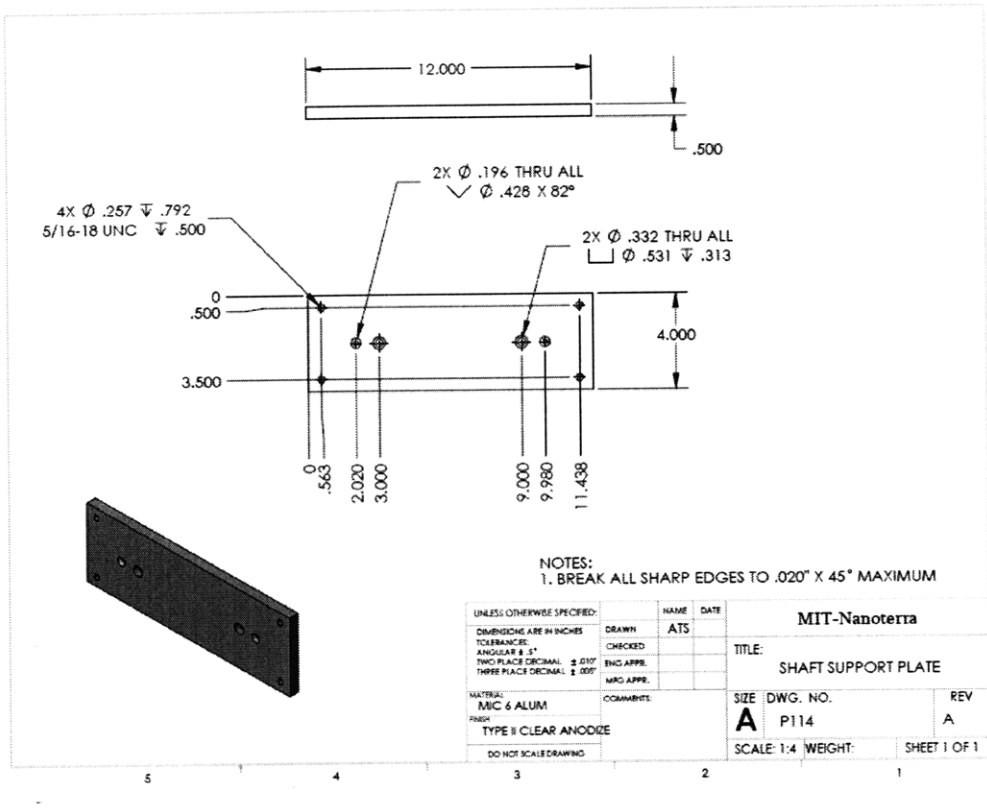
12.000
.500
2X Ø .196 THRU ALL
Ø .428 X 82°
4X Ø .257 ↧ .792
5/16-18 UNC ↧ .500
2X Ø .332 THRU ALL
Ø .531 ↧ .313
0
.500
3.500
4.000
0
.563
2.020
3.000
9.000
9.980
11.438
NOTES:
1. BREAK ALL SHARP EDGES TO .020" X 45° MAXIMUM
UNLESS OTHERWISE SPECIFIED:
DIMENSIONS ARE IN INCHES
TOLERANCES:
ANGULAR ± .5°
TWO PLACE DECIMAL ± .010"
THREE PLACE DECIMAL ± .005"
MATERIAL: MIC 6 ALUM
FINISH: TYPE II CLEAR ANODIZE
DO NOT SCALE DRAWING
DRAWN ATS
CHECKED
ENG APPR.
MFG APPR.
COMMENTS:
MIT-Nanoterra
TITLE: SHAFT SUPPORT PLATE
SIZE A
DWG. NO. P114
REV A
SCALE: 1:4
WEIGHT:
SHEET 1 OF 1

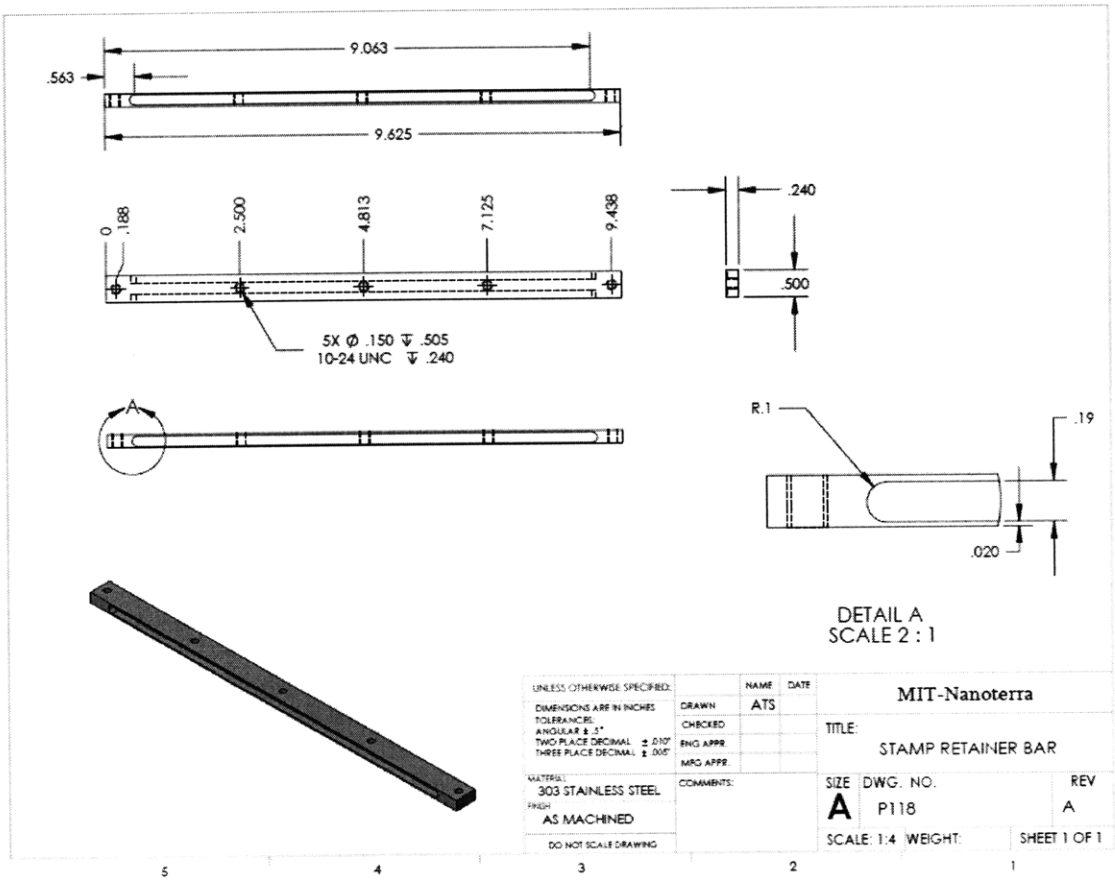
9.063
.563
9.625
0
.188
2.500
4.813
7.125
9.438
.240
.500
5X Ø .150 ↧ .505
10-24 UNC ↧ .240
A
R.1
.19
.020
DETAIL A
SCALE 2 : 1
UNLESS OTHERWISE SPECIFIED:
DIMENSIONS ARE IN INCHES
TOLERANCES:
ANGULAR ± .5°
TWO PLACE DECIMAL ± .010"
THREE PLACE DECIMAL ± .005"
MATERIAL: 303 STAINLESS STEEL
FINISH: AS MACHINED
DO NOT SCALE DRAWING
DRAWN ATS
CHECKED
ENG APPR.
MFG APPR.
COMMENTS:
MIT-Nanoterra
TITLE: STAMP RETAINER BAR
SIZE A
DWG. NO. P118
REV A
SCALE: 1:4
WEIGHT:
SHEET 1 OF 1

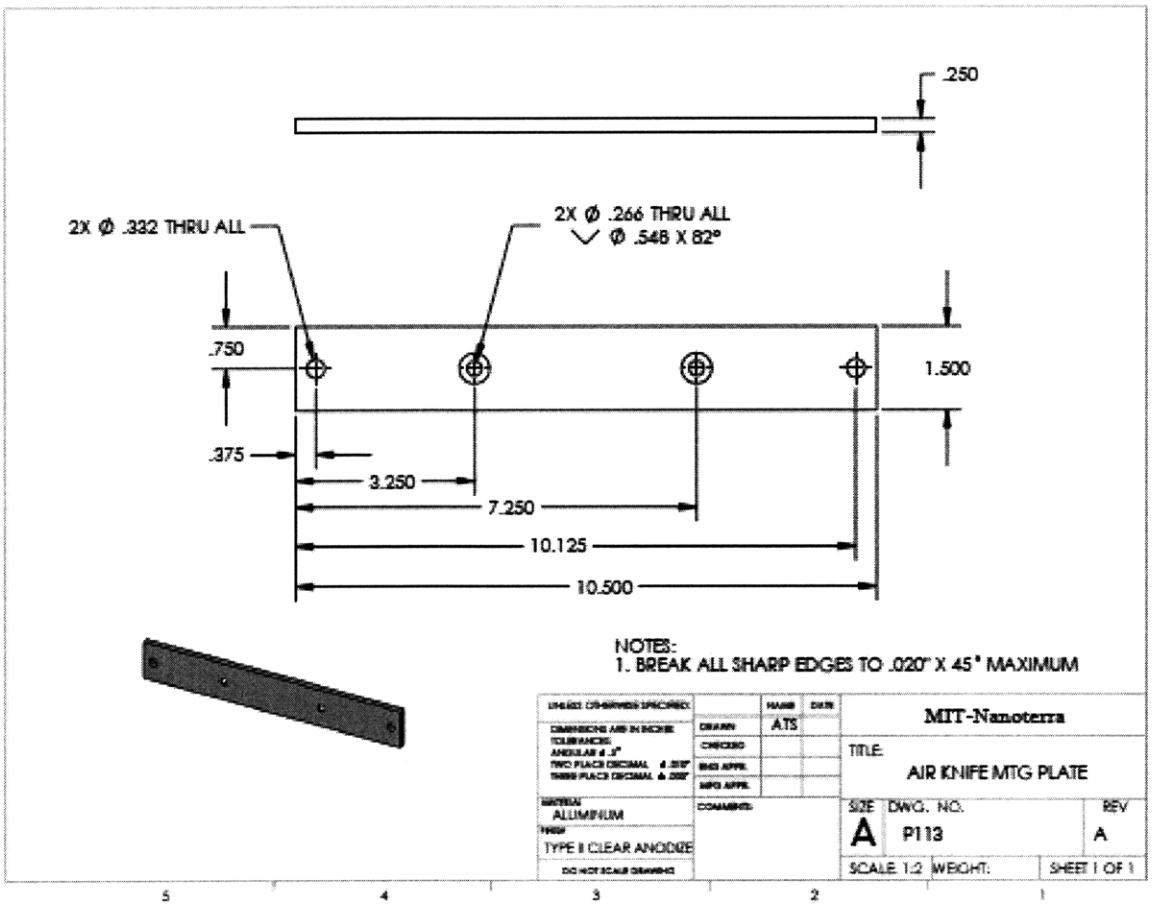
.250
2X Ø .332 THRU ALL
2X Ø .266 THRU ALL
Ø .548 X 82°
.750
1.500
.375
3.250
7.250
10.125
10.500
NOTES:
1. BREAK ALL SHARP EDGES TO .020" X 45° MAXIMUM
ALUMINUM
TYPE II CLEAR ANODIZE
DRAWN
ATS
MIT-Nanoterra
TITLE:
AIR KNIFE MTG PLATE
SIZE
A
DWG. NO.
P113
REV
A
SCALE: 1:2
WEIGHT:
SHEET 1 OF 1

Bill of Materials, Printing Machine

Project #:	Pxxx
Project Name:	μCP Machine

Item	Description	Qty	MFG	Vendor	Part #
1	MODULE PLATE, SUPPLY	1	NT-MIT	MD Belanger	P100
2	MODULE PLATE, PRINT	1	NT-MIT	MD Belanger	P101
3	MODULE PLATE, COLLECT	1	NT-MIT	MD Belanger	P102
4	BEARING BLOCK	10	NT-MIT	Dynatech	P104
5	IDLER ROLLER	4	NT-MIT	Dynatech	P105
6	BONE ROLLER	2	NT-MIT	Dynatech	P106
7	SPOOL ROLLER	2	NT-MIT	Dynatech	P107
8	PRINT ROLLER	1	NT-MIT	Dynatech	P108
9	INKING ROLLER	1	NT-MIT	Dynatech	P109
10	MOTOR MOUNT PLATE	5	NT-MIT	MD Belanger	P110
11	BEARING PLATE, PRINT	1	NT-MIT	MD Belanger	P111
12	STAMP TUBE	1	NT-MIT	Dynatech	P112
13	AIR KNIFE MTG PLATE	1	NT-MIT	Dynatech	P113
14	SHAFT SUPPORT PLATE	1	NT-MIT	MD Belanger	P114
15	PRESSURE PLATE	1	NT-MIT	MD Belanger	P115
16	IMPRESSION FIXED PLATE	1	NT-MIT	MD Belanger	P116
17	SUBSTRATE SPOOL END	4	NT-MIT	Dynatech	P117
18	STAMP RETAINER BAR	1	NT-MIT	Dynatech	P118
19	ADAPTER SHAFT	1	NT-MIT	MIT	P202
20	CLUTCH DISC	1	NT-MIT	MIT	P201
21	24VDC POWER SUPPLY, 360W	1		A-D	PSM24-360S
22	PLC, 20 IN 16 OUT (SOURCE)	1		A-D	D0-06DD2-D
23	ANALOG INPUT MODULE	1		A-D	F0-08ADH-2
24	CIRCUIT BREAKER, 20A	1	EATON	A-D	WMS1D20
25	CIRCUIT BREAKER, 5A	3	EATON	A-D	WMS1D05
26	CONTACTOR	1		A-D	SC-E04G-24VDC
27	START/STOP BUTTON BOX	2		A-D	E22ASB204
28	ELECTRONICS ENCLOSURE	1		A-D	N412202008C
29	IDLER ROLLER ASSY	1	DFE	DFE	IR3-8-45

30	TRANSDUCER ROLL	3	DFE	DFE	NWIS-10-50-6
31	TENSION TRANSDUCER AMPLI-FIER	2	DFE	DFE	TI201L
32	TRANSDUCER CABLE	2	DFE	DFE	721-1556
33	AIR KNIFE	1	EXAIR	EXAIR	110009
34	STEPPER MOTOR NEMA34	3	IMS	IMS	MDRIVE 34AC
35	CORDSET-PROTO DEV	3	IMS	IMS	MD-CS100-000
36	CORDSET-POWER	3	IMS	IMS	MD-CS200-000
37	PARAMETER SETUP CABLE	1	IMS	IMS	MD-CC300-000
38	ADAPTER	1	IMS	IMS	MD-ADP-M23
39	PM CLUTCH	2	MAGPOWR	MAGPOWR	HC5-58
40	BALL BEARING, 1" ID 2" OD	21	SKF	M-C	3760T350
41	WAVE WASHER	10		M-C	9714K650
42	BEARING LOCKNUT	10		M-C	6343K160
43	HOSE CLAMP, 4.75-5.5 ID (PKG 5)	1		M-C	5076K27
44	SHAFT COUPLING	5		M-C	2463K15
45	LINEAR BEARING ASSY	2	THOMPSON	M-C	64825K36
46	LINEAR SHAFT, .750"	2	THOMPSON	M-C	6649K61
47	SHAFT MOUNT	2		M-C	6068K27
48	KNOB	2		M-C	6092K470
49	WASHER, .750" ID	2		M-C	98029A036
50	SHOULDER BOLT, .625"	2		M-C	90298A834
51	WASHER, SPOOL	2		M-C	92303A103
52	MACHINE TABLE, 30" HEIGHT	1		M-C	6403T42
53	ALUM EXTRUSION, 1.5" X 3.0" X 8'	3	80/20	M-C	47065T81
54	ALUM EXTRUSION, 1" X 2.0" X 8'	2	80/20	M-C	47065T126
55	ALUM EXTRUSION, 1.5" X 1.5" X 8'	1	80/20	M-C	47065T23
56	EXTRUSION END CAPS	8		M-C	47065T16
57	CORNER CONNECTORS	4	80/20	M-C	47065T51
58	CORNER CONNECTORS	4	80/20	M-C	47065T19
59	PUSHBUTTON (ILLUMINATED), YEL	2	BACO	M-C	6749K365
60	EMERGENCY STOP BUTTON	2	BACO	M-C	6785K21
61	CORD GRIPS	6		M-C	7529K171
62	CORD GRIP MOUNTING KIT	6		M-C	7466K37
63	ROTARY ON/OFF SWITCH, 25A	1		M-C	6759K231
64	DIN RAIL, 2 METER	2		M-C	8961K16
65	FUSE HOLDER	4		M-C	7641K351
66	DISTRIBUTION BLOCK, 3 CIR-CUIT	1		M-C	6367T19
67	TERMINAL BLOCK, 3 TERMINAL	10	WECO	M-C	9473T8
68	END SECTION	2	WECO	M-C	9473T132
69	END STOP	10	WECO	M-C	9473T144
70	JUMPER	10	WECO	M-C	9473T112
71	FEP SHRINK TUBING	1		M-C	8703K86
72	NEOPRENE RUBBER SHEET	1		M-C	8583K234
73	CORD GRIP, NYLON	2		M-C	7529K173

74	CLAMP COLLAR, .75" ID	2		M-C	6435K16
75	BEARING SPACER	10		MISUMI	U-CLBS D2-L1.25
76	MICROMETER	2	NEWPORT	NEWPORT	HR-13
77	LOAD CELL	2	TT	TRANSDUCER TECH	TT-MLP
78	LOAD CELL AMPLIFIER	2	TT	TRANSDUCER TECH	TM0-1-24VDC

References

[1] Xia, Y. and Whitesides, G. M., 1998, "Soft Lithography", Annual Review Mater. Sci. 1998. 28:153–84

[2] Michel, B. et al., 2000, "Printing Meets Lithography: Soft Approaches to High-resolution Patterning", IBM Journal of Research and Development, 45(5)

[3] Xia, Y.; Zhao, X. M.; and G. M. Whitesides, "Pattern Transfer: Self-Assembled Monolayers as Ultrathin Resists," Microelectron. Eng. **32,** 255 (1996).

[4] Great Lakes Regional Pollution Prevention Roundtable, <http://www.glrppr.org>. Accessed 3/15/2008

[5] International Paper Knowledge Center, <http://glossary.ippaper.com>. Accessed 3/15/2008.

[6] Whitesides, George M. "Soft Lithography". Harvard University. January 1998. <www.wtec.org/loyola/nano/US.Review/04_02.htm>.

[7] Rogers, J.A., Paul, K.E. and Whitesides, G.M., 1997, "Quantifying Distortions in Soft Lithography", Journal of Vacuum Science and Technology B: Microelectronics and Nanometer Structures, 16(1), pp 88-97

[8] Helmuth, Jo A.; Schmid, H.; Stutz, R.; Stemmer, A.; and Wolf, H. "High-Speed Microcontact Printing", Journal of American Chemical Society 2006, 128: 9296-9297

[9] Slocum, Alex. Precision Machine Design. Michigan: Society of Manufacturing Engineers, 1992.

[10] Moore, Wayne R. Foundations of Mechanical Accuracy. Connecticut: The Moore Tool Company, 1970.

[11] Dover Flexo Electronics, Inc. <http://www.dfe.com>. Accessed 7/20/2008.

[12] Mcmaster Carr, Inc. <http://www.mcmaster.com>. Accessed 7/15/2008.

[13] Magpowr, Inc. <http://www.magpowr.com>. Accessed 7/15/2008

[14] NanoterraInc, <http://www.nanoterra.com/i/self_assembly_diagram_1.gif>. Accessed 8/1/2008.

[15] Khanna, K. "Analysis of the Capabilities of Continuous High-Speed Microcontact Printing". Massachusetts Institute of Technology. August 19, 2008.

[16] Goel, A.; Laxminarayanan, S.; Xia, Y., "Understanding and Developing Capabilities for Large Area and Continuous Micro Contact Printing". Massachusetts Institute of Technology. August 29, 2007.

[17] Chestnut Engineering, Inc. <http://www.chesnuteng.com>. Accessed 3/15/2008.

[18] Delamarche, E., Schmid, H., Michel, B. and Biebuyck; 1997; "Stability of Molded Polydimethylsiloxane Microstructures"; Advanced Materials; 9 pp 741-746

[19]Bietsch, A. and Michel, B., "Conformal Contact and Pattern Stability of Stamps Used for Soft Lithography," *J. Appl. Phys.* **88,** 4310 (2000).

[20]Hardt, D.E., 1996, "Manufacturing Processes and Process Control". Massachusetts Institute of Technology. February, 1996.

[21]Delamarche, E.; Schmid, H.; Bietsch, A.; Larsen, N.B.; Rothuizen, H.; Michel, B.; Biebuych, H.; "Transport Mechanisms of Alkanethiols during Microcontact Printing on Gold," J. Phys. Chem. B., 1998, Vol. 102(18), pp.3324-3334.

[22]Roisum, David. "Web 101.00, Web Handling and Converting". <www.SeminarsForEngineers.com>.

[23]Roisum, David. Mechanics of Winding. Georgia: TAPPI, 1994.

[24]Web Handling and Converting Blog. "An Interview with Dr. Roisum". <http://www.webhandlingblog.com/blog/2005/08/an_interview_wi.html>. August 16, 2005. Accessed 7/25/2008.

[25]Shen, Shawn. "Design and Analysis of High-speed Continuous Micro-Contact Printing". Massachusetts Institute of Technology. August 19, 2008.

[26]Parish, G.J.; "Calculation of the behavior of rubber-covered rollers". British Cotton Industry Research Association. July 1961. Issue 7.